Spatial Relationships of Suspended Solids and Phosphorus in Bioretention Cells

by

Hallie Douglas

A thesis submitted to the Graduate Faculty of
Auburn University
in partial fulfillment of the
requirements for the Degree of
Master of Science

Auburn, Alabama
December 16, 2017

Keywords: Bioretention cells, hydraulic conductivity, infiltration, stormwater,

Approved by

Thorsten Knappenberger, Chair, Assistant Professor of Crop, Soil
and Environmental Sciences
Eve Brantley, Co-Chair, Extension Specialist and Associate Professor of
Crop, Soil and Environmental Sciences
Wesley Zech, Brasfield and Gorrie Professor of Construction Engineering and Management
Julie Howe, Associate Professor of Soil and Crop Sciences, Texas A&M University

Abstract

According to the United Nations, 54% of people live in urban areas. By 2050, that number will increase to 66% (UN Department of Economic and Social Affairs, 2016). The addition of impervious surfaces, such as parking lots, rooftops, and buildings, increases stormwater peak flows, degrades surface water quality, and generates higher pollutant loads compared to runoff originating from undeveloped areas. In order to improve stormwater management, it is necessary to transition from direct discharge of runoff into streams to innovative retention and treatment to protect water resources.

Bioretention cells (BRC) are a stormwater practice designed to infiltrate, store, and treat the first flush of stormwater, typically the most polluted. Pollutants are removed in BRCs by plant uptake, microbial activity, adsorption, and filtered by the media before entering surface waters (Li and Davis, 2008c; Dietz and Clausen, 2005; Prince George's County Department of Environmental Resources, 1993; Liu et al., 2014b). These cells help mitigate stormwater flow volume, flow rate, and remove nutrients. Suspended sediments that are commonly found in stormwater runoff decrease BRC infiltration rates over time, rendering the practice less effective.

Research on the effects of suspended sediments on infiltration rates has only been conducted in 1-D columns; additionally, it is unclear how stormwater pollutants (i.e, phosphorus) flow through clogged BRC media. Bioretention cells interact with water flow, sediment, and pollutants multi-dimensionally, thus 3-D studies are crucial for understanding their dynamics. The goal of this research was to assess how phosphorus flow is affected in non-clogged, semi-clogged, and clogged BRC systems and evaluate if the current maintenance recommendations are sufficient.

Water was pumped through a 3-D flow cell (62.5 x 5 x 32.5 cm) with an inflow tube and outflow ports, and the spatial variability of the filtration media was analyzed. Trial 1 had no additional solids, Trial 2 was a "semi-clogged" system with 300 g of solids placed on half of the BRC media surface, and Trial 3 was a "clogged system" with 600 g solids placed on the entire BRC media surface. For each trial, synthetic stormwater containing phosphorus fertilizer mixed with iron oxides was pumped through the cell. After the stormwater flush, media samples were analyzed for phosphorus concentration. Correlations between the amount of added solids and location of phosphorus adsorption were made by analyzing the BRC media grid. The lowest phosphorus levels were found in the clogged layer and higher phosphorus levels were found in the media layer. Results support the current practice of periodically removing the top surface layers in order to remove accumulated solids and nutrients from BRC media.

Acknowledgments

I would like to thank my advisors, Dr. Thorsten Knappenberger and Dr. Eve Brantley, for their support, knowledge, and guidance throughout this research project. I would also like to thank my committee members, Dr. Wesley Zech and Dr. Julie Howe, for their gracious support and guidance. I would like to thank my fellow graduate students, as well as professors, undergraduate workers, and technicians within the Crop, Soil, and Environmental Sciences Department for their knowledge, support and problem solving skills. And lastly, I would like to thank my family and friends for their continuous, unwavered support and love from across the country.

Table of Contents

List of Figures

List of Tables

Chapter 1

Introduction

The number of people living in rural areas compared to urban areas has changed over the past century. In the developing world, populations are moving from rural areas to urban areas, and in the developed world, suburban populations are expanding (Economist, 2016). By the year 2050, 66% of the world's population will be living in urban areas compared to the 54% living in them today (UN Department of Economic and Social Affairs, 2016). Environmental challenges are associated with urbanization and mass population movement; the biggest challenge includes integrating urban and non-urban areas while preserving and maintaining natural resources. Increasing urbanization causes a high transition rate of farmland, grassland, and otherwise non-developed land into developed, impervious land. Impervious land includes asphalt and concrete, containing structures such as sidewalks, buildings, and parking lots that disturb the natural soil characteristics by the processes of land grading and compaction (Rhea et al., 2015). Urban development alters stream geomorphology, as well as, negatively affects water quality, aquatic organisms, and habitat (Liu et al., 2014b; Alberti et al., 2007; Booth et al., 2002; Carey et al., 2013; Cianfrani et al., 2006).

Water from rainfall and snowmelt affect the landscape in various ways. In vegetated and forested areas, precipitation makes contact with the canopy, which provides a natural shield for the soil below. This layer of protection decreases particle detachment and erosion rates, while increasing groundwater recharge, infiltration rates, and maintains overall surface water quality (Liu et al., 2014a; University of Arkansas, 2010). Surface runoff originating from impervious surfaces has higher peak flow due to the smooth, un-textured surface (Miguez et al., 2015; Page et al., 2015; Li and Davis, 2008c; Hsieh and Davis, 2005b). Runoff can mobilize and transport pollutants, resulting in degraded downstream water quality (Miguez

et al., 2015; Page et al., 2015; Li and Davis, 2008c; Hsieh and Davis, 2005b; Gobel et al., 2007; Liu et al., 2014b). As pollutant loads increase, biological integrity of receiving water bodies degrades, biological assemblages are disrupted, and the overall physical and chemical composition are altered (Page et al., 2015; Saalfeld et al., 2012). Stormwater is typically conveyed to its end of pipe location, which could include a storm drainpipe, a water treatment plant, or in some cases a stream, lake, or river (Miguez et al., 2015).

Surface water bodies receive pollution from both point and nonpoint sources. Point source pollution, as defined by the amended 1987 Clean Water Act, is any pollution from a defined and discrete conveyance, such as a pipe, conduit, ditch or channel (Novotny, 2003). Point source pollution can be pipe discharges from factories or wastewater treatment plants (Novotny, 2003). In contrast, nonpoint source pollution originates from diffuse sources that do not have a well-defined point of discharge. This includes runoff from agricultural lands, urban and suburban development, construction runoff, rangeland, animal feeding operations, and pastures. Nonpoint source pollution was not federally recognized until the Clean Water Act was reauthorized in 1972. At one time, all pollution was nonpoint source pollution, and it was not until urban centers started collecting urban runoff and wastewater to one point for disposal that point source pollution became a common practice (Novotny, 2003).

Stormwater moving through urban and impervious areas contain various pollutants including sediments, nutrients, heavy metals, organic compounds, pesticides, herbicides, trash and toxins (Akan, 1993). Roads and parking lots, two common impervious surfaces, generate a large portion of runoff containing pollutant loads from automobiles (Brown and Hunt, 2008). Stormwater from developed areas carrying higher pollutant loads into local water bodies can contribute to the "urban stream syndrome" (Askarizadeh et al., 2015). Symptoms of the "urban stream syndrome" include altered streamflow, impaired water and sediment quality, and shifts in biological composition and ecosystem services (Askarizadeh et al., 2015). Hydrologic drivers of these symptoms include increased watershed imperviousness, increased formal drainage systems (i.e., grey infrastructure), lining streams with

concrete, and surface water impoundments (Askarizadeh et al., 2015). To alleviate these symptoms, holistic hydrologic approaches such as Low Impact Development (LID) practices may be implemented to address the impacts of conventional stormwater management.

1.1 Low Impact Development

Conventional development practices promote installation of impervious surfaces and centralized stormwater management without considering the changes in hydrology from pre-construction to post-construction conditions (Thompson, 2009; Wilson et al., 2015). Pre-development hydrographs have lower runoff rates and a later peak discharge compared to post-development hydrographs. Pre-development hydrographs demonstrate a higher stream baseflow, while post-development hydrographs have a lower baseflow (Thompson, 2009).

Low Impact Development is a holistic management practice that incorporates pre-development hydrology into urban drainage systems as a means to address the challenges of conventional development and restore the natural water balance (Liu et al., 2014a; Askarizadeh et al., 2015; Liu et al., 2014b). It was first developed in Prince George's County, MD, in the 1990s as a response to the high costs, both economic and environmental, of conventional stormwater management techniques (Prince George's County Department of Environmental Resources, 1999a). The main goal of LID is to enhance infiltration, reduce runoff, and increase groundwater recharge (Prince George's County Department of Environmental Resources, 1999b).

Low Impact Development practices provide hydrologic relief, as well as, aesthetic benefits. Implementation of LID practices is driven by four hydrologic considerations, including: the control of runoff volume, peak runoff rate, flow frequency and duration, and water quality (Prince George's County Department of Environmental Resources, 1999a; Ahiablame et al., 2013). Various LID techniques can be implemented depending on the site specific conditions and hydrologic considerations. Techniques include, but are not limited to, green roofs, rain barrels, cisterns, permeable pavement, vegetated buffer strips, vegetated swales,

and bioretention cells (Arnold and Gibbons, 1996; LeFevre et al., 2010). These techniques provide relief areas for water retention, infiltration, and storage to occur, as opposed to being conveyed within a typical grey infrastructure system to an end of pipe location.

1.2 Bioretention Cells

Stormwater Best Management Practices (BMPs) are technologies designed to improve stormwater runoff (Hsieh and Davis, 2005b). Widely used BMPs are bioretention cells (BRCs), which are common due to their versatility and high level of performance (Brown and Hunt, 2011a). Compared to other BMPs, bioretention methods are cost effective (Wossink and Hunt, 2003). A BRC can be characterized as a landscaped depression, designed and sized accordingly to receive runoff from surrounding impervious surfaces (Liu et al., 2014a).

BRCs are typically sized at 5-10% of the total drainage area and are designed to infiltrate, store, and treat the first flush of stormwater, typically the first 2.5 - 3.8 cm (1 - 1.5 in), which tends to be the most polluted (Hsieh and Davis, 2005a; Brown and Hunt, 2008; Davis et al., 2009; Davis, 2007; Davis et al., 2001, 2006; Hunt et al., 2008). BRCs consist of multiple filtration constituents, including a vegetated layer underlain by a mulch layer, as well as, a blended layer containing sand, soil, fines, and organic matter (Liu et al., 2014a; Davis et al., 2001; Liu et al., 2014b). BRCs have the ability to treat pollutants such as sediment, bacteria, pathogens, oil and grease, nutrients, and metals. Pollutants entering a BRC are treated by physical, chemical, and biological processes, including plant uptake, microbial and biological interaction, sedimentation, filtration, decomposition, ion exchange, volatilization and adsorption (Li and Davis, 2008c; Dietz and Clausen, 2005; Prince George's County Department of Environmental Resources, 1993; Liu et al., 2014b).

1.2.1 Phosphorus in Stormwater

Phosphorus is a particular pollutant of concern in stormwater runoff, and is the limiting nutrient in temperate fresh water systems (Erickson et al., 2007; Aldridge and Ganf,

2003; Schindler, 1977). High phosphorus concentrations in water bodies can cause excessive algae growth and eutrophication, reduce oxygen levels and reduce the overall aesthetic and recreational value of water bodies (Hunt et al., 2006; Kim et al., 2003; Li and Davis, 2016).

Agricultural non-point source pollution (including phosphorus fertilizer) has been identified as the leading source of water quality deterioration in freshwater systems (Wang et al., 2013). Erosion of particulate phosphorus and surface movement of dissolved phosphorus are methods of introduction into freshwater systems; phosphorus does not have an atmospheric component, therefore it has a high accumulation rate once presented to a system (Mallin et al., 2009; Sims et al., 1998; Nash and Halliwell, 2000). Total P concentrations found in stormwater have shown a mean value of 0.3 mg/L based on NPDES data (Pitt et al., 2004; Li and Davis, 2016).

When introduced to soils, surface adsorbed phosphorus in soil colloids is considered gradually fixed, becoming less available over time due to the slow solid-state diffusion into soil particles (Baken et al., 2016; Barrow, 1983). Phosphorus release from soils has a fast initial release, followed by a slow release spanning several months (Baken et al., 2016; Koopmans et al., 2004; Lookman et al., 1995). Additionally, phosphorus has a high affinity to bind with iron and aluminum oxides due to several mechanisms: adsorbing to the surface of existing minerals and binding during the formation of iron rich minerals (Baken et al., 2016; Li and Davis, 2016; Bortoluzzi et al., 2015; Zhang et al., 2001; Jain and Loeppert, 2000). Studies by Jain and Loeppert (2000) reported that when in competition with a competing ion such as arsenate, phosphate adsorbed to ferrihydrite, an iron oxide derived in the lab, at 85% at pH 7.5. This demonstrated phosphates high affinity to bind with ferrihydrite in a competing scenario (Jain and Loeppert, 2000).

The capacity of BRC media to adsorb phosphorus is reduced depending on the concentration of background phosphorus present and if fine sediments have accumulated onto the media surface. Background phosphorus concentrations present in BRC media depend

on the particular media specifications, and can affect the phosphorus uptake capacity from stormwater (Li and Davis, 2016).

1.3 Bioretention Cell Maintenance Strategies

Removal of the surface layer of a BRC is a highly regarded preventative maintenance strategy to remove pollutants and potential clogged areas due to fine sediments. However, there remains an overall lack of maintenance and construction oversight for bioretention systems, which diminishes performance (Brown and Hunt, 2012). BRCs, compared to other types of stormwater control measures, such as detention/retention basins, are more susceptible to construction and maintenance complications due to the accumulation of fine particles in unstable catchments that clog over time (Brown and Hunt, 2011a; Bean et al., 2007; Asleson et al., 2009; Fassman and Blackbourn, 2010; Brown and Hunt, 2012).

1.4 Media Clogging by Fine Particle Accumulation

If designed properly, BRCs can meet both water quality and landscape objectives, and can be aesthetically pleasing and beneficial to the landscape (Hunt et al., 2006). However, if the media mix or BRC size is designed incorrectly, media clogging, increased ponding depth, decreased pollutant removal, and overflow can occur, allowing untreated stormwater to enter water bodies. Media clogging by fine sediments can be detrimental to the cells filtration performance and lifespan; studies conducted by Langergraber et al. (2003), Schuh (1990), and Hatt et al. (2007) found that clogging of bioretention media occurred in the top 0.1 m (4 in), and that the fine textured component of the media clogs over time, limiting the cells lifespan (Li and Davis, 2008a).

Table 1.1: Suspended solids clogging research gap in stormwater and bioretention cell studies.

Article	Clogging Findings
Hatt et al. (2007) Langergraber et al. (2003) Schuh (1990)	Clogging occurs in top 100 mm
Lindsey et al. (1992) Le Coustumer et al. (2009)	After 2 years, 40-60% of previously installed BRCs are not functioning as designed due to clogging
Li and Davis (2008a)	Fine textured media component clogs over time, limiting the lifespan of the cell

1.5 Research Objectives

Field scale BRC media research focuses on short term hydrologic performance (Brown and Hunt, 2008, 2011b, 2012; Davis, 2008) and water quality performance (Brown and Hunt, 2011b, 2012; Hathaway and Hunt, 2011). Lab scale BRC media column studies has focused on phosphorus removal and hydraulic conductivity reduction (Hsieh et al., 2007; Le Coustumer et al., 2012). However, long term fine particle accumulation and clogging negatively affect BRC performance; there is a lack of research that further investigates how the fate and transport of pollutants, particularly phosphorus, through BRC media are affected by fine particle accumulation and clogging.

Column studies provide a controlled environment to observe these interactions unable to be isolated in field scale studies; however, to further investigate how BRC media affected by fine particle accumulation and clogging interacts with water flow and pollutant transport, 3-D studies within a rectangular flow cell of larger dimensions is crucial for understanding these dynamics.

The objectives of this study are to (a) address the spatial variability of fine particle accumulation and clogging of BRC media on phosphorus mobility and retention, (b) simulate water flow and pollutant load multi-dimensionally, and (c) determine any correlations between background phosphorus levels in BRC media on phosphorus sorption capacity by conducting mass balance calculations.

The tasks to complete this work include (a) conducting clogging experiments to determine hydraulic conductivity decline of BRC media, (b) conducting phosphorus flow experiments to determine phosphorus retention on several clogged media conditions, (c) analyzing BRC media for phosphorus levels, (d) flushing media with blue dye to visualize changes in flow patterns, (e) comparing results to current maintenance practices, and (f) predicting hydraulic conductivity decline in field-scale BRCs to improve future maintenance practices.

1.6 Thesis Structure

To address the objectives and tasks listed in Section 1.5, the thesis begins with a literature review (Chapter 2), followed by materials and methods used (Chapter 3), results and discussion (Chapter 4), and conclusions and recommendations for future research (Chapter 5).

Chapter 2

Literature Review

2.1 Bioretention Cell Media Selection and Depth

BRCs are able to remove both particulate and dissolved pollutants (Li and Davis, 2008c). During precipitation events, water is directed to the BRC and excess water can pond temporarily at the surface or be stored in the upper media layer once the rainfall intensity surpasses that of the infiltration capacity of the media (Hsieh et al., 2007; Hsieh and Davis, 2005b). Storing runoff in the upper media layers is a useful pollutant removal mechanism compared to water ponding at the surface (Hsieh and Davis, 2005b). Hsieh and Davis (2005b) studied bioretention columns and observed that when storage occurs in the upper layers, pollutants have a greater chance of being sorbed onto the media or assimilated by microorganisms (Hsieh and Davis, 2005b). Some BRCs contain an internal water storage system that creates anaerobic conditions in order to increase denitrification and reduce total nitrogen in the system (Brown and Hunt, 2008). BRCs may also contain an overflow inlet, designated inflow path (i.e., grass, vegetated, or stone-lined), and a temporary ponding area.

Although BRCs are gaining in popularity, there remain concerns with the technology, especially pertaining to media selection and determination (O'Neill and Davis, 2010). Due to inconsistent media specifications and varying treatment goals depending on cost and location, a standardized bioretention soil medium has yet to be produced (O'Neill and Davis, 2010). Selection of proper media is key when designing a BRC and can vary depending on pollutant removal efficiency, cost, and location suitability (Liu et al., 2014a). For a BRC to function properly, the media must have sufficient hydraulic conductivity for large volumes of water to infiltrate (Hsieh and Davis, 2005b). Hydraulic conductivity depends on the size of the conducting pores, in which larger pores conduct water at a faster rate (Hillel, 1998).

Soil properties including porosity, infiltration, and particle size distribution can affect the transport and retention of water through the BRC media and overall effluent water quality (Carpenter and Hallam, 2010; Liu et al., 2014b). However, the hydraulic conductivity should not be so rapid that no retention of pollutants occurs.

A bioretention blend contains a ratio of sand, mulch/organic matter, and a fine fraction of silt and clay (Liu et al., 2014a). Sand may be a majority of the mix, up to 90%, and the remaining fraction is a mix of fines and organic matter. The fine fraction, a mixture of silt and clay, is increased if phosphorus is the pollutant of concern. BRC media should contain less than 10% fine material as above 8% clay can be detrimental to the cell, reduce infiltration rates, and increase total suspended solids (TSS) in the effluent (Liu et al., 2014a; O'Neill and Davis, 2010; Stander and Borst, 2010; Liu et al., 2014b). The fine fraction is chemically active, which requires an active balance between chemical reactions and media permeability parameters (Hsieh and Davis, 2005b). If certain parameters such as soil texture or compaction are out of balance, the efficiency of the cell can be compromised. Unfortunately, most performance parameters are not known until the cell is built and in use (Hsieh and Davis, 2005b).

By using highly permeable media, a BRC can promote rapid stormwater infiltration that achieves the goals of preserving water quality and flood control (Hsieh et al., 2007). However, using a highly permeable media without a fine fraction can reduce the cells hydraulic retention time, resulting in the cell media being unable to adequately treat and remove nutrients (Brown and Hunt, 2011b).

Brown and Hunt (2008) monitored two BRCs at two locations (Rocky Mount and Nashville, NC) in the Coastal Plain region of North Carolina with different media mixes; one site had 98% sand and 2% fines and the other had 86-89% sand and 11-14% fines (i.e., silt and clay) (Brown and Hunt, 2008). The site with 98% sand and 2% fines had a total nitrogen removal rate of 80%, total phosphorus removal rate of 72%, and a total suspended solids (TSS) removal rate of 92%; all three reductions above the North Carolina Department

of Water Quality (NCDWQ) pollutant removal thresholds for specified design requirements (Brown and Hunt, 2008). Brown and Hunt (2011b) conducted an additional monitoring study at Rocky Mount, NC, from Brown and Hunt (2008), but altered the internal water storage (IWS) depth and the media mix with 96% sand, 2.9% silt, and 1.1% clay (Brown and Hunt, 2011b, 2008). Brown and Hunt (2011b) discovered the percentage of runoff leaving the site by evapotranspiration and exfiltration was 87% for an internal water storage depth of 1.03 m (3.38 ft) and 75% for an internal water storage depth of 0.73 m (2.39 ft) (Brown and Hunt, 2011b). The new media mix configuration contained increased silt and clay, and hydraulic retention time increased and resulted in all nitrogen species and TSS concentrations decreasing in the effluent (Brown and Hunt, 2011b). It is important that the media selected be tested for background extractable phosphorus, especially if phosphorus reduction is a primary concern (Davis et al., 2009; Davis, 2007; Davis et al., 2001, 2006; Hunt et al., 2008). Phosphorus removal depends highly on the amount of background phosphorus already present; media that contains high extractable phosphorus is more likely to contribute to leaching (Davis et al., 2009; Davis, 2007; Davis et al., 2001, 2006; Hunt et al., 2008). Davis (2008) constructed a BRC in College Park, MD, with 50% construction sand, 30% topsoil, 20% compost with less than 10% clay (Davis, 2008). This cell noted a 44-63% peak flow reduction from a data set of 49 rainfall events (Davis, 2008).

Media depth can vary depending on location, type of soil, and cost, and is characterized on a case-by-case basis depending on the specific site needs. In general, a media layer thickness of 0.7 - 1 m (2.3 - 3.3 ft) is recommended for BRCs, and in some cases it could be beneficial to incorporate two distinct media layers, an upper layer for vegetation and a bottom layer for filtration (Liu et al., 2014a; US Dep of Housing and Urban Development, 2003). However, different media layers must be fully characterized; an impermeable surface layer could form if layer characterization is not performed. A comparison study of six BRCs in North Carolina and Maryland found that cells with deeper media depths promoted infiltration, evapotranspiration, and predevelopment hydrology (Brown and Hunt, 2011a; Li

et al., 2009). In BRC studies conducted by Brown and Hunt (2008) in Rocky Mount and Nashville, NC, 0.6 m (2 ft) and 0.9 m (3 ft) cells were monitored and the deeper media depth exhibited higher runoff volume reduction compared to the shallow media depth (Brown and Hunt, 2008).

2.2 Pollutant Remediation

2.2.1 Nitrogen and Phosphorus Removal

Nitrogen and phosphorus are considered pollutants of concern in many areas of the United States, especially coastal zones (Hunt et al., 2006). The USEPA provides a limit of 0.05 mg/L of total phosphorus in streams that enter lakes and 0.1 mg/L in flowing water to control eutrophication (USEPA, 1986; Li and Davis, 2016). BRC filtration technology can reduce concentrations of nitrogen and phosphorus; however, current technology does not support the reduction of nitrate-nitrogen levels (NO_3-N) (Hunt et al., 2006; Davis et al., 2001, 2003; Hsieh and Davis, 2005a). BRC systems are less effective at reducing total nitrogen unless aided by an internal water storage system (Passeport et al., 2009; Liu et al., 2014b). Davis et al. (2001) noted that nitrate was produced in bioretention systems due to the accumulation of organic and ammonia-nitrogen (Davis et al., 2001; Kim et al., 2003). Nitrate-nitrogen must be in the form of nitrogen gas to be removed from the media, which requires a carbon source and an anaerobic environment (Hunt et al., 2006). Hunt (2003) and Kim et al. (2003) studied how the addition of a saturated anoxic layer increased the conversion rate to nitrogen gas via denitrification.

Phosphorus treatment in bioretention is highly variable; research has shown cases where effluent concentrations are higher than influent concentrations (Li and Davis, 2016; Brown and Hunt, 2011a; Dietz and Clausen, 2005, 2006; Hunt et al., 2006; Li and Davis, 2009; Palmer et al., 2013; Sharkey, 2006). Additionally, research has shown cases of reduction in effluent phosphorus compared to influent concentration (Li and Davis, 2016; Brown and

Hunt, 2011b; Davis, 2007; Hunt et al., 2008; Komlos and Traver, 2012; Liu and Davis, 2014; Passeport et al., 2009).

The treatment processes for the removal of phosphorus from BRCs include precipitation, adsorption, filtration, and plant uptake (Liu et al., 2014a). Phosphorus has several forms, and can be found in particulate form, which can be removed by filtration mechanisms, and in dissolved form, which are effectively immobilized when adsorbed onto the media during transport (Li and Davis, 2016, 2008a,b, 2009; Liu and Davis, 2014; Lucas and Greenway, 2008, 2011). Nutrient removal can be maximized by promoting plant growth and microbial activity (Henderson, 2008; Liu et al., 2014b). Phosphorus ions are easily adsorbed onto soil particles, approximately two-thirds of phosphorus in stormwater is bound to other particles and sediments, which simplify phosphorus removal in the cell when the soil media is eventually replaced (Liu et al., 2014a; Davis et al., 2009; Davis, 2007; Davis et al., 2001, 2006; Hunt et al., 2008).

2.2.2 Metal Accumulation

Metals in stormwater runoff are of concern due to their environmental accumulation potential (Liu et al., 2014a; Jones and Davis, 2013). Within BRC media, the mulch/organic matter portion play a role in the removal of metals to prevent downstream metal toxicity (Li and Davis, 2008c). Studies by Davis et al. (2001) and Li and Davis (2008c) showed instances of high metal removal rates taking place in the top 0.2 m (0.7 ft) of a media. Copper (Cu), Zinc (Zn) and Lead (Pb) can be removed in the mulch layer due to its high cation exchange capacity and ability to bind metals (Davis et al., 2001). Metals have been shown to decrease with depth in typical BRC media profiles (Li and Davis, 2008c; Dechesne et al., 2005). Hunt et al. (2006) studied a BRC in urban North Carolina for 2 years and reported that after 23 rain storms, effluent concentrations of Cu, Zn, and Pb decreased (Liu et al., 2014a; Hunt et al., 2006).

2.2.3 Suspended Solids and Clogging

Excessive suspended solids can be detrimental to water bodies. Sediments can be abrasive to fish gills, create turbid water, and reduce water quality. Bioretention systems can effectively treat suspended sediments, in addition to heavy metals and nutrients (Davis et al., 2001; Le Coustumer et al., 2009; Zinger et al., 2007). Suspended solids can be removed from the BRC through sedimentation within the cell and by filtration of the media (Liu et al., 2014a). However, suspended sediments can clog the BRC media and render parts of the cell insufficient at successfully filtering out pollutants. Once a BRC has accumulated solids, current maintenance practices suggest removal of the surface layer containing phosphorus and suspended solids and replacement with fresh media.

2.3 Design Challenges

2.3.1 Media Specifications and Configuration

There are several challenges regarding media specifications addressed in current research. The majority of BRC media design is based on soil texture – sand, silt, and clay – where particle size and soil chemical properties can vary immensely within the three textural categories depending on the soil type (Hsieh and Davis, 2005b). Minor textural size differences can result in larger differences in infiltration rates (Hsieh and Davis, 2005b).

Furthermore, the configuration of the media layers can result in differences in performance among similarly designed BRCs. If the hydraulic conductivity of the different media layers is not known, infiltration rates can be compromised. A layer with high silt and clay content with low hydraulic conductivity and low permeability will affect overall BRC performance if placed at the surface of the cell instead of the bottom (Hsieh and Davis, 2005b). A cell would have much slower infiltration rates if a layer with low permeability was placed at the surface compared to the bottom of the cell (Hsieh and Davis, 2005b). There will also be

differences in a cells performance if the different layers were mixed compared to individually placed (Hsieh and Davis, 2005b).

Additionally, there are inherent levels of background phosphorus associated with components of BRC media, including sand, silt, clay, mulch, and other organic components (Li and Davis, 2016). They can be sorbed to particles or bound as organic phosphorus (Li and Davis, 2016). Levels of background phosphorus vary among BRC media mixes depending on location, soil type, and climate. The level of background phosphorus present in a BRC media affects the phosphorus sorption capacity from stormwater runoff (Li and Davis, 2016). Palmer et al. (2013) used soil amendments to enhance phosphorus sorption capacity when already exposed to high levels of background phosphorus. The presence of amorphous iron oxides and aluminum oxides within BRC media can increase the sorption capacity (Li and Davis, 2016; Bortoluzzi et al., 2015; Zhang et al., 2001).

2.3.2 Cell Size

BRCs are designed and sized to receive runoff from surrounding impervious surfaces, and are typically sized at 5-10% of the total drainage area (Liu et al., 2014a; Hsieh and Davis, 2005a; Brown and Hunt, 2008; Davis et al., 2009; Davis, 2007; Davis et al., 2001, 2006; Hunt et al., 2008). If not constructed according to the drainage area, filtration potential and pollutant removal can be compromised. Li et al. (2009) demonstrated that deep media depths promote infiltration and pollutant removal more than shallow depths (Brown and Hunt, 2011a; Li et al., 2009). However, in order to reduce costs, shallow cells are preferred and sometimes design standards are not met during the construction process.

Brown and Hunt (2011a) conducted BRC studies on intentionally undersized cells to see how size affects overall performance. Three cells were built with a 0.6 m (2 ft) media depth, while 4 cells had a 0.9 m (3 ft) media depth. The actual surface storage volume for the 0.6 m (2 ft) cells was 28% and 35% for the 0.9 m (3 ft) cells. Out of 64 storm events measured, overflow should have been generated in 17% of the events; however, 59% and 55% of the 0.6

m (2 ft) and 0.9 m (3 ft) cells, respectively, produced overflow. The higher percentage of overflow allowed for more untreated stormwater runoff to enter surface waters (Brown and Hunt, 2011a).

2.3.3 Clogging of Fine Sediments

Current BRC research reports a large percentage of bioretention studies as being negatively affected by clogging of fine sediments. Brown and Hunt (2011a) conducted a study observing the performance of undersized BRCs and found that the cells were clogged with granite fines associated with the gravel base layer from parking lot construction (Brown and Hunt, 2011a). The cell media was installed prior to the paving of the parking lot, and although a geotextile fabric was placed to mediate the problem, fine particles still passed through (Brown and Hunt, 2011a).

Clogging of BRCs can be caused by a combination of mechanical, biological, and chemical processes, which can reduce the overall hydraulic conductivity of the cell (Le Coustumer et al., 2012; Langergraber et al., 2003). Hsieh et al. (2007) conducted column studies and discovered that placing a medium with a higher hydraulic conductivity in the upper profile would prevent a capillary barrier from forming. Studies conducted by Langergraber et al. (2003), Schuh (1990), and Hatt et al. (2007) found that clogging of bioretention media occurred in the top 0.1 m (4 in). Lindsey et al. (1992) and Le Coustumer et al. (2009) reported that after 2 years of operation, between 40 and 60% of previously installed bioretention systems were not functioning as designed. A majority of the malfunctions were due to negative changes in the hydraulic conductivity (Le Coustumer et al., 2012, 2009; Lindsey et al., 1992).

BRCs, in particular, are highly susceptible to construction and maintenance complications, specifically clogging of fine particles, compared to other LID practices (Brown and Hunt, 2012; Bean et al., 2007; Asleson et al., 2009; Fassman and Blackbourn, 2010; Brown and Hunt, 2011a).

Bioretention studies conducted by Brown and Hunt (2012) revealed that when the top 7.5 cm (3 in) of fill media was removed from two different BRCs, the surface storage volume increased by 90%, and the overflow volume decreased from 35-37% and 11-12%, respectively (Liu et al., 2014a; Brown and Hunt, 2012). This result demonstrated that restorative maintenance directly correlates to BRC performance, especially within the top media layer, where clogging occurred most frequently (Liu et al., 2014a; Brown and Hunt, 2012).

2.3.4 Bioretention Cell Design Challenges Summary

Media depth, media mix, and cell size are important components of BRCs that allow them to operate as designed. If one of the components is not designed correctly, it could impact the overall cell performance. Table 2.1 provides details regarding the component and its importance within the literature.

Table 2.1: Bioretention cell components and challenges.

Component	Importance	Literature	Challenges
Media depth	Runoff volume reduction	Brown and Hunt (2008)	Ponding depth Decreased pollutant removal
Media mix	Filtration capacity Pollutant removal	Liu et al. (2014a)	Fine sediment clogging
BRC size	Ponding depth	Brown and Hunt (2011a)	Overflow

For the purposes of this research, the media mix component will be further analyzed and fine sediment clogging will be the focus.

2.4 Column Studies

To further understand the effects that suspended solids have on BRCs, researchers conducted column studies using BRC media with synthetic stormwater runoff. Column studies can be effective small-scale laboratory techniques that eliminate most variables in large-scale

fieldwork yet still yield reproducible results. Hsieh and Davis (2005b) conducted column studies using bioretention media and demonstrated a significant removal of total suspended solids (Hsieh and Davis, 2005b). Li and Davis (2008a) conducted column studies to determine whether bioretention media are limited by the clogging of suspended solids, the depth of particulate movement, and to assess media replacement as a means to maintain BRC facilities (Li and Davis, 2008a). Their studies concluded that the fine grain component of BRC media would clog, limiting the lifespan of the BRC (Li and Davis, 2008a). Specifically, the clay-sized components dominate the clogging potential compared to sand and silt. Additionally, particle deposition will limit the cell's ability to filter out pollutants; surface media replacement could be an effective maintenance requirement (Li and Davis, 2008a). However, column studies lack the dimensions to properly simulate water flow and sediment load in field scale BRC studies.

2.5 Maintenance Strategies

Surface layer replacement is a maintenance method that removes pollutants and clogged areas with a buildup of fine sediments. Langergraber et al. (2003), Schuh (1990), and Hatt et al. (2007) conducted studies on bioretention media and concluded that clogging of the media from fine sediments occurred in the top 0.1 m (4 in) (Langergraber et al., 2003; Schuh, 1990; Hatt et al., 2007). Liu et al. (2014a) and Brown and Hunt (2012) conducted studies on bioretention media and once the top 7.5 cm (3 in) of media was removed, the surface storage volume increased by 90% (Liu et al., 2014a; Brown and Hunt, 2012). Combined, these studies confirmed the current maintenance strategy suggesting removal of the surface media layer.

2.6 Infiltration

Infiltration is the process of which water flows into the soil, which can occur uniformly across the entire surface, across sections of the surface in a non-uniform manner, or can enter

upwards from a source below (Hillel, 2004). However, infiltration generally refers to water moving downward from the soil surface, known as vertical infiltration (Jury and Horton, 2004). When water moves through the surface, it gets absorbed into consecutively deeper levels of the soil profile (Hillel, 2004). During vertical infiltration, the soil becomes wetter with time, and water at the front line of the wetting pattern remains ahead of the matric potential gradient influence and gravity as it advances into drier soil regions (Jury and Horton, 2004). In this case, the gravitational force is overpowered by the matric potential gradient, allowing water to enter the soil (Jury and Horton, 2004).

Vertical infiltration in unsaturated soils occurs under the combination of the suction effect (sorptivity) and gravity effect (conductivity) (Hillel, 2004). As the wet soil increases (i.e., water moving downward into the profile), the suction gradient decreases as it spans over a larger and larger area (Hillel, 2004). The suction gradient eventually disappears, resulting in water movement solely due to the gravity effect (Hillel, 2004). Due to the unsaturated nature of the soil, saturation will never be reached unless all entrained air is evacuated from the soil (Hillel, 2004). Vertical flow can be described in Darcy's equation, shown in Equation 2.1,

$$q = -K\frac{dH}{dz} = -K\Big[\frac{d(H_p - z)}{dz}\Big] \tag{2.1}$$

where q is flux, K is hydraulic conductivity, H is total hydraulic head (sum of H_p and z), H_p is pressure head, and z is gravity head (Hillel, 2004).

Equation 2.1 can be combined with the continuity equation to give a flow equation shown in Equation 2.2,

$$\frac{\partial\theta}{\partial t} = \frac{\partial}{\partial z}\Big(K\frac{\partial H}{\partial z}\Big) = -\frac{\partial}{\partial z}\Big(K\frac{\partial\psi}{\partial z}\Big) - \frac{\partial K}{\partial z} \tag{2.2}$$

where θ is volumetric water content and ψ is suction head (Hillel, 2004). If ψ and θ are related, the left side of Equation 2.2 can be transformed, as shown in Equation 2.3.

$$C\frac{\partial\psi}{\partial t} = \frac{\partial}{\partial z}\Big(K\frac{\partial\psi}{\partial z}\Big) + \frac{\partial K}{\partial z} \tag{2.3}$$

where C is the specific or differential water capacity (change in water content in a unit volume of soil per unit change in matric potential) (Hillel, 2004). Equations 2.2 and 2.3 are forms of the Richards equation, which was the first attempt in combining Darcy's equation with the continuity equation (Hillel, 2004; Richards, 1931).

Equations 2.2 and 2.3 both contain two terms on the right-hand side. The first term relates to the suction effect, sorptivity, and the second term relates to the gravity effect, conductivity (Hillel, 2004). The antecedent moisture conditions of the soil determine which term overpowers the other (Hillel, 2004). In a dry soil, the suction effect, sorptivity, overpowers gravity, conductivity; however, in a wet soil, the suction effect, sorptivity, is overpowered by gravity (Hillel, 2004).

The volume flux of water flowing into the profile per unit of soil surface area affects vegetation, particularly the rooting zone (Hillel, 2004). Additionally, the rate at which water enters the soil affects overland flow and the potential for soil erosion (Hillel, 2004). Knowledge of infiltration patterns is crucial for soil, water, and land management, especially when pertaining to a small-scale, specialized microcosm that is a BRC.

Infiltrability refers to the infiltration flux when water at atmospheric pressure is freely available at the soil surface (Hillel, 2004, 1971). When the rate of water entering at the surface is smaller than the infiltrability of the soil, water infiltrates as fast as it arrives and is considered flux controlled or supply controlled (Hillel, 2004). When the surface entry rate exceeds the infiltrability of the soil, the process is then considered to be soil controlled, either on the surface, surface controlled, or within the profile, profile controlled (Hillel, 2004). Infiltrability at the soil surface, when dry, is high, and decreases until it reaches a steady-state or constant rate (Hillel, 2004). Decreasing infiltrability results from decreases in the matric suction gradient (Hillel, 2004). Additionally, the movement of small particles, weakening soil structure, shrink-swell clays, and entrapped air can decrease infiltrability (Hillel, 2004).

2.6.1 Types of Infiltrometers

An infiltrometer measures infiltration rate. There are different types of infiltrometers, including single-ring, double-ring, tension, and pressure infiltrometers.

Single- and Double-Ring Infiltrometers

Single- and double-ring infiltrometers consist of an open-ended cylinder containing water placed on the surface of the soil (Burgy and Luthin, 1956). The double-ring infiltrometer consists of two concentric cylinders with water ponded to the same height. The rate of water entry is determined by the amount of lateral movement between the two cylinders; the outer cylinder reduces lateral movement from the inner cylinder in order to produce a more accurate infiltration rate (Burgy and Luthin, 1956). Both the single- and double-ring infiltrometers can be used to measure cumulative infiltration, infiltration rate, and field-saturated hydraulic conductivity (Reynolds et al., 2002). The single-ring infiltrometer has a cylinder diameter of 10 - 50 cm and length of 10 - 20 cm, whereas the double-ring infiltrometer has a cylinder diameter of 10 - 20 cm, length of 10 - 20 cm with an additional cylinder diameter of 50 cm (Reynolds et al., 2002). The cylinders are inserted to a soil depth of 3 - 10 cm, kept as straight as possible, and ponded with a constant depth of water until quasi-steady flow (equilibrium time) is achieved by monitoring the discharge out of the cylinder (Reynolds et al., 2002). Equilibrium is reached in 10 - 60 min for small cylinders with coarse-textured materials and in several hours to several days for larger cylinders containing fine-textured material (Reynolds et al., 2002; Scotter et al., 1982).

Equation 2.4 represents quasi-steady state infiltration through a ring infiltrometer (Reynolds and Elrick, 1990; Reynolds et al., 2002),

$$\frac{q_s}{K_{fs}} = \frac{Q}{\pi a^2 K_{fs}} = \frac{H}{C_1 d + C_2 a} + \frac{1}{[\alpha(C_1 d + C_2 a)]} + 1 \tag{2.4}$$

where q_s is quasi-steady state infiltration, K_{fs} is field saturated hydraulic conductivity, Q is quasi-steady flow rate, a is ring radius, H is steady depth of ponded water in the ring, d is ring insertion depth, $C_1 = 0.316\pi$ and $C_2 = 0.184\pi$ are dimensionless quasi-empirical constants, and α is the soil macroscopic capillary length parameter (Reynolds and Elrick, 1990; Raats, 1976; Youngs et al., 1995; Philip, 1983; Jury and Horton, 2004).

The simplest method to determine field-saturated hydraulic conductivity overlooked the first two terms on the right side of Equation 2.4, producing Equation 2.5 (Reynolds and Elrick, 1990; Reynolds et al., 2002).

$$K_{fs} = q_s \tag{2.5}$$

However, Equation 2.5 overestimates K_{fs} by various degrees depending on the magnitudes of the neglected terms in Equation 2.4.

Tension Infiltrometers

A tension infiltrometer (or disk permeameter) measures saturated and near-saturated infiltration rates with a constant negative pressure head at the surface (Reynolds et al., 2002, 2000; Perroux and White, 1988; Reynolds and Elrick, 1991; Ankeny et al., 1991; Everts and Kanwar, 1993; Mohanty et al., 1998). A porous plate at the base of the infiltrometer allows suction to be maintained on the inside of the tube, and can be adjusted if needed (Reynolds et al., 2002). An example of a tension infiltrometer is the mini-disk infiltrometer (Decagon Devices, Inc., Pullman, WA, USA). The water within the mini-disk infiltrometer is controlled by adjustable suction (-7 - -0.5 cm); therefore, infiltration is controlled by negative suction, and macropores are eliminated (Decagon Devices, 2016). The hydraulic conductivity measured with the mini-disk infiltrometer is that of the soil matrix (less spatially variable), and not of the macropores (more spatially variable) (Decagon Devices, 2016).

Within the mini-disk infiltrometer, the bubble chamber is filled three-quarters of the way with water, the porous disk is placed at the bottom of the chamber, and the suction rate is chosen before it is placed on a soil surface (Decagon Devices, 2016).

Zhang (1997) introduced a method to calculate hydraulic conductivity from tension infiltrometer data (Equation 2.6),

$$I = C_1 t + C_2 \sqrt{t} \tag{2.6}$$

where C_1 is related to hydraulic conductivity, C_2 is soil sorptivity, and t is time. Hydraulic conductivity (k) of the soil is then computed in Equation 2.7,

$$K = \frac{C_1}{A} \tag{2.7}$$

where K is hydraulic conductivity, C_1 is the slope of the curve of cumulative infiltration versus square root of time, and A is computed from specific van Genuchten soil parameters: disk radius and suction rate (Equations 2.8 and 2.9, respectively) (Zhang, 1997; Decagon Devices, 2016).

$$A = \frac{11.65(n^{0.1} - 1)exp[2.92(n - 1.9)\alpha h_0]}{(\alpha r_o)^{0.91}} \tag{2.8}$$

$$A = \frac{11.65(n^{0.1} - 1)exp[7.5(n - 1.9)\alpha h_0]}{(\alpha r_o)^{0.91}} \tag{2.9}$$

where n and a are van Genuchten parameters, r_o is the disk radius, and h_o is the disk surface suction (Zhang, 1997; Decagon Devices, 2016). Carsel and Parrish (1988) determined the van Genuchten parameters (n and a in Equations 2.8 and 2.9) for 12 soil textural classes (Zhang, 1997; Decagon Devices, 2016; Carsel and Parrish, 1988).

Pressure Infiltrometers

The pressure infiltrometer is used to measure field saturated hydraulic conductivity (K_fs) (Reynolds et al., 2002). A 10 - 20 cm diameter ring is inserted 3 - 10 cm into the ground, similar to the single-ring infiltrometer (see Section 2.6.1) (Reynolds et al., 2002). A constant head reservoir is attached to the cap, located on top of the ring; the Mariotte reservoir system is commonly used and can be commercially purchased or individually constructed (Reynolds et al., 2002). The height of water in the column determines the pressure head of water acting on the infiltration surface; the infiltrometer operates properly when air bubbles rise into the reservoir from the base of the column (Reynolds et al., 2002). Water flow rate was measured by monitoring the discharge out of the reservoir, and when it becomes constant, has reached quasi-steady state (Reynolds et al., 2002). For highly permeable media, quasi-steady state was reached in approximately 5 - 60 minutes and can take hours to days for low permeability soils (Reynolds et al., 2002).

Single-head, two-head or multiple-head pressure infiltrometer measurements can be utilized depending on the situation. The simplest analysis for pressure infiltrometer measurements is the single-head pressure analysis, as it only requires one ponded head of water (Reynolds et al., 2002). However, the single-head analysis provides less accuracy then the two-head or multiple-head method (Reynolds et al., 2002). Equation 2.10 describes how K_{fs} and ϕ_m are determined using a pressure infiltrometer method.

$$K_{fs} = \frac{\alpha \cdot GAR_1}{[a(\alpha H_1 + 1) + G\alpha\pi a^2]} \tag{2.10}$$

where K_{fs} is field saturated hydraulic conductivity, α is the soil macroscopic capillary length parameter, G is a dimensionless shape factor (Equation 2.12), A is the cross sectional area of the pressure infiltrometer reservoir, R_1 is the quasi steady rate of fall of the water level in the pressure infiltrometer reservoir, a is the inner reservoir radius, and H_1 is the steady

pressure head of water on the infiltration surface (Reynolds et al., 2002; Reynolds and Elrick, 1990; Raats, 1976; Youngs et al., 1995; Philip, 1983; Jury and Horton, 2004).

Table 2.2: Soil texture-structure categories for estimation of α (Reynolds et al., 2002; Elrick et al., 1989)

Soil Texture and Structure Category	α (cm^{-1})
Compacted, structureless, clayey or silty materials such as landfill caps and liners, lacustrine or marine sediments	0.01
Most structured soils from clays through loams; also includes unstructured medium and fine sands. Most applicable for agricultural soils	0.04
Coarse and gravelly sands; may also include highly structured or aggregated soils, as well as soils with numerous cracks and/or macropores	0.12
Soils both fine textured (clayey and silty) and unstructured; can include fine sands	0.36

$$\phi_m = \frac{GAR_1}{[a(\alpha H_1 + 1) + G\alpha\pi a^2]} \tag{2.11}$$

Equation 2.11 determines the matrix flux potential (ϕ_m) with an equation similar to Equation 2.10 where G is a dimensionless shape factor (Equation 2.12), A is the cross sectional area of the pressure infiltrometer reservoir, R_1 is the quasi steady rate of fall of the water level in the pressure infiltrometer reservoir, α is the soil macroscopic capillary length parameter, a is the inner reservoir radius, and H_1 is the steady pressure head of water on the infiltration surface (Reynolds et al., 2002; Reynolds and Elrick, 1990; Raats, 1976; Youngs et al., 1995; Philip, 1983; Jury and Horton, 2004).

$$G = 0.316\left(\frac{d}{a}\right) + 0.184 \tag{2.12}$$

Equation 2.12 determines the dimensionless shape factor needed for Equations 2.10 and 2.11, where G is a dimensionless shape factor, d is the depth of ring insertion into the soil, and a is the inner reservoir radius (Reynolds et al., 2002; Reynolds and Elrick, 1990; Raats, 1976; Youngs et al., 1995; Philip, 1983; Jury and Horton, 2004). Equation 2.12 was developed for 5 cm $\leq a \leq$ 10 cm, 3 cm $\leq d \leq$ 5 cm, and 5 cm $\leq H_1 \leq$ 25 cm (Reynolds et al., 2002; Reynolds and Elrick, 1990). However, studies conducted by Youngs et al. (1995) indicated there would be no significant reduction in accuracy if numbers were used outside of the given range.

$$S = [\gamma(\theta_{fs} - \theta_i)\phi_m]^{1/2} \tag{2.13}$$

Equation 2.13 determines sorptivity from pressure infiltrometer data, where S is sorptivity, γ is a dimensionless constant pertaining to wetting front shape ($\gamma \approx 1.818$), θ_{fs} is field saturated volumetric water content, θ_i is the antecedent volumetric water content, and ϕ_m is the matrix flux potential (Reynolds et al., 2002; White and Sully, 1987).

2.6.2 Infiltration Models

There are many ways to quantify infiltration rates in different environmental conditions. Well-known infiltration models include the Horton Equation, Green-Ampt, and Philips Equation.

Horton Equation

Horton influenced the study of infiltration with an equation that combined infiltration in different soils with the physical concept (Equation 2.14).

$$i = i_f + (i_0 - i_f)exp(-\beta t) \tag{2.14}$$

where i_f is the final infiltration rate, i_0 is the initial infiltration rate, and β is a soil parameter describing the rate of soil decrease (Horton, 1933, 1939; Jury and Horton, 2004). Cumulative infiltration is calculated from the integral of Equation 2.14 (Equation 2.15),

$$I = i_f t + \frac{i_0 - i_f}{\beta}[1 - exp(-\beta t)] \tag{2.15}$$

where I is cumulative infiltration, i_f is the final infiltration rate, i_0 is the initial infiltration rate, and β is a soil parameter describing the rate of soil decrease (Horton, 1933, 1939; Jury and Horton, 2004).

Horton (1940) determined that decreases in infiltration rates were caused by swelling of soil colloids that slowly sealed the surface, as well as overall compaction of the bare surface soil by means of precipitation.

Green-Ampt

Green and Ampt (1911) derived an infiltration theory incorporating simplified assumptions of the wetting process in dry, coarse-textured soils (Green and Ampt, 1911; Jury and Horton, 2004; Hillel, 2004). The assumptions include the existence of a sharp wetting front characterized by constant matric suction moving continuously downward regardless of time and position (Green and Ampt, 1911; Jury and Horton, 2004; Hillel, 2004). Equation 2.16 incorporates Darcy's law to calculate vertical infiltration,

$$-i = -K_0 \frac{h_F - L - h_0}{-L - 0} = -\frac{K_0}{L}(\Delta h + L) \tag{2.16}$$

where K_0 is hydraulic conductivity, h_F is matric potential, L is wet region thickness, h_0 is constant matric potential head (equal to h_F), and $\Delta H = h_0 - H_F$ (Green and Ampt, 1911; Jury and Horton, 2004; Hillel, 2004).

Philips Equation

The Richards equation (Section 2.6, Equations 2.2 and 2.3) encountered solving difficulties due to its non-linear nature (Jury and Horton, 2004). J.R. Philips developed an infiltration solving technique (both horizontal and vertical infiltration) for infinitely deep homogenous mediums at uniform initial water content with a boundary at a higher water content (Philip, 1957a,b,c,d,e,f).

The Richards equation was modified to develop the horizontal infiltration equation (Equation 2.17),

$$i = \frac{1}{2} S t^{-\frac{1}{2}} \tag{2.17}$$

where i is the infiltration rate, S is the sorptivity, and t is time (Jury and Horton, 2004; Philip, 1957a,b,c,d,e,f). Cumulative horizontal infiltration is shown by Equation 2.18,

$$I = S t^{\frac{1}{2}} \tag{2.18}$$

where I is cumulative infiltration, S is sorptivity, and t is time (Jury and Horton, 2004; Philip, 1957a,b,c,d,e,f). The vertical infiltration equation contains two expressions for the short and long times post infiltration commencement, with the short time expressed as an infinite series of powers,

$$I = S t^{\frac{1}{2}} + A_1 t + A_2 t^{\frac{3}{2}} + ... \tag{2.19}$$

where I is cumulative infiltration, S is sorptivity, t is time, and $A_1, A_2, ...$ are water content dependent constants (Jury and Horton, 2004; Philip, 1957a,b,c,d,e,f). Approximating the first two terms in Equation 2.19 gives Equation 2.20,

$$I = S t^{\frac{1}{2}} + At \tag{2.20}$$

where I is cumulative infiltration, S is sorptivity, t is time, and A and S are constant under a uniform initial matric potential (Jury and Horton, 2004; Philip, 1957a,b,c,d,e,f).

2.7 Field Use of Infiltration

Field infiltration data commonly utilizes the single-ring infiltrometer due to its ease of operation. Le Coustumer et al. (2009) conducted hydraulic evaluations on 37 different BRCs throughout Australia using a single-ring infiltrometer measured at both deep and shallow depths to determine hydraulic conductivity (Le Coustumer et al., 2009). The method does not require much additional field equipment and can be mobilized easily when working on multiple field sites.

2.8 Alternative Water Flow Experimentation

2.8.1 Dye Tracer Usage

In addition to using infiltration measurements as a means of gathering quantitative soils data, dyes can be used as tracers to qualitatively document flow patterns and pathways throughout soil media. Dyes are important tracers that investigate subsurface water movement; they can provide clues about changes in the hydrologic cycle as well as flow and transport processes (Flury and Wai, 2003). Industrial uses of tracers include analyzing agrochemicals applied to the soil surface, toxic spills, and contaminant leaching (Flury and Wai, 2003).

Preferential Flow

Even if a soil receives the same amount of water at the same rate, there are minor differences in structural voids, biological channels, and local obstacles that cause water to funnel into narrow plumes that can carry water at higher velocities at different points of the soil matrix (Jury and Horton, 2004; Kung, 1990a). In some cases, preferential flow

paths constitute dominant flow patterns (Kung, 1990a). Preferential flow can be observed as macropore flow through soil with a structural void, fingering flow ("funneled" flow), consisting of uniform flow splitting into fingers due to instability associated with soil air compression or at a horizontal boundary where fine soil overlies a course sand layer (Kung, 1990b).

Chapter 3

Materials and Methods

3.1 Experimental Setup

To meet the objectives and tasks listed in Section 1.5, two experiments were conducted on a rectangular, acrylic flow cell. The cell contained inflow and outflow tubes and was packed with BRC media. The first set of experiments, titled clogging experiments, were conducted on the cell to determine when surface hydraulic conductivity decreased and water flow severely impeded due to fine particle clogging and accumulation. The second set of experiments, titled phosphorus flow experiments, evaluated phosphorus retention in synthetic stormwater under three clogging conditions: a non-clogged condition (Trial 1), semi-clogged condition (Trial 2), and clogged condition (Trial 3). Figure 3.1 depicts the steps performed throughout the entirety of the research project, whereas Figure 3.2 and 3.3 differentiate the clogging experiments and phosphorus flow experiments.

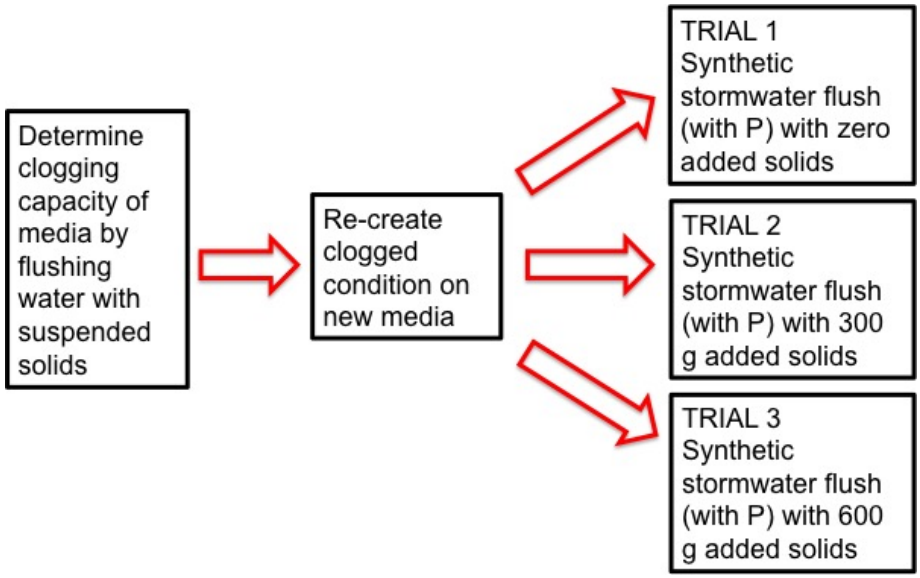

Figure 3.1: Experimental setup for clogging and phosphorus flow experiments.

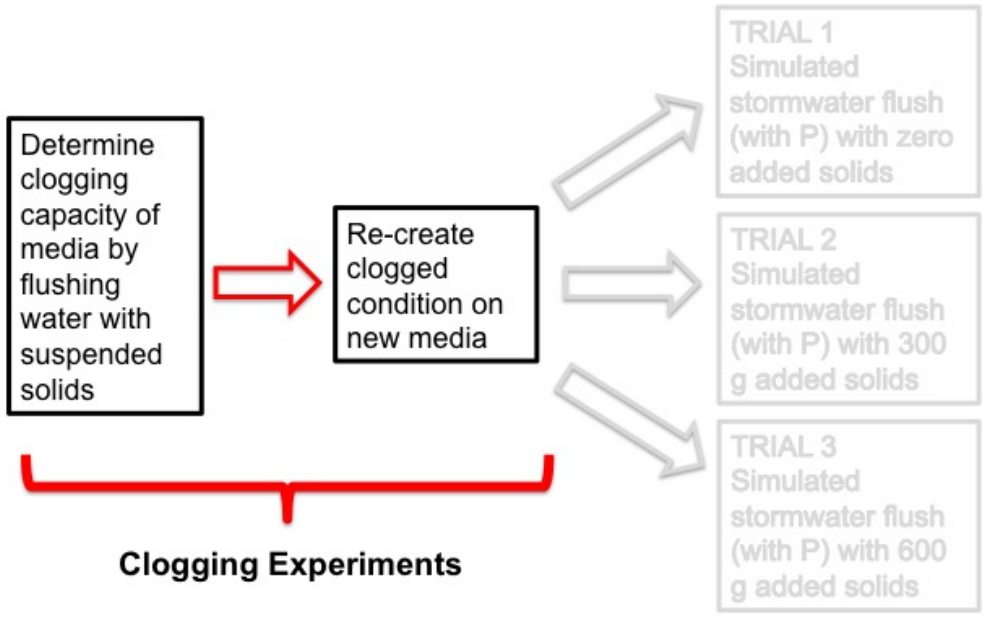

Figure 3.2: Experimental setup focused on clogging experiments.

Table 3.1 describes the procedure used for the clogging experiments. Ground silica (SilCoSil 106, US Silica, Frederick, MD, USA) was used in the suspended solids mixture pumped onto the BRC media surface. Silica concentration was increased due to time constraints. WCP and surface infiltration measurements are further explained in Section 3.3.3. Additional materials and methods for the clogging experiments can be found in Section 3.3.

Table 3.1: Procedure for clogging experiments.

Step	Description
1	Media added to the cell
2	WCP measurement
3	Surface infiltration measurement
4	Suspended solids pumped onto media at 2 g/8 L water
5	WCP measurement
6	Surface infiltration measurement
7	Steps 4 - 6 repeated at 2, 25, 50, and 100 g/8 L water, respectively, until semi-clogged and clogged conditions determined for phosphorus flow experiments

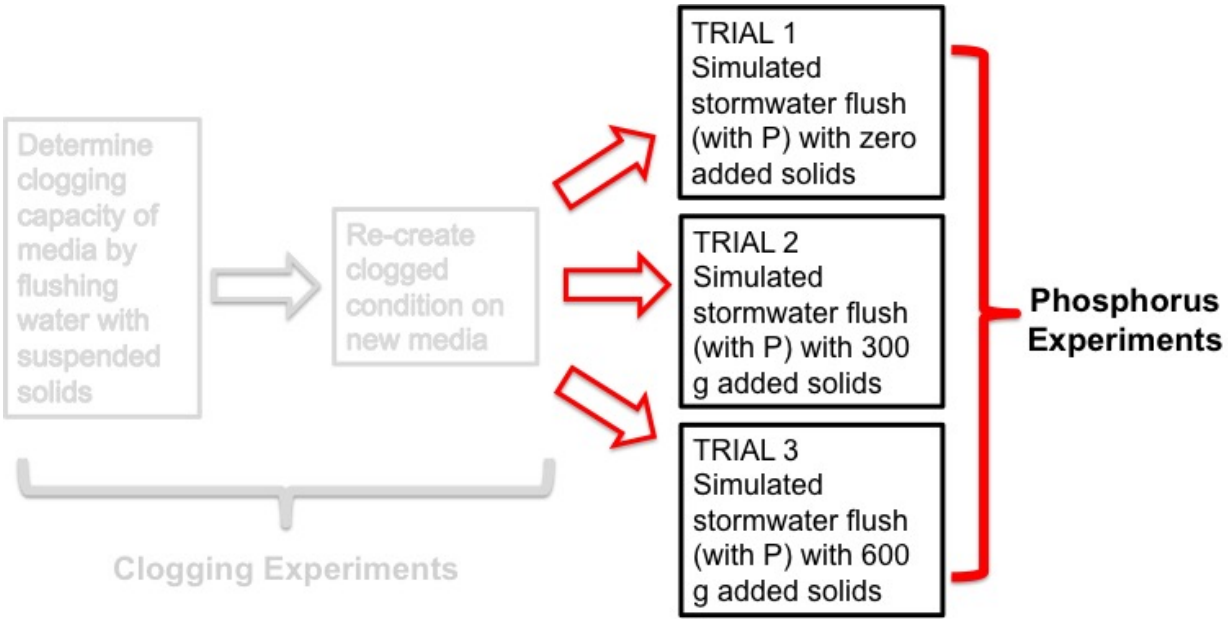

Figure 3.3: Experimental setup focused on phosphorus flow experiments.

Table 3.2 describes the procedure used for the three trial conditions of the phosphorus flow experiments. WCP and surface infiltration measurements were taken (similar to the clogging experiments), but surface solids (ground silica) were placed in specific amounts as opposed to suspended in water and flushed through the media. Synthetic stormwater containing phosphorus and iron oxides was flushed through the system, blue dye was flushed through the system to document preferential flow patterns (if applicable), and the media, ground silica layer, and effluent water was sampled and analyzed for phosphorus concentration.

Table 3.2: Procedure for phosphorus flow experiment trials.

Step	Trial(s)	Description
1	1, 2, 3	Media added to cell
2	1, 2, 3	WCP measurement (replicated 3x)
3	1, 2, 3	Surface infiltration measurement (replicated 3x)
4	2, 3	300/600 g surface solids placed on media
5	2, 3	Water flush
6	2, 3	WCP measurement (replicated 3x)
7	2, 3	Surface infiltration measurement (replicated 3x)
8	1, 2, 3	Synthetic stormwater flush
9	1, 2, 3	Blue dye flush/time lapse video
10	1, 2, 3	Media, silica, and effluent sampling

3.2 Bioretention Media Mix

A media mix of sand, mulch, and fine material were used in the clogging and phosphorus flow experiments. Based on data from Hsieh et al. (2007), Brown and Hunt (2008), and Davis (2008), a BRC media mix containing 85% sand, 10% fines, and 5% mulch was prepared (Hsieh et al., 2007; Brown and Hunt, 2008; Davis, 2008). The fine fraction was obtained from a City of Auburn stockpile of a silt/clay soil, the coarse sand obtained from the Auburn University Turfgrass Unit, and the mulch (pine bark mulch) was purchased from a local garden center.

3.2.1 Particle Size Analysis

Particle size analysis was performed on the silt/clay material obtained from a City of Auburn stockpile to determine particle size composition. A modified hydrometer method adapted from Day (1965) and ASTM (1985) was used (Klute, 1986; Day, 1965; ASTM, 1985). A standard hydrometer with a Bouyoucos scale (g/L), sodium-hexametaphosphate (HMP) solution, an electric stirrer, metal dispersing cups, rubber stoppers, sedimentation cylinders, 7.6 cm (3 in) sieve set, weighing jars, and an electric oven were utilized (Klute, 1986).

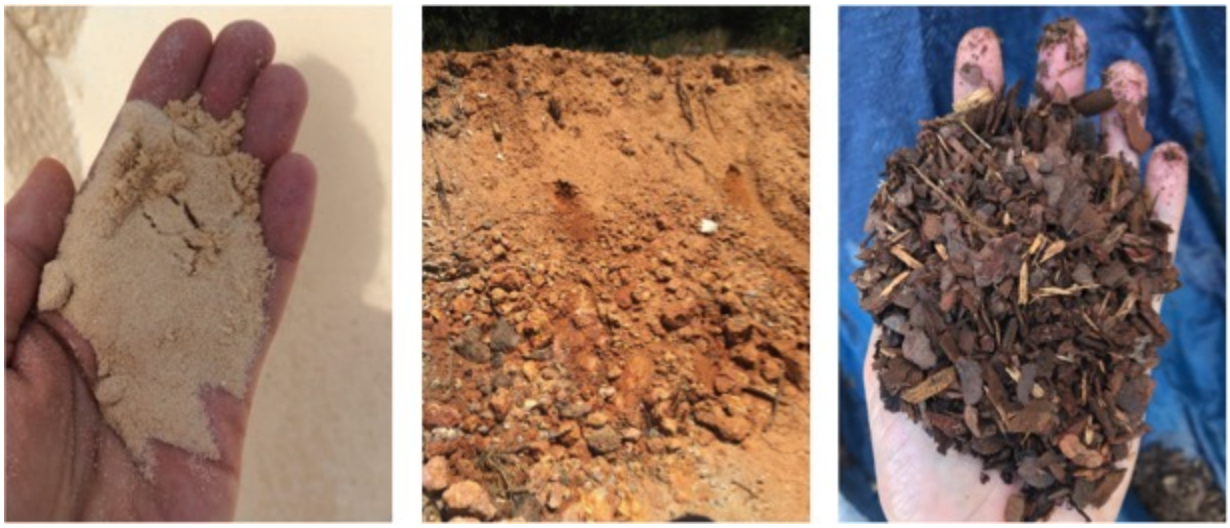

Figure 3.4: Components of the BRC media mix containing 85% sand, 10% fines, and 5% mulch. Left: sand; middle: fine fraction; right: pine bark mulch.

Three 1,000 mL cylinders were used, the blank cylinder with 100 mL HMP solution (5 g/L) and water, and samples A1 and A2 (replicate) containing 40 g of soil, 250 mL of deionized (DI) water, and 100 mL of HMP solution (5 g/L) (Table 3.3). Samples A1 and A2 soaked in solution overnight, the mixture was agitated in metal dispersion cups on the electric mixer for 5 minutes, transferred to a sedimentation cylinder, and brought to volume (Klute, 1986).

Table 3.3: Sample IDs and sample contents used in particle size analysis.

Sample ID	**Sample Contents**
Blank	100 mL HMP 900 mL DI water
A1	40 g soil 100 mL HMP 250 mL DI water
A2 (replicate)	40 g soil 100 mL HMP 250 mL DI water

The samples were mixed with a plunger and hydrometer and temperature readings were recorded (Klute, 1986). After 24 hours, the samples were passed through a 270-mesh (53-micrometers) sieve and the remaining material oven-dried at 105°C. The oven dried material passed through a set of sieves (1000, 500, 250, 106, and 53-micrometers), shaken for 3 minutes, and the remaining sand, silt, and clay fractions were weighed and recorded (Klute, 1986). The soil texture analysis reported 64% sand, 18% silt, and 16% clay, considered a sandy loam (Figure 3.5).

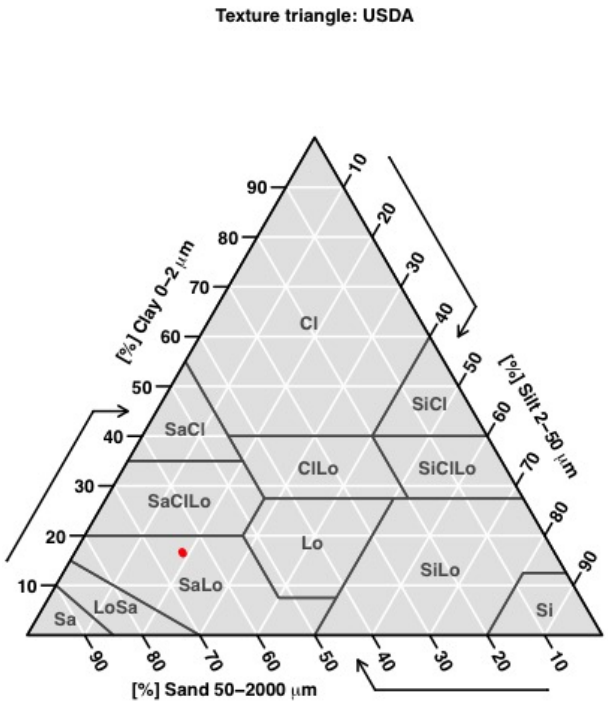

Figure 3.5: Results of the particle size analysis reported fine fraction soil texture as a sandy loam with 64% sand, 18% silt, and 16% clay.

3.2.2 Surface Silica Bulk Density

The ground silica used as suspended solids in the clogging experiments and placed on the surface of Trials 2 and 3 of the phosphorus flow experiments was measured for bulk density (g/cm^3), based on a method from Jury and Horton (2004). A metal cylinder with a volume of 127 cm^3 was placed in a crucible and filled to volume with ground silica. The cylinder and crucible were weighed previous to the addition of silica. The silica was oven dried at 105^o for 24 hours. The crucible, cylinder, and silica were weighed, and the crucible and cylinder masses subtracted from the total weight. Equation 3.1 determined bulk density of the silica.

$$\rho_b = \frac{m_s}{V} = \frac{1.2 \text{ g}}{cm^3} \tag{3.1}$$

3.2.3 Elemental Analysis Sample Preparation

The media and silica samples collected from the phosphorus flow trials were prepped for inductively coupled plasma (ICP) spectroscopy (Spectro Ciros CCD, side on plasma, SPECTRO Analytical Instruments Inc., Kleve, Germany) analysis by a modified USEPA Method 3051A Microwave Assisted Digestion of Sediments, Sludges, Soils, and Oils (Step 10, Table 3.2) (USEPA, 2007). This method used nitric acid (NNO_3) based on USEPA Method 200.2 and 3050 (USEPA, 2007). A microwave, filter paper, filter funnel, and analytical balance were utilized for the method. The media samples were ground in a mortar and pestle before each sample was weighed to 0.5 g. Grinding samples produce variability as volatilization of particles attached to larger pieces of mulch in the BRC mix can occur, which can misrepresent initial media constituents (85% sand, 10% fines, and 5% mulch) and produce high variability in background phosphorus levels and phosphorus retention throughout the media (USEPA, 2007).

Weighed samples were placed in digestion containers and 10 mL nitric acid was added to each under a fume hood, then sealed and placed in the microwave for digestion. The

samples cooled for 5 minutes, the contents transferred to another bottle and centrifuged at 2,000-3,000 rpm for 10 minutes. The remaining samples were filtered and the liquid diluted and prepped for elemental analysis (USEPA, 2007). Media, silica, and water samples were analyzed for phosphorus levels.

3.3 Clogging Experiments

The clogging experiments further explored the effects that solids accumulation had on infiltration and hydraulic conductivity. The media was flushed with a mixture containing ground silica, simulating suspended solids found in stormwater runoff.

3.3.1 Flow Cell Materials and Setup

The flow cell was built with acrylic sheets with dimensions 58 x 6 x 29 cm (22.8 x 2.4 x 11.4 in). Acrylic (Plexiglass) is less likely to scratch compared to polycarbonates and glass (Lewis and Sjostrom, 2010). Four outflow points were located at the bottom of the flow cell. Clear, interconnected drainage tubes allowed the effluent to drain out of the system. Figure 3.6 shows the flow cell and the drainage direction from the four outflow ports. Darcy's Law was used to describe water flow throughout the cell (Equation 3.2) (Jury and Horton, 2004).

$$J_w = -K_s \frac{H_2 - H_1}{z_2 - z_1} \tag{3.2}$$

where J_w is the soil water flux, K_s is saturated hydraulic conductivity across points 1 and 2, H_1 is the hydraulic head at point z_1 and H_2 is the hydraulic head at point z_2.

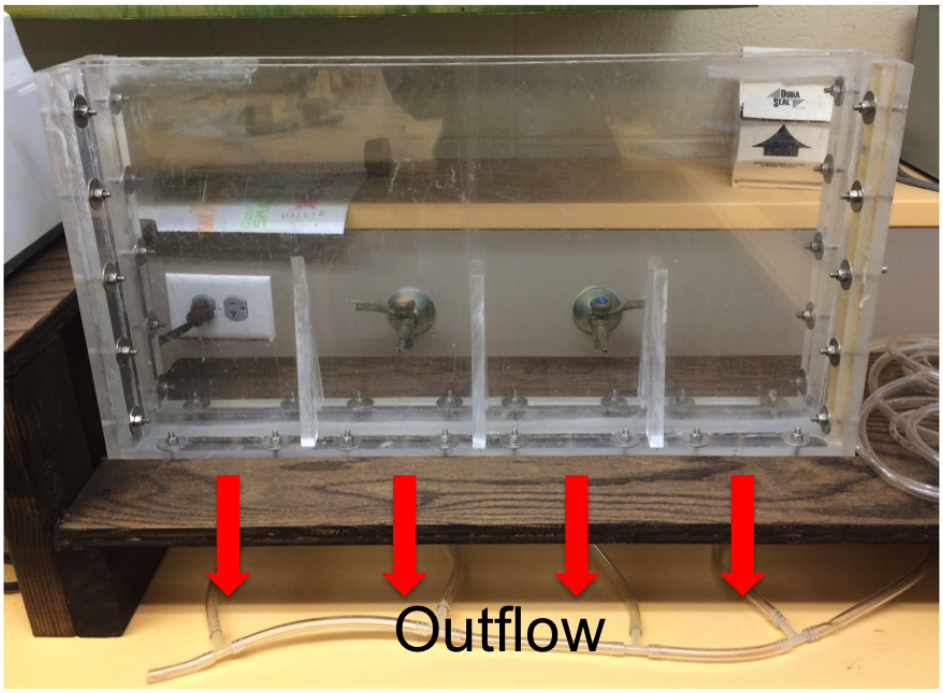

Figure 3.6: Flow cell used in clogging experiments. Drainage direction depicted by red arrows through four outflow ports at the bottom of the cell.

3.3.2 Media Placement and Packing

The flow cell was packed utilizing a modified version of the dry packing method (Lewis and Sjostrom, 2010; Begin et al., 2003; Communar et al., 2004; Ghodrati et al., 1999; Hrapovic et al., 2005). Media lifts of approximately 4 cm (1.6 in) were added one layer at a time and smoothed over to eliminate macropores. Figures 3.7 - 3.10 demonstrate the addition of each media lift.

Figure 3.7: Placement of the first media lift. Each lift was 4 cm (1.6 in) thick. Upon placement, the surface was lightly compacted with a piece of rectangular wood with similar dimensions of the flow cell. The dry packing method was utilized when placing the layers (Lewis and Sjostrom, 2010; Begin et al., 2003; Communar et al., 2004; Ghodrati et al., 1999; Hrapovic et al., 2005).

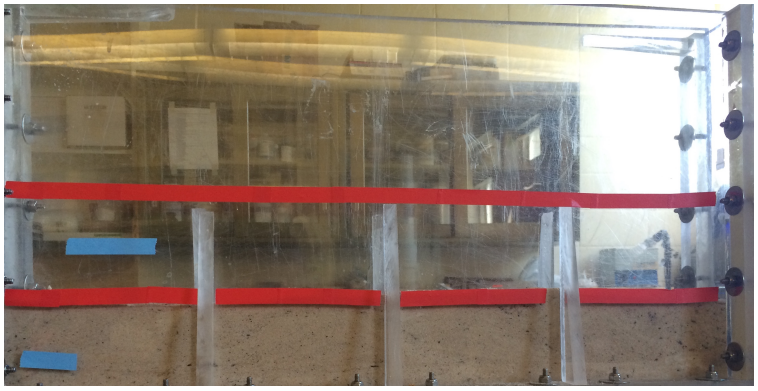

Figure 3.8: Placement of the second media lift. Each lift was 4 cm (1.6 in) thick. Upon placement, the surface was lightly compacted with a piece of rectangular wood with similar dimensions of the flow cell. The dry packing method was utilized when placing the layers (Lewis and Sjostrom, 2010; Begin et al., 2003; Communar et al., 2004; Ghodrati et al., 1999; Hrapovic et al., 2005).

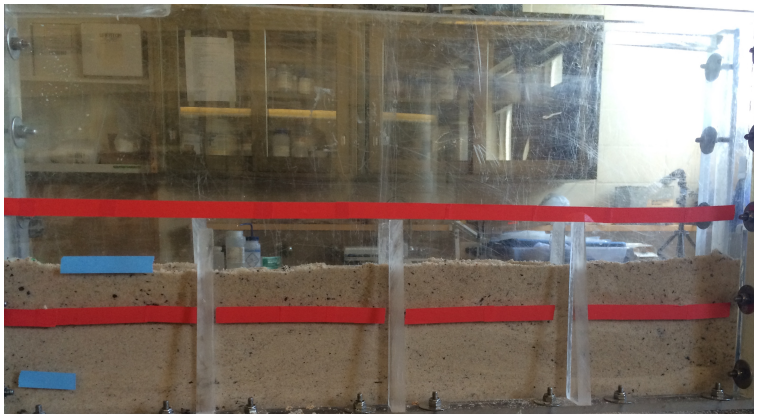

Figure 3.9: Placement of the third media lift. Each lift was 4 cm (1.6 in) thick. Upon placement, the surface was lightly compacted with a piece of rectangular wood with similar dimensions of the flow cell. The dry packing method was utilized when placing the layers (Lewis and Sjostrom, 2010; Begin et al., 2003; Communar et al., 2004; Ghodrati et al., 1999; Hrapovic et al., 2005).

Figure 3.10: Placement of the fourth media lift. Each lift was 4 cm (1.6 in) thick. Upon placement, the surface was lightly compacted with a piece of rectangular wood with similar dimensions of the flow cell. The dry packing method was utilized when placing the layers (Lewis and Sjostrom, 2010; Begin et al., 2003; Communar et al., 2004; Ghodrati et al., 1999; Hrapovic et al., 2005).

3.3.3 Trial Measurements

Two measurements were taken during the clogging experiments: (a) whole cell performance (WCP) and (b) infiltration. The WCP measurement determined the saturated hydraulic conductivity of the media once packed and placed in the cell. The outflow tubes were secured shut and a peristaltic pump gently pushed water through the media from the

bottom to the top, at a constant rate, to ensure no remaining air bubbles were present. This created a saturated condition containing only water in the soil pore spaces, guaranteeing all remaining air and gaseous phase present were expelled from the media (Lewis and Sjostrom, 2010; Casey et al., 2000; Jin et al., 1997; Liu et al., 2008). The water flowing up through the media ponded to a height of 11 cm from the surface. The outflow tube was opened and time was recorded when the water reached the surface of the media.

The saturated hydraulic conductivity from the WCP measurements was determined using Equation 3.3,

$$\frac{L}{t_1} \ln \frac{\beta_0 + L}{\beta_1 + L} = K_s \tag{3.3}$$

where L is the length of the soil column, t_1 is time, β_0 is initial ponded water height at t=0, and β_1 is the ponded water height at t=t_1 (Klute and Dirksen, 1986; Jury and Horton, 2004).

Infiltration was the second measurement taken. A modified pressure infiltrometer was built out of plastic tubing, with a height of 39.5 cm (15.5 in), an outer diameter of 2.5 cm (1 in), and an inner diameter of 1.8 cm (0.7 in) (Section 2.6.1). A circular cut of porous stone with a thickness of 0.5 cm (0.5 in) was glued to the bottom of the tube and wrapped with a thin mesh. A plastic stopper closed off the top of the tubing with a small hole for a glass tube with an inner diameter of 0.3 cm (0.12 in) and outer diameter of 0.4 cm (0.16 in). The tube was filled with 30 cm of water (83 cm^3 of water) and time was recorded as the water level dropped to 0 cm. The flow cell was divided into 4 columns, A, B, C, and D, with Column D below the inflow tube and Column A farthest away from the inflow tube. Surface infiltration measurements were taken in each column, as demonstrated in Figures 3.11 and 3.12.

Figure 3.11: Measurement of surface infiltration rates in the clogging trials using an infiltrometer.

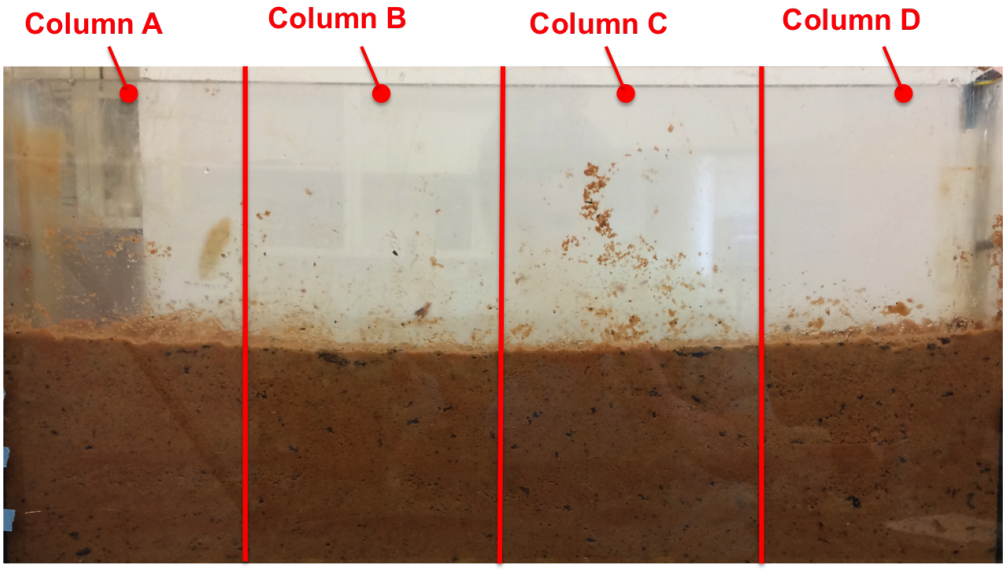

Figure 3.12: Flow cell divided into Columns A, B, C, and D.

3.3.4 Water Flush Trials

Water was flushed through the cell with no additional solids added to ensure proper flow cell set up. WCP and surface infiltration measurements (Columns A, B, C, and D)

were taken after 8 liters of water was flushed through the cell using a peristaltic pump and discharged out of the outflow tubing. The results from the initial water flush trials indicated that flow cell setup (including outflow tubing arrangement and height and placement of media) did not negatively affect water flow.

3.3.5 Solids Flush Trials

Water mixed with suspended solids (ground silica) was flushed through the media to allow solids accumulation to occur and effectively clog the BRC media by decreasing hydraulic conductivity. Rates at which suspended solids were introduced to the BRC media are described in Table 3.4. After each solids flush, a WCP measurement was taken and infiltration rates were measured in Columns A, B, C, and D.

Table 3.4: Flushed solids rates per trial in clogging experiments.

Experiment ID	**Trial #**	**Flushed solids per trial (g solids/8L water)**
1	1 - 5, odd (WCP) 2 - 6, even (Infiltration)	0
2	7 - 71, odd (Infiltration) 8 - 72, even (WCP)	2
3	73 - 77, odd (Infiltration) 74 - 78, even (WCP)	25
4	79 (Infiltration) 80 (WCP)	50
5	81 - 89, odd (Infiltration) 82 - 90, even (WCP)	100

3.4 Phosphorus Flow Experiments

Field-scale BRCs operate under less than optimal conditions when the filtration capacity is compromised due to fine solids accumulation. The mobility of stormwater pollutants through BRC media changes when clogging occurs. Synthetic stormwater containing phosphorus was flushed through three flow cell conditions (clogged, semi-clogged, and non-clogged) to document how mobility was affected.

3.4.1 Flow Cell Materials and Setup

An additional flow cell was built for the phosphorus flow trials, with dimensions of 62.5 x 5 x 32.5 cm (24.6 x 2 x 12.8 in) made of acrylic sheets (one being detachable). Five outflow points were located at the bottom of the cell that connected to clear drainage tubes, allowing water to expel from the cell. Darcy's Law was applied to the new flow cell (Section 3.3.1). Figures 3.13 - 3.15 show the construction of the flow cell.

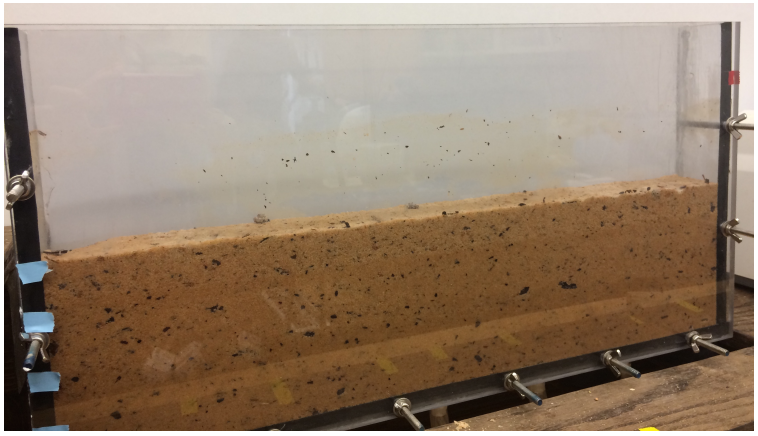

Figure 3.13: Flow cell with detachable side and packed with media. New cell used acrylic sheets with dimensions of 62.5 x 5 x 32.5 cm (24.6 x 2 x 12.8 in) and glued together with epoxy (Gorilla Epoxy, The Gorilla Glue Company, Cincinnati, OH, USA) and sealant (LEXEL Elastic Sealant, Sashco, Inc., Brighton, CO, USA).

Figure 3.14: Construction of flow cell. Detachable side getting glued together and compressed to allow the epoxy to set. Used acrylic sheets with dimensions of 62.5 x 5 x 32.5 cm (24.6 x 2 x 12.8 in) and glued together with epoxy (Gorilla Epoxy, The Gorilla Glue Company, Cincinnati, OH, USA) and sealant (LEXEL Elastic Sealant, Sashco, Inc., Brighton, CO, USA).

Figure 3.15: Construction of flow cell. Detachable side getting glued together and compressed to allow the epoxy to set. Used acrylic sheets with dimensions of 62.5 x 5 x 32.5 cm (24.6 x 2 x 12.8 in) and glued together with epoxy (Gorilla Epoxy, The Gorilla Glue Company, Cincinnati, OH, USA) and sealant (LEXEL Elastic Sealant, Sashco, Inc., Brighton, CO, USA).

3.4.2 Media Placement and Packing

The BRC media was wet-packed based on a modified version of ASTM D 1557 to maintain a level of reproducibility within the phosphorus flow trials (of Ecology Water Quality Program, 2014; ASTM, 2012; Lewis and Sjostrom, 2010; Seol and Lee, 2001). The BRC media was packed in four lifts of 4 cm (1.6 in) each with a total depth of 15 cm (5.9 in). After each packed layer, the surface was smoothed over by hand to eliminate any open macropores. Figures 3.16 and 3.17 describe the packing and light compaction of the first media lift.

Figure 3.16: First "lift" of media added to the new flow cell. Media was packed into the cell in four different layers with a layer thickness of 4 cm (1.6 in). Media packing was based on a modified version of ASTM D 1557 (of Ecology Water Quality Program, 2014; ASTM, 2012; Lewis and Sjostrom, 2010; Seol and Lee, 2001).

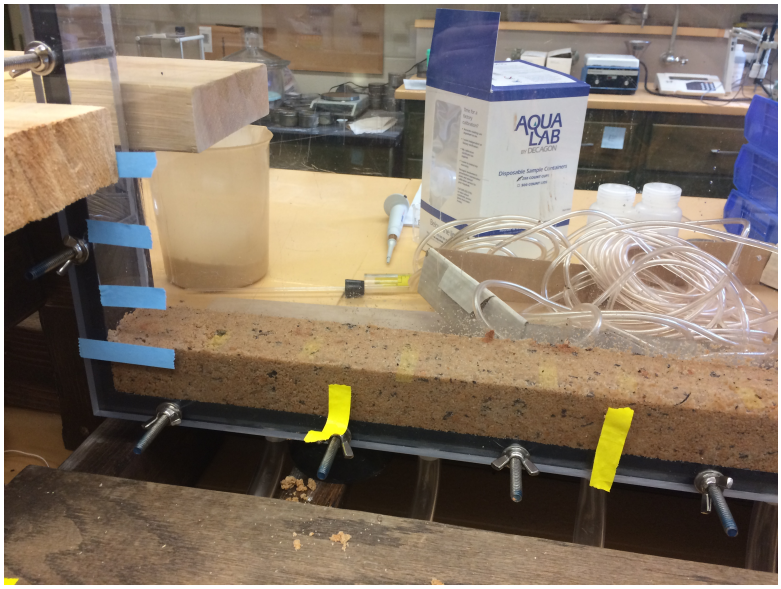

Figure 3.17: First "lift" of media added to the new flow cell and lightly compacted. Media was packed into the cell in four different layers with a layer thickness of 4 cm (1.6 in). Media packing was based on a modified version of ASTM D 1557 (of Ecology Water Quality Program, 2014; ASTM, 2012; Lewis and Sjostrom, 2010; Seol and Lee, 2001).

3.4.3 Trial Descriptions

The phosphorus flow experiments evaluated phosphorus retention in synthetic stormwater under three clogging conditions: a non-clogged condition (Trial 1), semi-clogged condition (Trial 2), and clogged condition (Trial 3). Each trial was replicated three times, and a 4-point composite sample of the BRC media was analyzed for background phosphorus levels.

Trial 1 flushed synthetic stormwater through the cell with no additional surface solids. The media depth was 15 cm (5.9 in) to allow for sufficient water ponding space during WCP measurements. The flow cell for Trial 1 was divided into Columns A, B, C, and D, where infiltration measurements occurred, further subdivided into 16 media sections, and composite sampled (labeled 1 - 16). Figure 3.18 demonstrates how the flow cell was sub-divided and sampled.

Trials 2 and 3 flushed synthetic stormwater through the cell with either 300 g or 600 g of placed silica on the surface, respectively. The media depth was 15 cm (5.9 in) to allow for

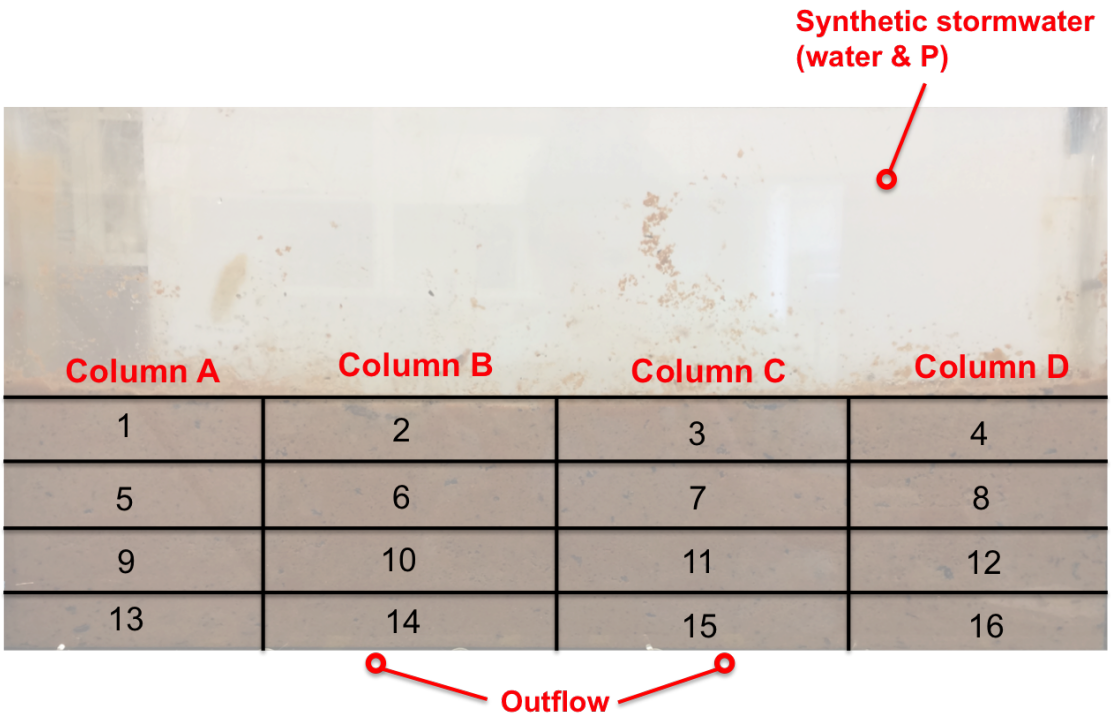

Figure 3.18: Trial 1 media sampling numbers containing no additional surface solids. Samples 1 - 16 were taken from Columns A, B, C, and D, further subdivided into media Sections 1 - 16, respectively, and analyzed for phosphorus levels.

sufficient water ponding space during WCP measurements. The flow cell for Trials 2 and 3 was divided into Columns A, B, C, and D, where infiltration measurements occurred, and further subdivided into 16 media sections and composite sampled (labeled 1 - 16). The silica layer was sub-divided into Sections 17, 18, 19, and 20 based on Columns A, B, C, and D, respectively, and composite sampled (Samples 17 - 20). Figure 3.19 demonstrates how the flow cell media and silica was sub-divided and sampled.

3.4.4 Trial Measurements

Two measurements were taken during the phosphorus flow experiments: (a) whole cell performance (WCP) and (b) infiltration. Section 3.3.3 described the methodology used for the measurements. Both measurements were conducted twice, pre-solids placement and post-solids placement, to quantify changes in the media by the addition of surface solids. The infiltration method used for the phosphorus flow experiments collected additional data

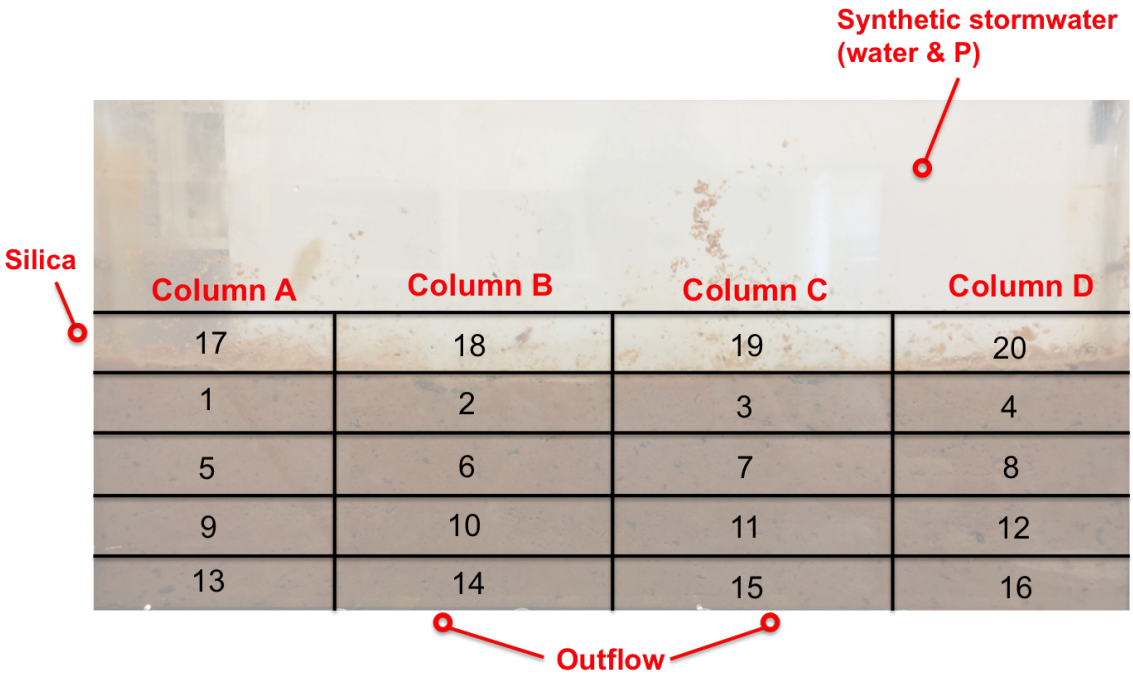

Figure 3.19: Trial 2 and 3 media sampling numbers containing 300 g or 600 g surface solids, respectively. Samples 1 - 16 were taken from media sections 1 - 16, respectively, and analyzed for phosphorus concentration. The upper silica layer was subdivided based on Columns A, B, C, and D, sampled (Samples 17 - 20), and analyzed for phosphorus levels.

points compared to the clogging experiments. Seven measurements were recorded as the water column dropped from 30 cm (11.8 in) to 25, 20, 15, 10, 5, and 0 cm (9.8, 7.9, 5.9, 3.9, 2, and 0 cm).

After synthetic stormwater was flushed through each trial replicate, the effluent stormwater was sampled and analyzed for phosphorus concentration, and finally, brilliant blue dye (4 g/L) was flushed through the flow cell and recorded with a time-lapse camera to identify potential occurrences of preferential flow. Screenshots of the dye flowing through the media at specific times were compared to phosphorus levels in order to further explore preferential flow.

The flow cell media was sampled and analyzed for phosphorus levels using the methods described in Section 3.2.3. For Trials 1 - 3, Samples 1 - 16 and 17 - 20 (if applicable) were each acid digested and analyzed 3 times. The average values and standard error were reported.

Mass balance calculations were conducted using the average phosphorus values to determine differences in total initial phosphorus levels and effluent phosphorus levels.

3.4.5 Infiltration Method

A modified version of the pressure infiltrometer method was used to measure infiltration during the phosphorus flow trials (Equation 2.10, Section 2.6.1; Section 3.3.3).

3.4.6 Synthetic Stormwater

Phosphorus was chosen as the pollutant of concern in the synthetic stormwater. There are various methods of phosphorus delivery within stormwater, including particulate phosphorus and dissolved phosphorus. Particulate phosphorus was introduced into the BRC media as phosphorus bound to ferrihydrite, an iron oxide derived in the lab. Ferrihydrite was chosen as the delivery method due to its adsorption with anions, including that of phosphorus, arsenic, and arsenite, to name a few. Additionally, ferrihydrite is easily synthesized in a lab setting.

The target phosphorus concentration within the synthetic stormwater was 3.7 mg/L with a total volume of 333 L of synthetic stormwater flushed through each trial replicate. The total amount of phosphorus introduced into each trial replicate was 1.23 g of Super Triple Phosphate (0-46-0), based on the target concentration of 3.7 mg/L.

3.4.7 Ferrihydrite Synthesis

Ferrihydrite was synthesized based on a modified version of Schwertmann and Cornell (2000), Raven et al. (1998), and Jain and Loeppert (2000). Briefly, two-line ferrihydrite was produced using 40 g $Fe(NO_3) \cdot 9\ H_20$ (ferric nitrate nonahydrate or Iron (III) nitrate nonahydrate, VWR International, LLC, Solon, OH, USA) dissolved in 500 mL distilled water. 1 M KOH (Fisher Scientific, Fair Lawn, NJ, USA) was added at a fixed rate of of 100 mL min^{-1} while being actively stirred with a magnetic stirrer until the pH of the solution

reached 7.5. The final 20 mL was added in dropwise until the desired pH was reached. The suspension was washed three times with 0.1 M NaCl (Aldrich Chemical Company, Milwaukee, WI, USA) and the remaining sediment separated by centrifuge at 2,500 g for 10 minutes. The final sediment was resuspended in 0.1 M NaCl, adjusted to pH 7.5, and diluted to a 1 L final volume with the ferrihydrite concentration in the final suspension approximating 10 g L^{-1}.

3.4.8 Phosphorus Adsorption on Ferrihydrite

To determine how much ferrihydrite was bound to phosphorus within the synthetic stormwater, phosphorus adsorption was analyzed over a five day period. Ferrihydrite and phosphorus were combined together using the same concentration used in the phosphorus flow experiments. The mixture was separated by centrifuge at 2,500 g for 10 minutes to allow for the ferrihydrite and bound phosphorus to settle out of solution. The supernatant was sampled in triplicate and allowed to sit for a period of four days; the mixture was centrifuged and agitated throughout that period to replicate the mixing that occurred during the phosphorus flow experiments. The mixture was sampled in triplicate after 48 and 96 total hours after initial sampling. Table 3.5 shows the phosphorus concentrations found in the samples after 0, 48, and 96 hours, respectively.

Table 3.5: Average phosphorus adsorption on ferrihydrite concentrations over a five day period. Error term reflects one standard error ($n = 3$)

	Time (hours)		
	Initial	**48 hours**	**96 hours**
P Conc (mg/L)	3.8±0	3.7±0	3.7 ±0

Based on the agitation of the samples that occurred during the duration of the experiment and the relatively stable concentrations that resulted, it can be concluded that a

majority of the phosphorus was dissolved in solution, and concentrations bound to ferrihydrite and considered out of solution were unable to be calculated. Further experimentation is required to determine the phosphorus concentration bound to ferrihydrite.

3.4.9 Mass Balance

Mass balance was calculated for all trial replicates. Total phosphorus in the synthetic stormwater, background phosphorus levels in the media, average retained phosphorus levels in the media, average retained phosphorus in the silica, and phosphorus present in the effluent were determined and separated into total initial phosphorus and total phosphorus in the outflow, reported in mg.

$$P_{initial} = P_{background} + P_{stormwater} \tag{3.4}$$

$$P_{outflow} = P_{effuent} + P_{media} + P_{silica} \tag{3.5}$$

Equations 3.4 and 3.5 show how each aspect of the phosphorus levels are categorized and labeled for mass balance purposes. $P_{background}$ was a media sample analyzed after each trial, and $P_{stormwater}$ was an estimated solution value (Equation 3.4). $P_{effluent}$ was a solution sample analyzed after each trial, P_{media} was a media sample analyzed after each trial, and P_{silica} was a media sample analyzed after each trial (Equation 3.5).

The total initial phosphorus in the synthetic stormwater remained constant for all trial replicates, at an estimated 1,228 mg. The concentration of phosphorus used was 3.7 mg/L, with 333 L of stormwater used for each trial replicate. Background phosphorus levels were sampled once and analyzed three times, and an average was calculated for each trial replicate. The sum of total phosphorus present in the stormwater and the average background phosphorus levels equaled the total initial phosphorus.

Background phosphorus levels were sampled once and analyzed three times to give an average concentration (mg/kg) for each trial replicate, and was converted to total mg in Equation 3.6,

$$\frac{\text{mg}}{\text{kg}} \cdot 4,420 \text{ cm}^3 \cdot \frac{1.3 \text{ g}}{\text{cm}^3} \cdot \frac{1 \text{ kg}}{1000 \text{ g}} \tag{3.6}$$

where 4,420 cm^3 is the volume and 1.3 g/cm^3 is the bulk density of the media (calculated based on a method from Klute (1986)).

Samples 1 - 16 in Trials 1, 2, and 3 were analyzed three times and an average concentration (mg/kg) was reported and converted to average phosphorus (mg) for each section. Equation 3.7 describes this process,

$$\frac{\text{mg}}{\text{kg}} \cdot 273 \text{ cm}^3 \cdot \frac{1.3 \text{ g}}{\text{cm}^3} \cdot \frac{1 \text{ kg}}{1000 \text{ g}} \tag{3.7}$$

where 273 cm^3 is the volume of each media section (1 - 16). The average phosphorus (mg) value for Sections 1 - 16 were added together to report the total average phosphorus (mg) value for the entire flow cell media. Background phosphorus was then subtracted from the total average phosphorus (mg) value to give total average phosphorus (mg) retention per trial replicate. Similar calculations were conducted for the silica layer (Samples 17 - 20); average phosphorus (mg) values were calculated for Sections 17 - 20 based on volume measurements and bulk density of the silica layer, as reported in Table 3.6 and Equation 3.8.

$$\frac{\text{mg}}{\text{kg}} \cdot \text{ V}olume(cm^3) \cdot \frac{1.2 \text{ g}}{\text{cm}^3} \cdot \frac{1 \text{ kg}}{1000 \text{ g}} \tag{3.8}$$

Water samples from the collected effluent were analyzed for phosphorus concentration (mg/L) and multiplied by the total volume of stormwater used (332 L) to report total phosphorus (mg) in the stormwater effluent. The sum of phosphorus retained in the media and silica, along with phosphorus levels in the effluent equaled the total phosphorus outflow.

Equation 3.9 was used to calculated percent P reduction,

Table 3.6: Silica volume estimates for Sections 17, 18, 19, and 20.

	Volume (cm^3)			
Trial	**Section 17**	**Section 18**	**Section 19**	**Section 20**
2	14	21	28	77
3	70	70	70	70

$$\frac{\text{Total Initial - Outflow}}{\text{Total Initial}} \cdot 100 \tag{3.9}$$

where a positive percent reduction correlated to a reduction in phosphorus levels in the effluent, and a negative percent reduction correlated to an increase in phosphorus levels in the effluent.

(Equation 3.9) was chosen as the preferred method over the alternative calculation shown in Equation 3.10.

$$\frac{\text{Retained P Media - Background P}}{\text{Total Initial}} \cdot 100 \tag{3.10}$$

Determining the best method for calculating mass balance is highly correlated to the measurements sampled with the highest accuracy. In this case, there were both solution samples and heterogenous media samples measured for phosphorus levels. Due to the non-homogenous nature of the BRC media, the solution samples were considered more accurate. The method used (shown in Equation 3.9) used the total initial value, comprised of both estimated solution values and media values, and outflow values, comprised of effluent solution values and media/silica values. The method that was not used, shown in Equation 3.10, relied on retained phosphorus values and background values, exclusively media sample values, which are not as accurate as solution values due to their non-homogenous nature.

3.5 Statistical Analysis

3.5.1 ANOVA

A two-way Analysis of Variance (ANOVA) evaluated the influence of two independent variables on the dependent variable (K_{fs}) gathered from the averaged two data points collected from the pressure infiltrometer. Three separate analyses were conducted; (A) analyzed potential interactions between trial (1, 2, 3) and location (Section A, B, C, D) on pre-solids placement K_{fs}; (B) analyzed potential interactions between solids placement timing (pre-solids placement and post-solids placement) and location (Section A, B, C, D) on K_{fs} in Trial 2, and (C) analyzed potential interactions between solids placement timing (pre-solids placement and post-solids placement) and location (Section A, B, C, D) on K_{fs} in Trial 3.

(A) Influence of location and trial on K_{fs}

A two-way ANOVA evaluated the effects of the independent variables of location and trial on the dependent variable of K_{fs}, and if interactions occurred. Interactions between variables test whether the effect of one variable depends on another variable; therefore, does the effect of trial (treatment) depend on the location within the flow cell. The dependent response was K_{fs}, and the independent, explanatory variables were location, with 4 levels, and trial, with 3 levels. The null hypothesis stated that trial does not significantly affect K_{fs}, location does not significantly affect K_{fs}, and interactions between trial and location did not significantly affect K_{fs}. The alternative hypothesis stated that significant interactions occurred. A 95% confidence interval was determined for the two-way ANOVA, with an alpha level of 0.05. Table 3.7 summarizes variables used in the ANOVA determination.

(B), (C) Influence of location and timing on K_{fs} in Trials 2 and 3

A two-way ANOVA evaluated the effects of the independent variables of location and timing on the dependent variable of K_{fs} in Trial 2 and Trial 3, respectively, and if interactions

Table 3.7: ANOVA variables: Influence of location and trial on K_{fs}.

Observations	108
Degrees of Freedom (DF)	96
alpha	0.05
Dependent variable(s)	K_{fs}
Independent variable(s)	Location, trial

occurred. Interactions between variables test whether the effect of one variable depends on another variable; therefore, does the effect of timing (pre-solids placement and post-solids placement) depend on the location within the flow cell. For both trials, the dependent response was K_{fs}, and the independent, explanatory variables were location, with 4 levels, and solids placement timing, with 2 levels. For both trials, the null hypothesis stated that solids placement timing does not significantly affect K_{fs}, location does not significantly affect K_{fs}, and interactions between solids placement timing and location did not significantly affect K_{fs}. The alternative hypothesis stated that significant interactions occurred. A 95% confidence interval was determined for the two-way ANOVA, with an alpha level of 0.05. Table 3.8 summarizes variables used in the ANOVA determination for Trials 2 and 3.

Table 3.8: ANOVA variables: Influence of location and timing on K_{fs} in Trials 2 and 3.

Observations	72
Degrees of Freedom (DF)	64
alpha	0.05
Dependent variable(s)	K_{fs}
Independent variable(s)	timing, trial

3.5.2 Wilcoxon Rank Sum Test

The Wilcoxon Rank-Sum Test is a non-parametric test used on independent samples of non-normal error distribution and was used to determine if the background phosphorus

concentrations were less than the total phosphorus concentration of the media after synthetic stormwater flush, and if the difference was significant (Crawley, 2015). The null hypothesis was no difference between data sets, and the alternative hypothesis was that total phosphorus concentrations within the media were higher then background levels post synthetic stormwater flush, based on the BRC goal of adsorbing phosphorus onto the media. The alpha level chosen was 0.05.

3.6 Summary

By conducting the clogging experiments and phosphorus flow experiments, tasks (a) through (d) described in Section 1.6 can be completed.

Chapter 4

Results and Discussion

4.1 Clogging Experiments

Results from the infiltration and WCP measurements were used to determine the clogged and semi-clogged conditions for the phosphorus flow experiments.

4.1.1 Infiltration Results

Infiltration rates (cm/min) from the clogging experiments were plotted with cumulative flushed solids (g) to determine how the addition of solids affects infiltration across Columns A, B, C, and D, as shown in Figure 4.1. Rates at which suspended solids were added to the system increased after infiltration rates remained constant after several additions.

When focusing on the mean infiltration rate of 5 cm/min, a relatively slow infiltration rate into the media, Column D reaches that rate after approximately 85 g of solids were added and stayed beneath that rate for the remainder of the measurements. Figure 4.1 illustrates when each column reached a mean infiltration rate of 5 cm/min, denoted by blue arrows, and remained below it. Column C reaches the rate of 5 cm/min after approximately 185 g of cumulative solids, while Columns B and A reach the same rate after 350 and 450 g of solids, respectively. The lagged pattern exhibited in Columns A through D correlate with differences in silica layer thickness among the surface. Column D, directly below the inflow tube, received the greatest amount of silica when suspended solids were pumped through. Column A, farthest away from the inflow tube, received the least amount of silica. A wedge shape formed on the surface of the media, with the thickest layer in Column D that tapered into a thin layer in Column A. Figure 4.2 illustrated the wedge shape of silica that formed on the surface, and the differences in silica layer thickness across the media surface.

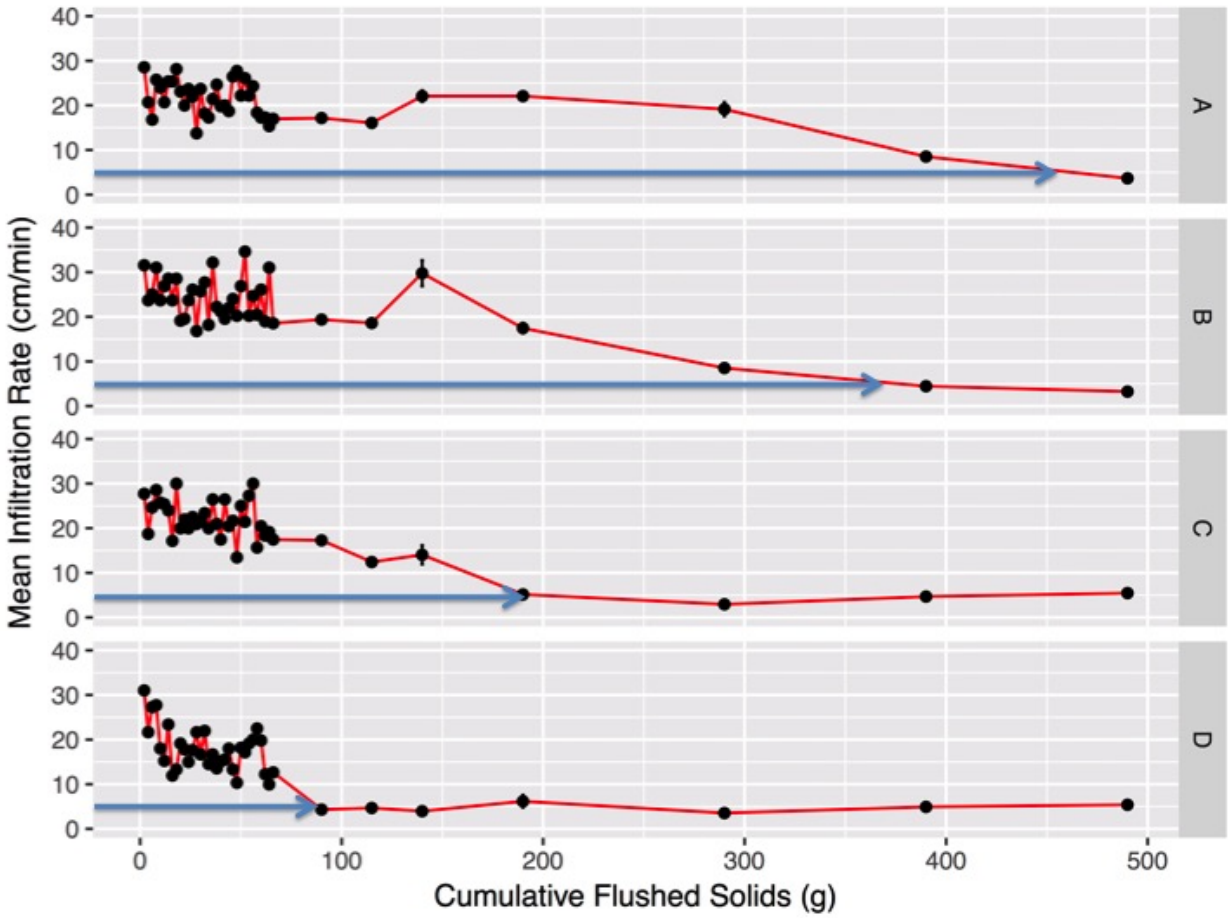

Figure 4.1: Mean infiltration rate (cm/min) compared to cumulative flushed solids (g) for Columns A, B, C, and D. Blue arrows show when the infiltration rate for each column reached 5 cm/min, illustrating the lagged pattern due to the wedge shape of solids that formed on the surface.

4.1.2 Whole Cell Performance

WCP measured the drainage time of a 10 cm water column (2,950 cm^3) out of the cell and determined saturated hydraulic conductivity. Similar to infiltration rates found in Section 4.2.1, hydraulic conductivity values in Figure 4.3 remained relatively constant from 0 to 66 g of cumulative flushed solids, correlating with the rate of 2 g/8L. After the rate increased to 25 g/8L and subsequently to 50 g/8L, the hydraulic conductivity gradually decreased until it plateaued at around 390 g of solids.

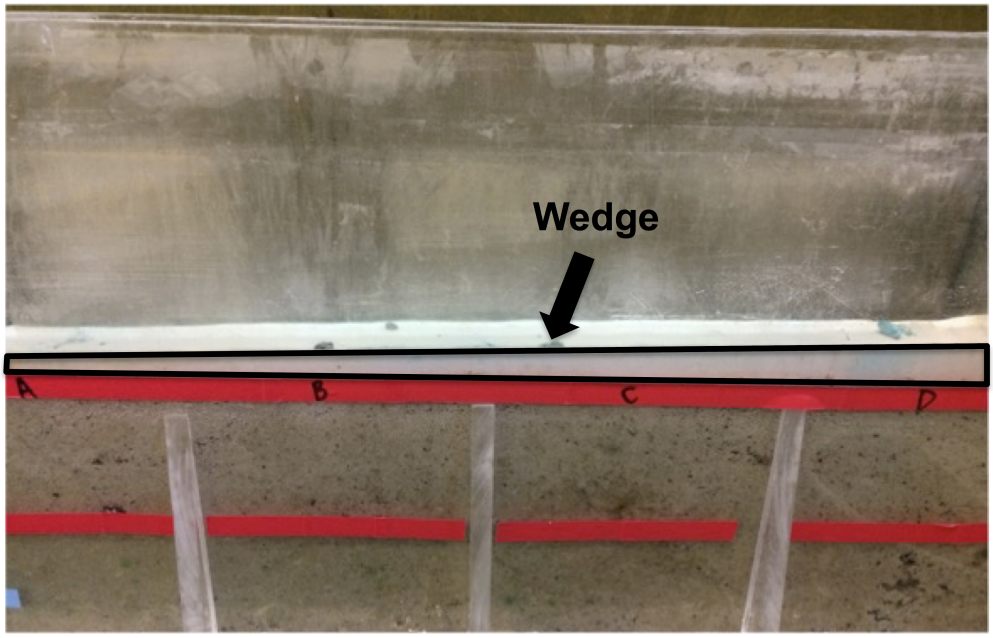

Figure 4.2: Wedge shape of suspended solids on media surface. The thickest section of the wedge shape occurred in Quadrant D, directly underneath the inflow tube, where initial solid buildup occurred.

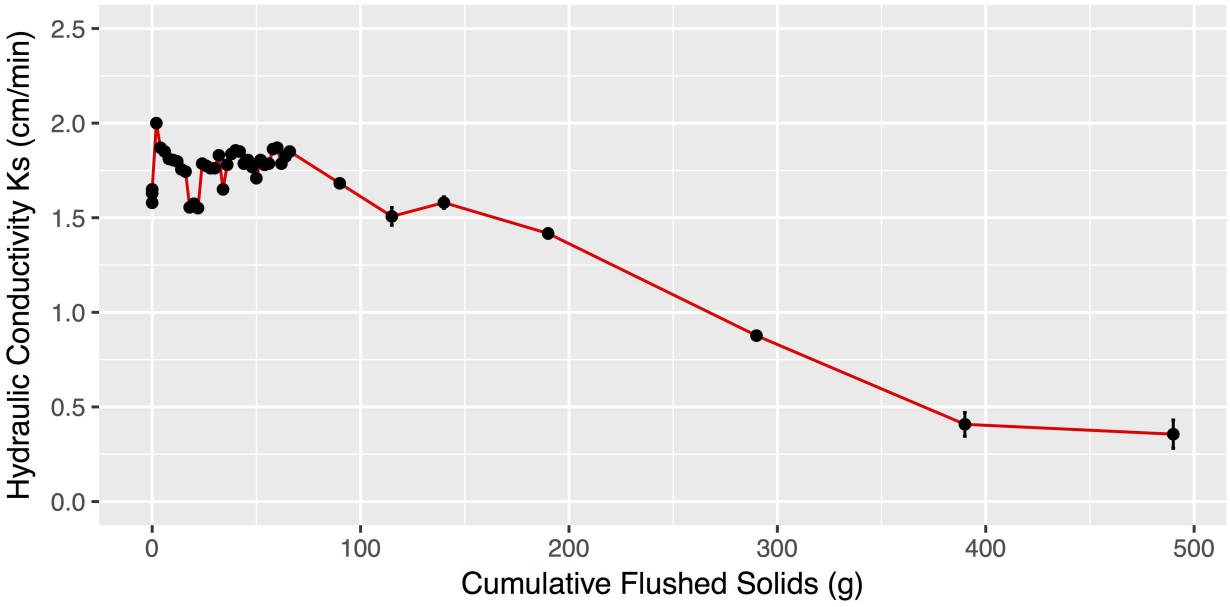

Figure 4.3: Saturated hydraulic conductivity measurements of the media surface after 490 g of cumulative flushed solids.

4.1.3 Determination of Phosphorus Flow Trial Initial Conditions

Infiltration and WCP data were used to determine the initial conditions for the phosphorus flow experiment. Figures 4.1 and 4.3 demonstrated initial decreases in both infiltration

rates and hydraulic conductivity at 100 g of solids, and plateaued between 400 and 500 g. Based on the plateaued infiltration rate for all columns in Figure 4.1 at the last two collected data points, it can be inferred that the infiltration rate would either stay the same or decrease with further experimentation, based on previous trends. The upper limit, or "clogged" condition for Trial 3, was 600 g, and covered the entire flow cell media surface. Infiltration rates and hydraulic conductivity decreased between 200 and 300 g of added solids at different rates. Based on the variability among the rates, 300 g solids was chosen as the "semi-clogged" condition in Trial 2, which covered approximately 66% of the flow cell media surface.

4.2 Phosphorus Flow Experiments

4.2.1 Infiltration

Trial 1 of the phosphorus flow trials evaluated phosphorus retention in BRC media without added surface solids. The average pre-solids placement field saturated hydraulic conductivity, K_{fs}, of the last two data points (25 cm and 30 cm) differed in Trial 1 and Trial 3 solely in Column A, with the remaining trials and columns not affected (Figure 4.4 A). K_{fs} values increased from Trials 1 to 3 in Column A, with significant differences among Trials 1 and 3 (Table 4.1). This result could be due to variations among media homogeneity and the packing method used. Trials 2 and 3 contained 300 and 600 g of added surface solids, respectively. Differences among pre- and post-placement average K_{fs} values for the last two data points were significant across Columns A, B, C, and D for Trial 2 (Figure 4.4 B) and Trial 3 (Figure 4.4 C). Although K_{fs} values presented a decreasing trend from Column A to Column D within the post-solids placement values in Figure 4.4 B, silica thickness was considered insignificant albeit the wedge shape was prominently thick in Column D (low K_{fs} values) and thin (high K_{fs} values) in Column A.

The data did not fit the Philip's infiltration model (Section 2.6.2) due to time and space limitations of the flow cell methodology. Antecedent moisture conditions determine

whether infiltration is dominated by sorption or conductivity; media wetness prior to starting the infiltration measurements varied from trial to trial, therefore the dataset captured the infiltration process dominated by sorption and not conductivity (Hillel, 2004). The first five infiltration data points were non-linear and not used in further analysis; the last two data points at 25 cm and 30 cm captured the very beginning of the linear portion of infiltration when quasi-steady state was reached and conductivity was the dominating process. The data was fit to a modified pressure infiltrometer equation. A two-way ANOVA was conducted on the data (method described in Section 3.5) in addition to computing 95% confidence intervals. A summary of the statistical data can be found in Table 4.1.

Table 4.1: Two-way ANOVA and 95% Confidence Interval variables and results.

	Figure (A)	**Figure (B)**	**Figure (C)**
Observations (n)	108	72	72
Degrees of Freedom (DF)	96	64	64
Dependent variable(s)	K_{fs}	K_{fs}	K_{fs}
Independent variable(s)	location, trial	location, timing	location, timing
Standard error	0.242	0.124	0.206
F-statistic	2.208	124.8	55.35
p-value	0.019	< 0.01	< 0.01

There is insufficient evidence to prove that flow is affected by the thickness of the accumulated solids layer, 300 and 600 g solids, in Figure 4.4 B and C, respectively. There was no statistically significant difference between column locations in Trial 2 (Figure 4.4 B), therefore the analysis failed to prove that the thin layer of silica in Column A had decreased infiltration rates compared to the thick layer of silica in Column D.

4.2.2 Whole Cell Performance and Saturated Hydraulic Conductivity

Figure 4.5 shows the average saturated hydraulic conductivity of Trials 1, 2, and 3. The blue line connects the average pre-solids placement measurements for Trials 1, 2, and 3.

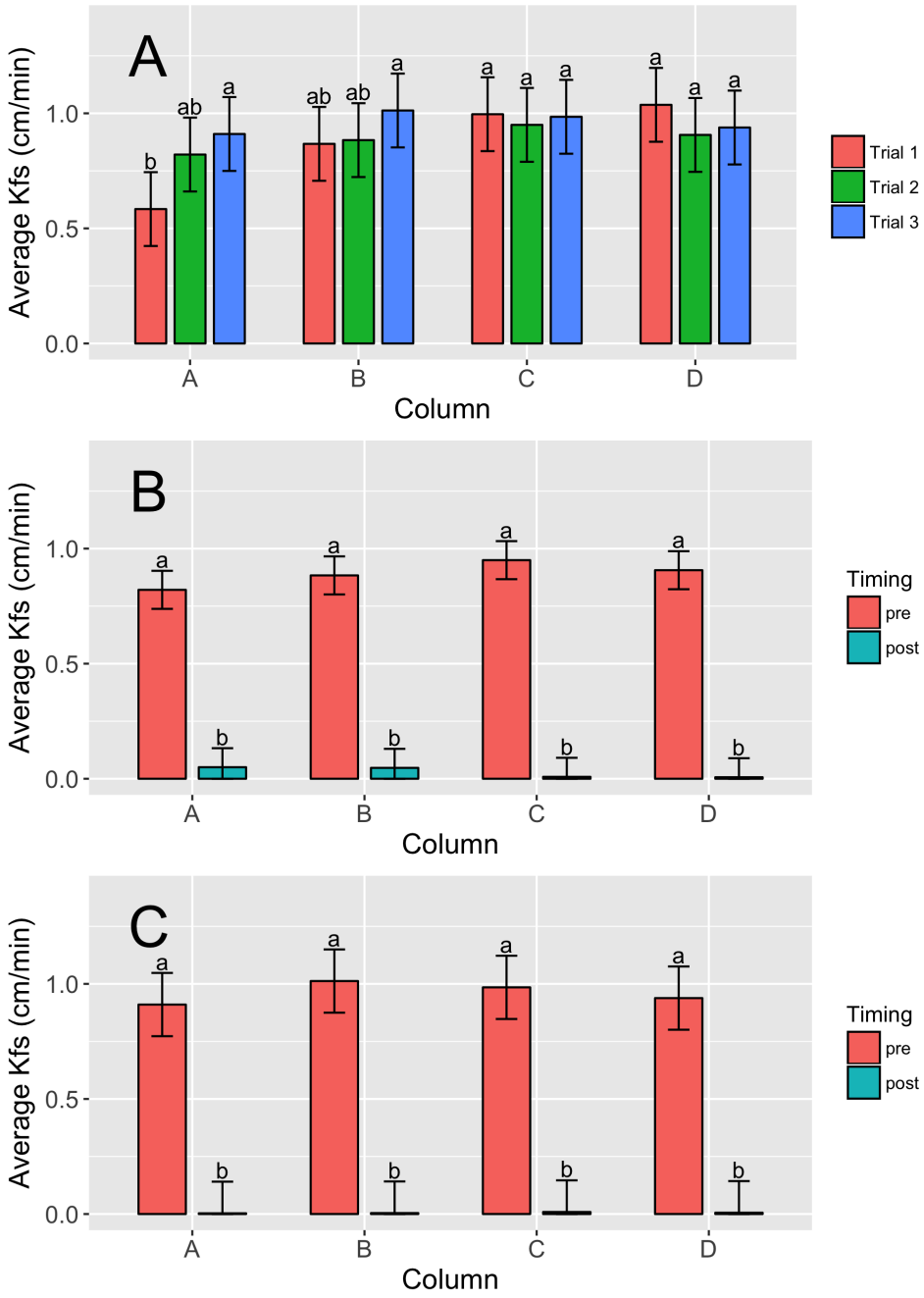

Figure 4.4: Phosphorus flow trial infiltration data; Figure (A) depicted the average pre-solids placement K_{fs} value at Columns A, B, C, and D for each trial replicate; Figure (B) depicted the average K_{fs} values for Trial 2 pre- and post-solids placement at Columns A, B, C, and D; Figure (C) depicted the average K_{fs} values for Trial 3 pre- and post-solids placement at Columns A, B, C, and D.

The red line connects the average post-solids placement measurements for Trials 2 and 3.

There was no average post-solids placement measurement for Trial 1 due to the absence of

surface solids. Average saturated hydraulic conductivity values, standard error and number of observations are reported in Table 4.2.

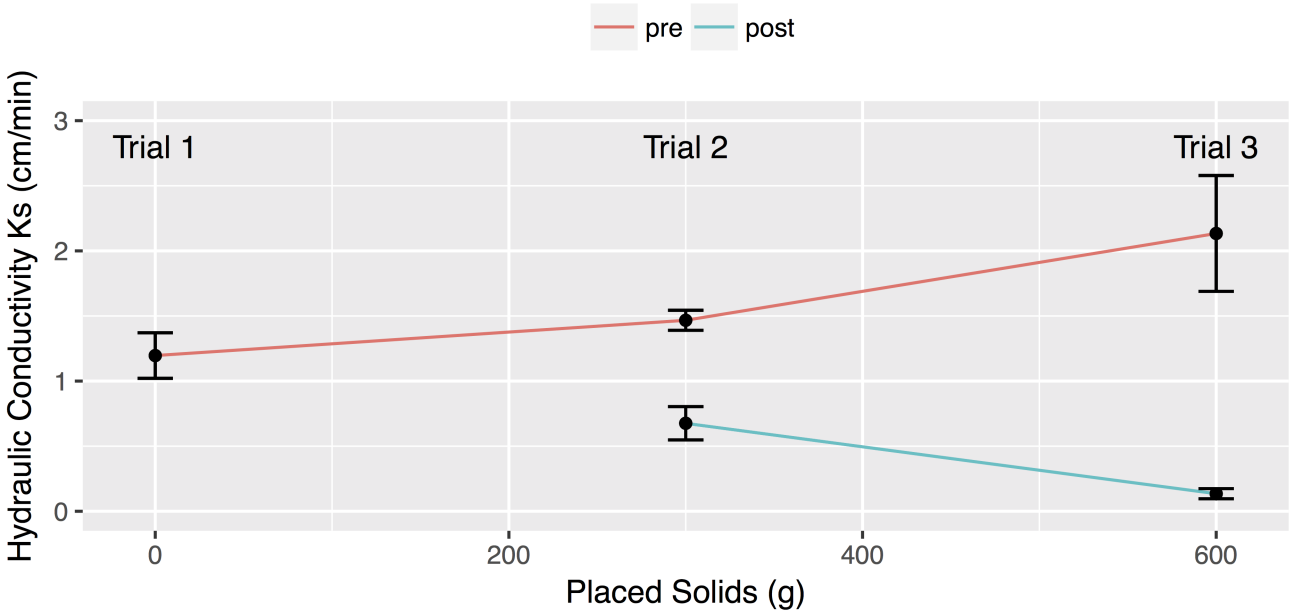

Figure 4.5: Average saturated hydraulic conductivity for Trials 1, 2, and 3. The blue line indicated average pre-solids placement measurements and the red line indicated average post solids placement measurements. Black lines indicated standard error bars.

The pre-placement solids hydraulic conductivity measurements for Trials 1, 2, and 3 were between 1 and 2.5 cm/min, post-placement measurements for Trials 2 and 3 were between 0 and 1 cm/min. The higher saturated conductivity values for the pre-placement trials represented ease of water flow through the media without the negative effects of a restrictive surface silica layer. The lower values for the post-placement trials represented decreased water flow rates through the media due to the added restrictive layer of ground silica on the surface. Trial 2 contained 300 g of solids, showed in Figure 4.6, covering a large portion of the media surface with a thick layer in Quadrant D and thin layer in Quadrant A. Trial 3 contained 600 g of surface solids, creating a thick, restrictive layer covering the entire surface, slowing down all water movement through the media.

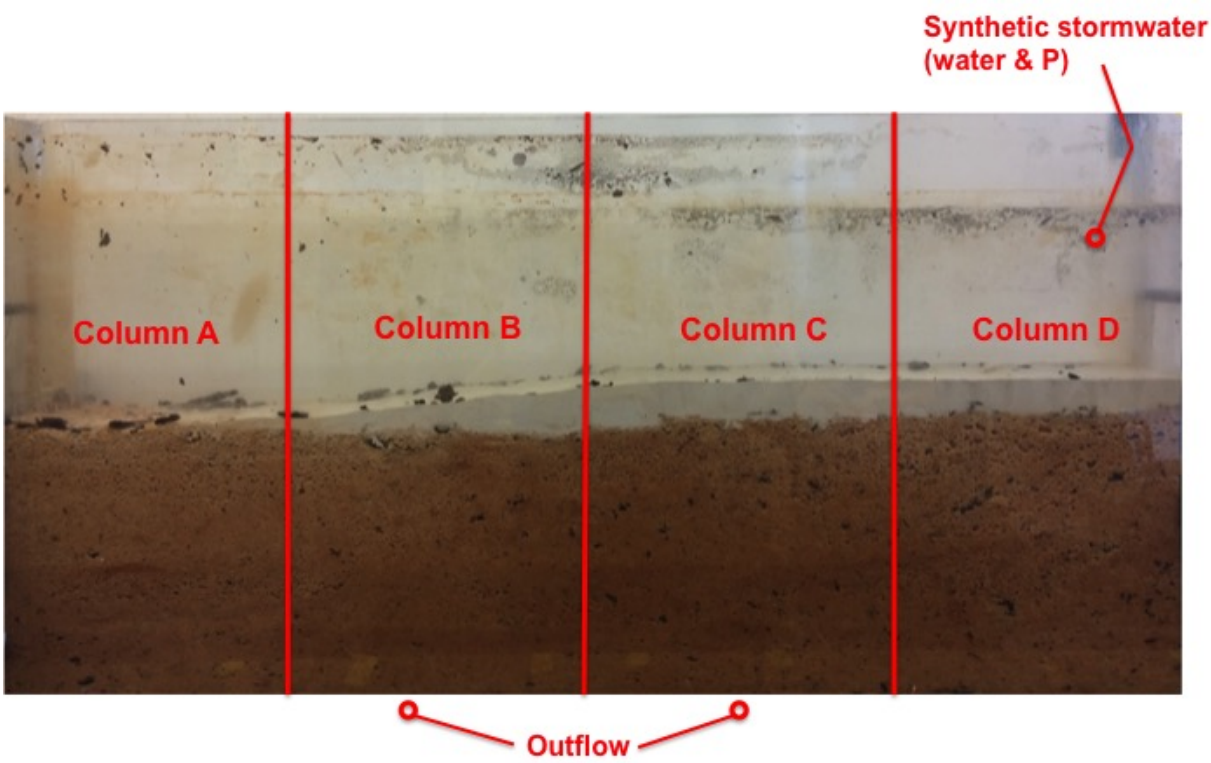

Figure 4.6: Wedge shape of solids found on Trial 2; approximately 66% of the surface is covered with the silica.

Table 4.2 reported average saturated hydraulic conductivity values and standard error for all trials. Trial 3, pre-solids placement had the highest standard error, potentially due to variability within the media mix components.

Table 4.2: Average saturated hydraulic conductivity (K_s) for pre-solids and post-solids placement of surface solids. Error term reflects one standard error ($n = 9$).

Trial	**Timing**	**Observations**	**Surface Solids (g)**	**Average Saturated Hydraulic Conductivity (cm/min)**
1	pre	9	0	1.20±0.17
2	pre	9	0	1.47±0.08
2	post	9	300	0.68±0.13
3	pre	9	0	2.13±0.44
3	post	9	600	0.13±0.04

4.2.3 Phosphorus Media Distribution and Concentration

Average phosphorus values were analyzed to determine phosphorus retention throughout the BRC media. Figures 4.7 - 4.15 present the average phosphorus values (mg) per section (media sections 1 - 16, silica sections 17 - 20) for all trial replicates.

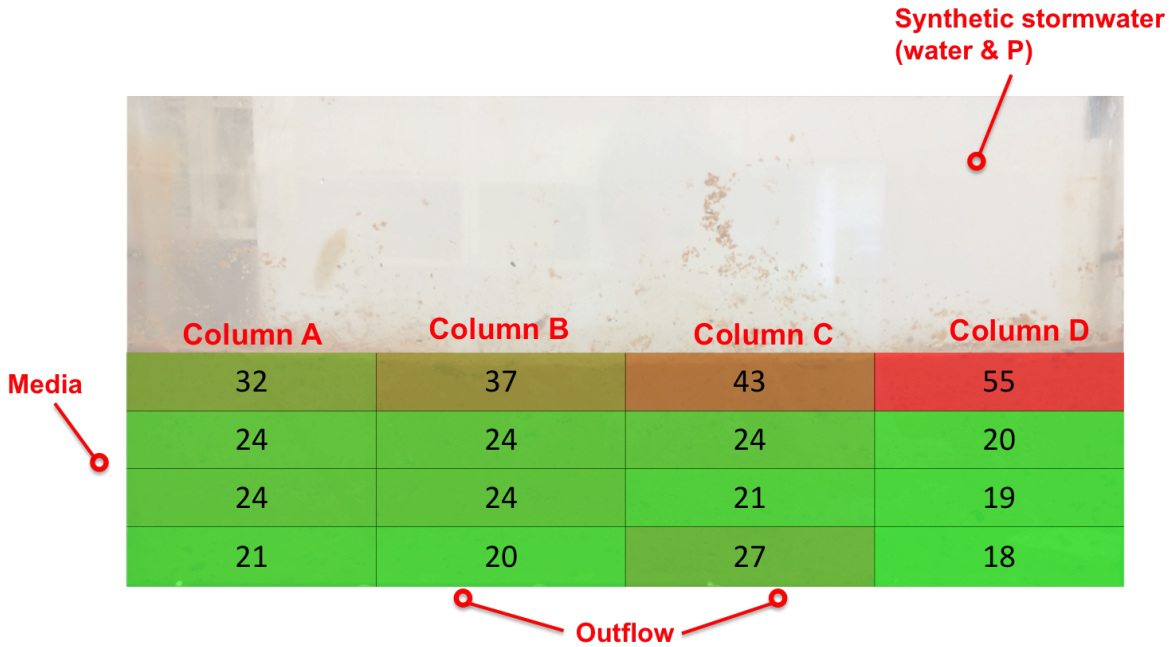

Figure 4.7: Trial 1 Rep 1 average composite phosphorus values (mg). Background phosphorus included. Image depicts high levels in red and low levels in green. Maximum phosphorus value was 55 mg, minimum phosphorus level was 18 mg.

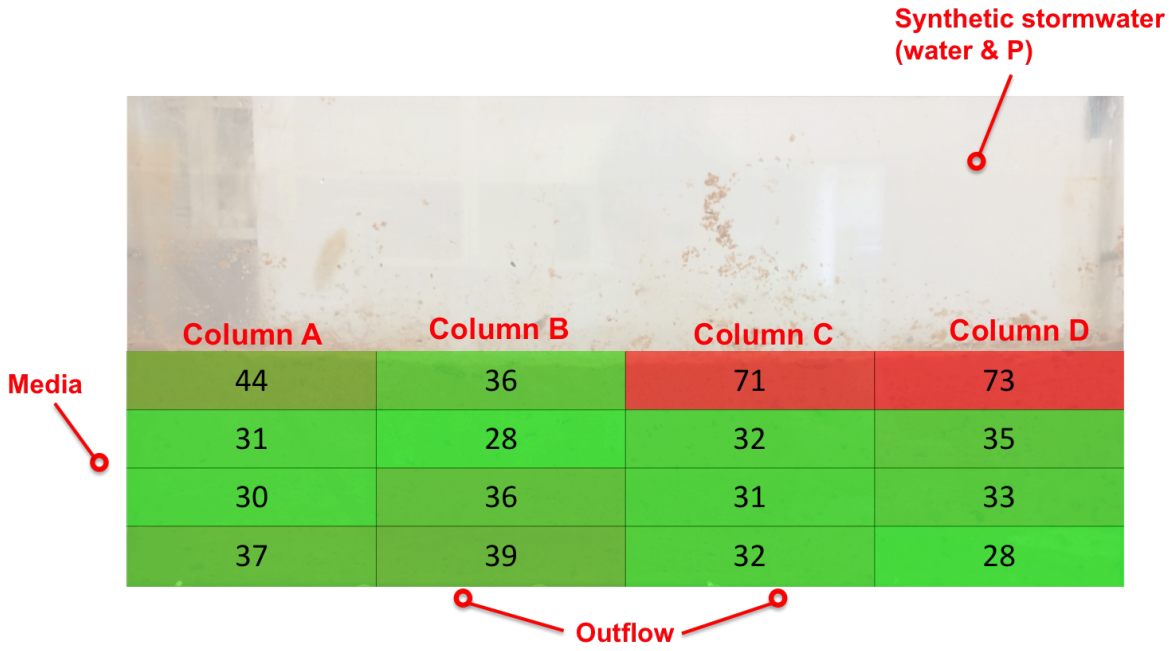

Figure 4.8: Trial 1 Rep 2 average composite phosphorus values (mg). Background phosphorus included. Image depicts high levels in red and low levels in green. Maximum phosphorus value was 73 mg, minimum phosphorus value was 28 mg.

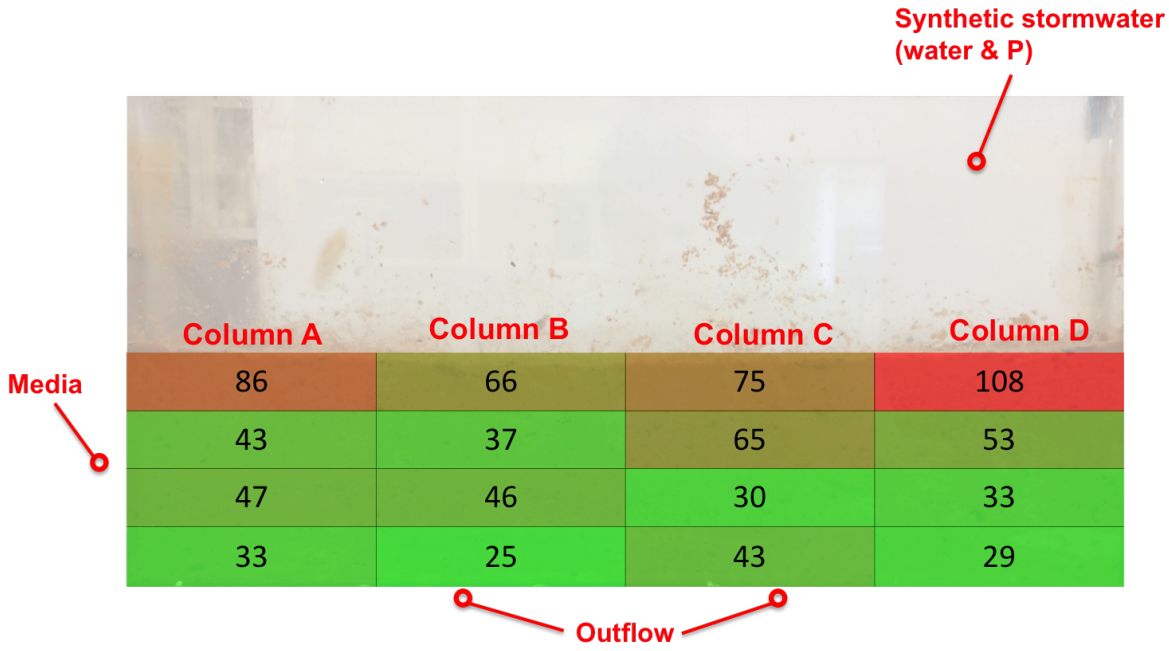

Figure 4.9: Trial 1 Rep 3 average composite phosphorus values (mg). Background phosphorus included. Image depicts high levels in red and low levels in green. Maximum phosphorus value was 108 mg, minimum phosphorus value was 25 mg.

Figures 4.7 - 4.9 illustrate the average phosphorus values (mg) for sections 1 - 16 for all replicates of Trial 1. For all three replicates, the highest phosphorus levels were found in the top layer underneath the inflow tube, with the lowest concentrations found in the bottom layer. This trend depicts a short transport time downward through the media due to early phosphorus retention throughout the stormwater flush.

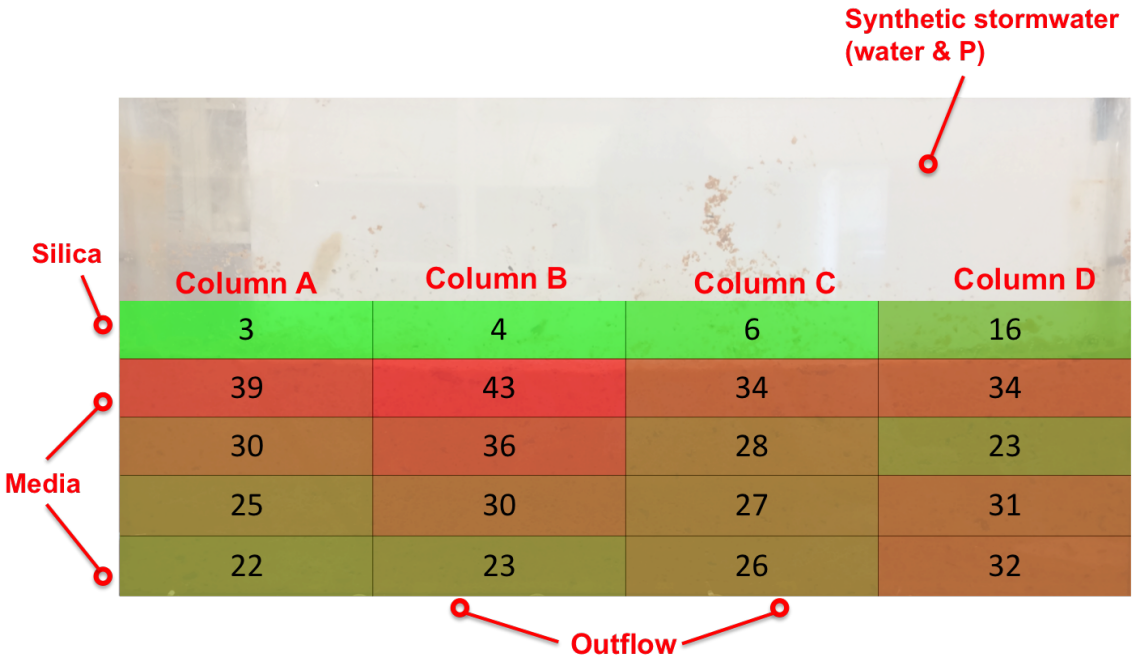

Figure 4.10: Trial 2 Rep 1 average composite phosphorus values (mg). Background phosphorus included. Image depicts high levels in red and low levels in green. Maximum phosphorus value was 43 mg, minimum phosphorus value was 3 mg.

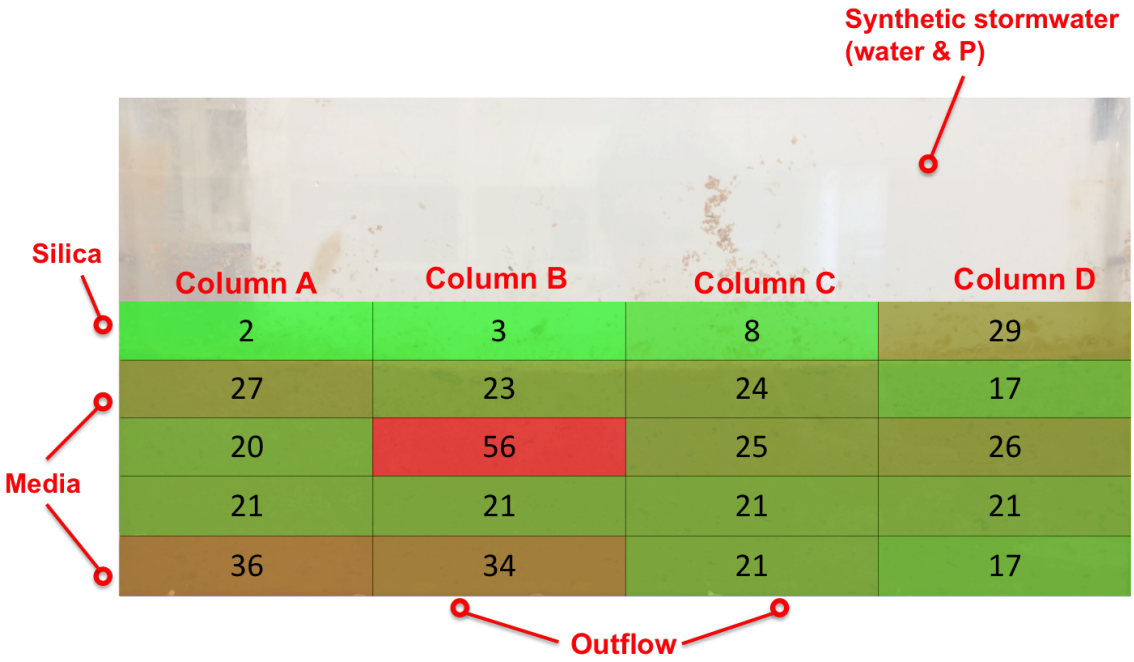

Figure 4.11: Trial 2 Rep 2 average composite phosphorus values (mg). Background phosphorus included. Image depicts high levels in red and low levels in green. Maximum phosphorus value was 56 mg, minimum phosphorus value was 2 mg.

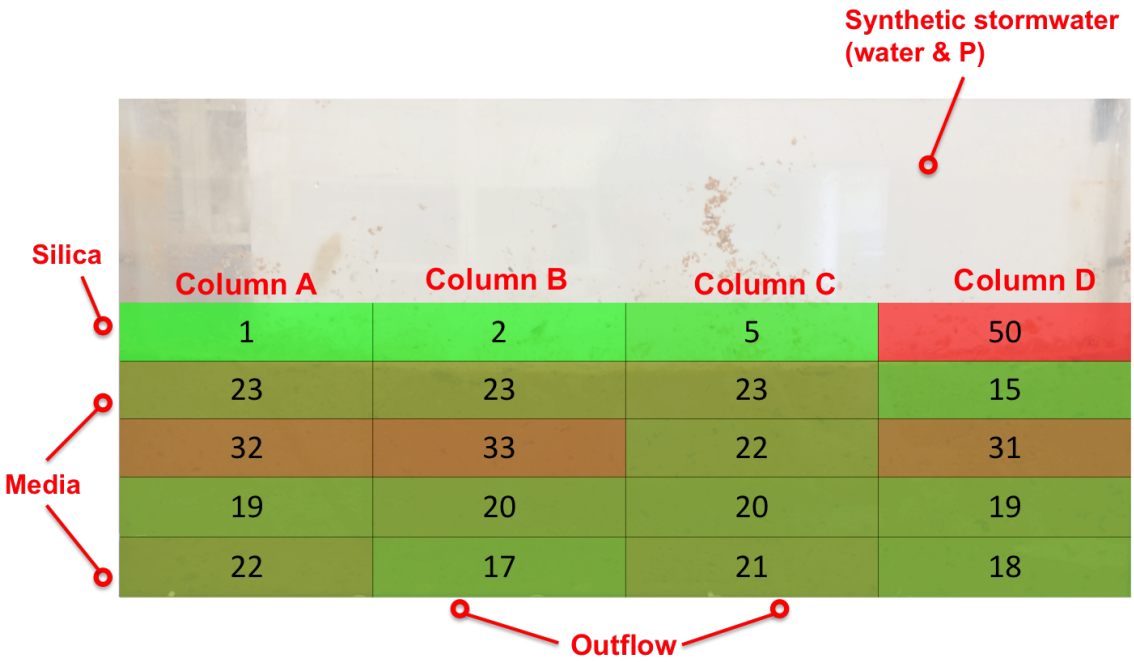

Figure 4.12: Trial 2 Rep 3 average composite phosphorus values (mg). Background phosphorus included. Image depicts high levels in red and low levels in green. Maximum phosphorus value was 50 mg, minimum phosphorus value was 1 mg.

Figures 4.10 - 4.12 illustrate the average phosphorus values (mg) for media sections 1 - 16 and silica sections 17 - 20 for all replicates of Trial 2. For all replicates, the lowest phosphorus levels were found in the silica layers, due to the low likelihood of phosphorus adsorption onto the silica. For Rep 1, the highest phosphorus levels were found in the media layer directly underneath the silica layer. For Reps 2 and 3, the highest phosphorus values were found in different layers, one being in the middle media layer (Rep 2) and the other being in the silica layer (Rep 3), alongside the lowest phosphorus levels.

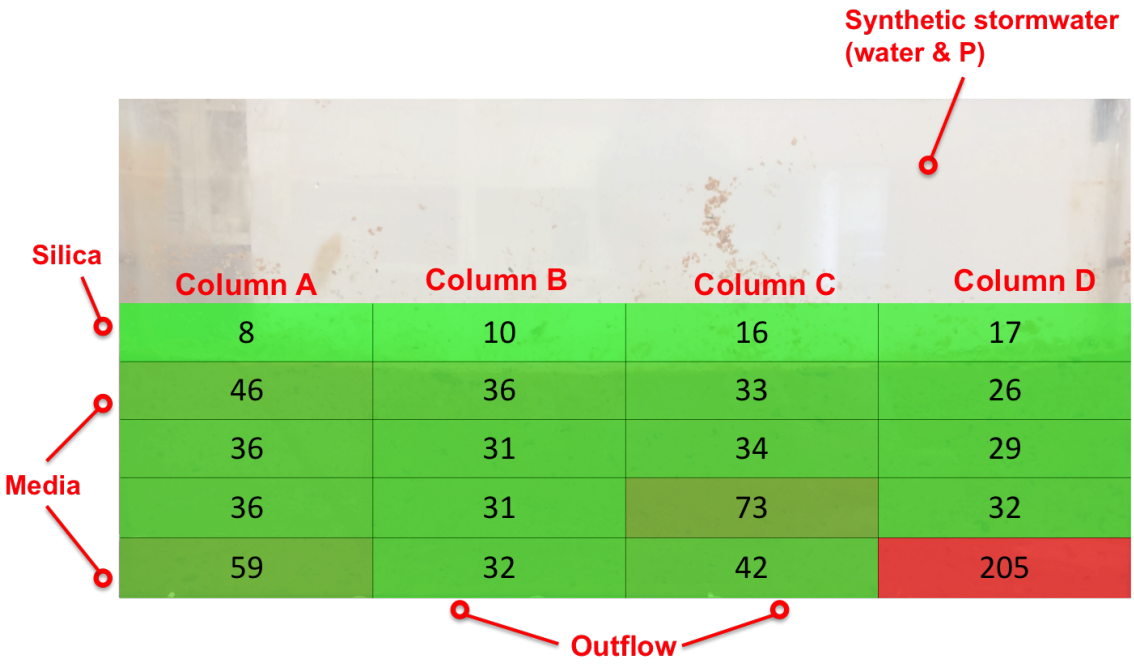

Figure 4.13: Trial 3 Rep 1 average composite phosphorus values (mg). Background phosphorus included. Image depicts high levels in red and low levels in green. Maximum phosphorus value was 205 mg, minimum phosphorus value was 8 mg.

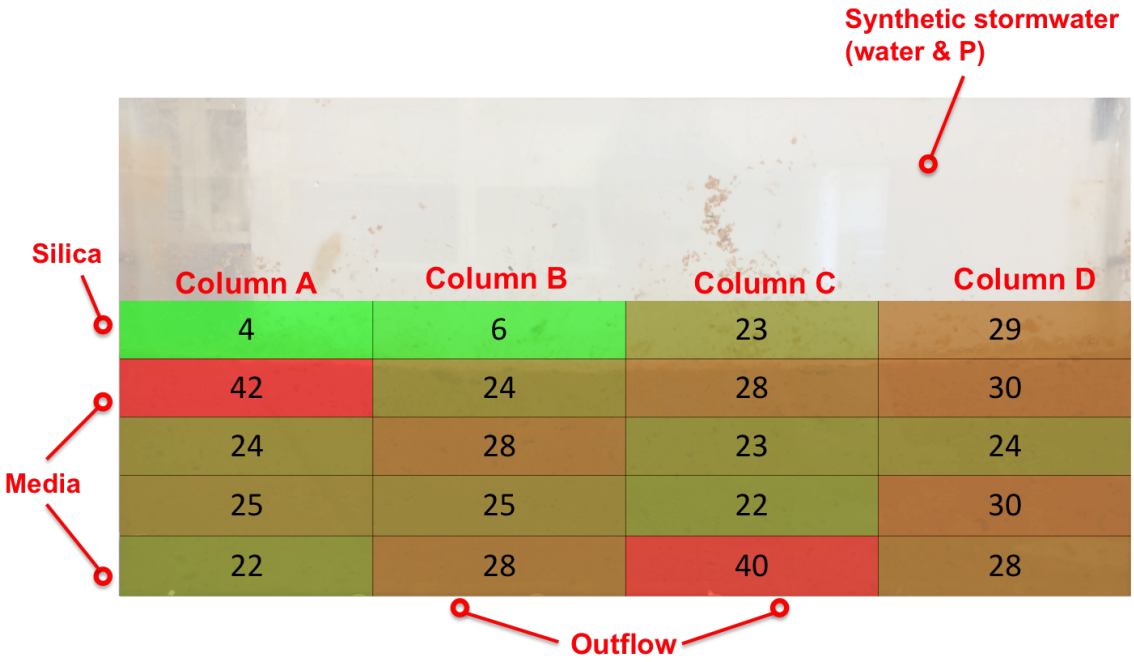

Figure 4.14: Trial 3 Rep 2 average composite phosphorus values (mg). Background phosphorus included. Image depicts high levels in red and low levels in green. Maximum phosphorus value was 42 mg, minimum phosphorus value was 4 mg.

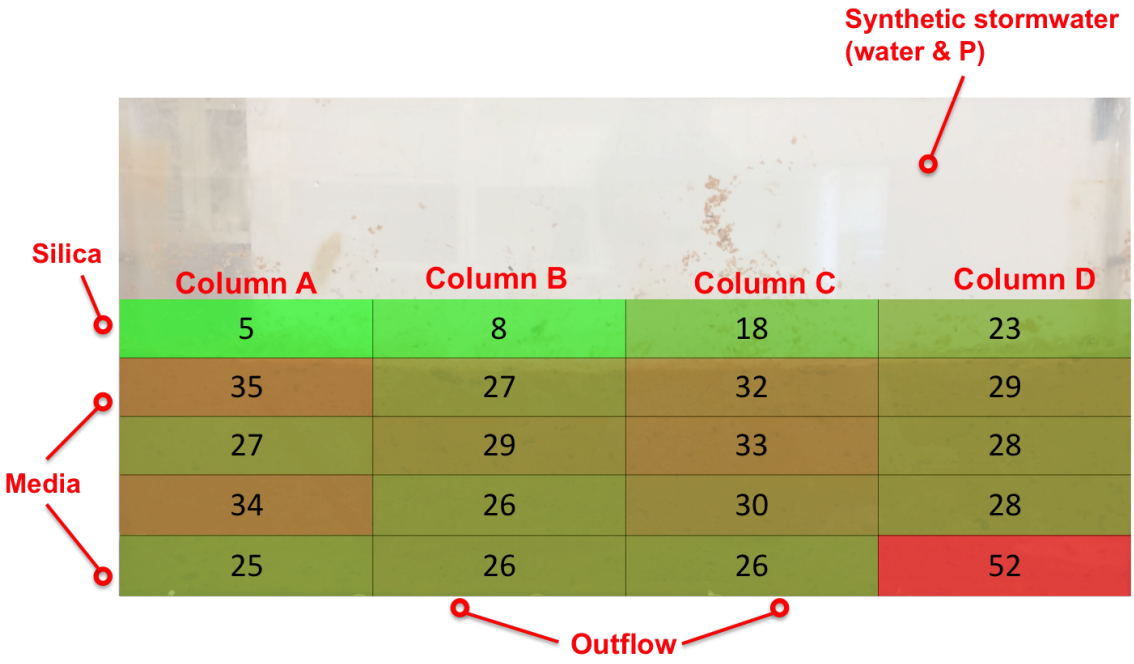

Figure 4.15: Trial 3 Rep 3 average composite phosphorus values (mg). Background phosphorus included. Image depicts high levels in red and low levels in green. Maximum phosphorus value was 52 mg, minimum phosphorus value was 5 mg.

Figures 4.13 - 4.15 illustrate the average phosphorus values (mg) for media sections 1 - 16 and silica sections 17 - 20 for all replicates of Trial 3. For all replicates, the lowest phosphorus levels were found in the silica layers, due to the low likelihood of phosphorus adsorption onto the silica. The highest phosphorus levels were found in different places in each replicate; Rep 1 was in the bottom media layer, Rep 2 was in the upper media layer, and Rep 3 was also in the bottom media layer. Relatively high concentrations (compared to surrounding sections) found in the lowest layers could correlate with preferential flow pathways, further described in Section 4.2.4. Average phosphorus data can be found in Table 4.3. Raw phosphorus data can be found in Appendix B, Table B.1.

Table 4.3: Average phosphorus (mg) for all trials based on position within flow cell. Error term reflects one standard error ($n = 3$). Media positions can be found in Figures 3.18 and 3.19.

		– Average P (mg) –		
Trial	**Position**	**Rep 1**	**Rep 2**	**Rep 3**
1	1	32±6	44±5	86±44
1	2	37±1	36±3	66±23
1	3	43±7	71±9	75±11
1	4	55±5	73±5	108±12
1	5	24±6	31±4	43±4
1	6	24±5	28±3	37±3
1	7	24±7	32±3	65±25
1	8	20±3	35±5	53±23
1	9	24±8	30±4	47±12
1	10	24±4	36±7	46±14
1	11	21±6	31±3	30±6
1	12	19±5	33±2	33±5
1	13	21±4	37±10	33±5
1	14	20±4	39±9	25±1
1	15	27±8	32±4	43±11
1	16	18±6	28±4	29±6
2	1	39±15	27±0	23±2
2	2	43±5	23±1	23±2
2	3	34±4	24±5	23±3
2	4	34±2	17±1	15±1
2	5	30±1	20±1	32±7
2	6	36±6	56±37	33±12
2	7	28±1	25±5	22±4
2	8	23±3	26±2	31±7
2	9	25±1	21±0	19±1
2	10	30±0	21±2	20±0
2	11	27±3	21±1	20±4
2	12	31±4	21±0	19±4
2	13	22±2	36±11	22±3
2	14	23±3	34±11	17±4
2	15	26±4	21±6	21±3
2	16	32±12	17±2	18±1

Continued on next page

Continued from previous page

		– Average P (mg) –		
Trial	**Position**	**Rep 1**	**Rep 2**	**Rep 3**
2	17	3±0	2±0	1±0
2	18	4±0	3±0	2±0
2	19	6±0	8±0	5±0
2	20	16±0	29±1	50±2
3	1	46±6	42±8	35±5
3	2	36±7	24±3	27±2
3	3	33±6	28±2	32±2
3	4	26±3	30±1	29±1
3	5	36±6	24±4	27±2
3	6	31±6	28±2	29±5
3	7	34±1	23±3	33±5
3	8	29±7	24±4	28±2
3	9	36±1	25±3	34±7
3	10	31±6	25±4	26±1
3	11	73±32	22±4	30±2
3	12	32±4	30±3	28±2
3	13	59±26	22±4	25±1
3	14	32±9	28±3	26±1
3	15	42±6	40±13	26±1
3	16	205±70	28±12	52±27
3	17	8±2	4±0	5±1
3	18	10±1	6±0	8±0
3	19	16±2	23±2	18±1
3	20	17±0	29±1	23±1

4.2.4 Blue Dye Experimentation

Screenshots of the brilliant blue dye flush were compared to phosphorus retention values (mg) to visualize flow patterns and instances of preferential flow. Figures 4.16 - 4.18 present average phosphorus levels (mg) and blue dye flush screenshots of all trial replicates.

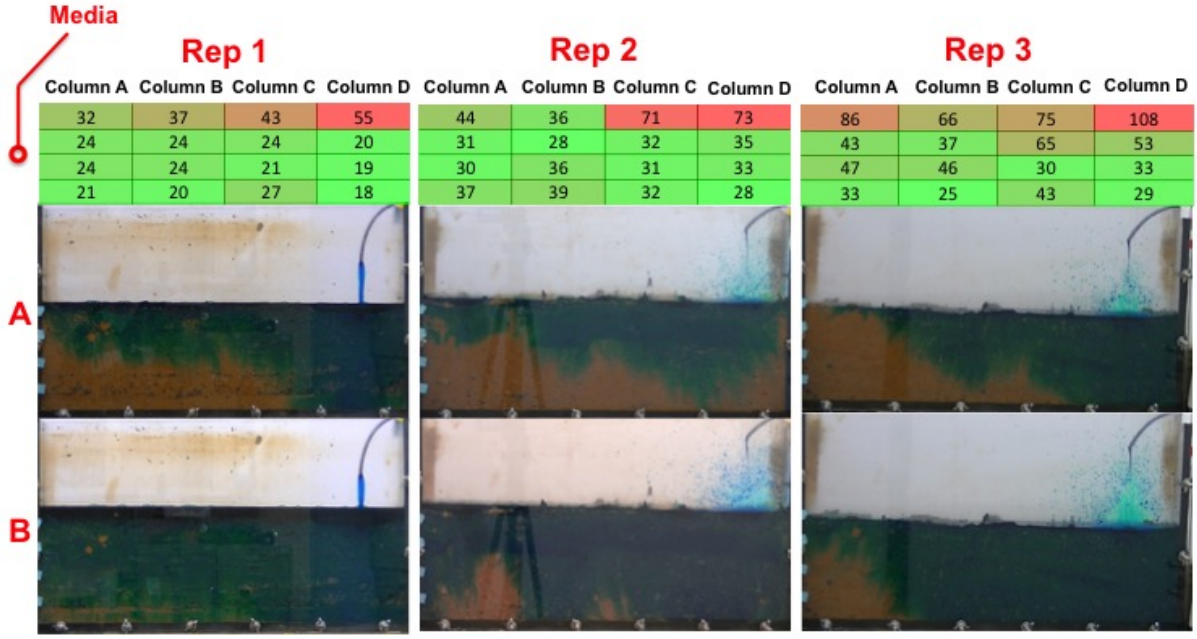

Figure 4.16: Comparison of blue dye flush with phosphorus retention (mg) across the media in Trial 1 Replicates 1, 2, and 3. Figure A illustrates flow patterns after approximately 0.06 L of blue dye had been flushed through the media, and Figure B illustrates flow patterns after approximately 1.5 L of blue dye had been flushed through the media.

Figure 4.16 compared average phosphorus values of media samples 1 - 16 (mg) to flow patterns within the media after 0.06 L (Figure 4.16 A) and 1.5 L (Figure 4.16 B) of dye had been flushed through in Trial 1. Replicate 1 demonstrates the highest amount of ponding compared to replicates 2 and 3. Additionally, Figure 4.16 B for replicate 1 demonstrated the earliest instance of blue dye flow through the entire media; replicates 2 and 3 still had patches of media untouched by the dye after 1.5 L had been flushed through. For all three replicates after 0.06 L had been flushed through, a similar flow pattern was present; the dye appeared to initially flow downward in Columns C and D, and flow horizontally across the

surface after 1.5 L had been flushed (Figure 4.16 B). For replicates 2 and 3, the bottom media layer in Column A was untouched by the dye after 1.5 L had been flushed through.

For all three replicates, the highest phosphorus values were found in the upper media layer underneath the inflow tube. Based on positioning of the highest phosphorus values and similar flow patterns among replicates, it can be inferred that preferential flow did not occur in Trial 1.

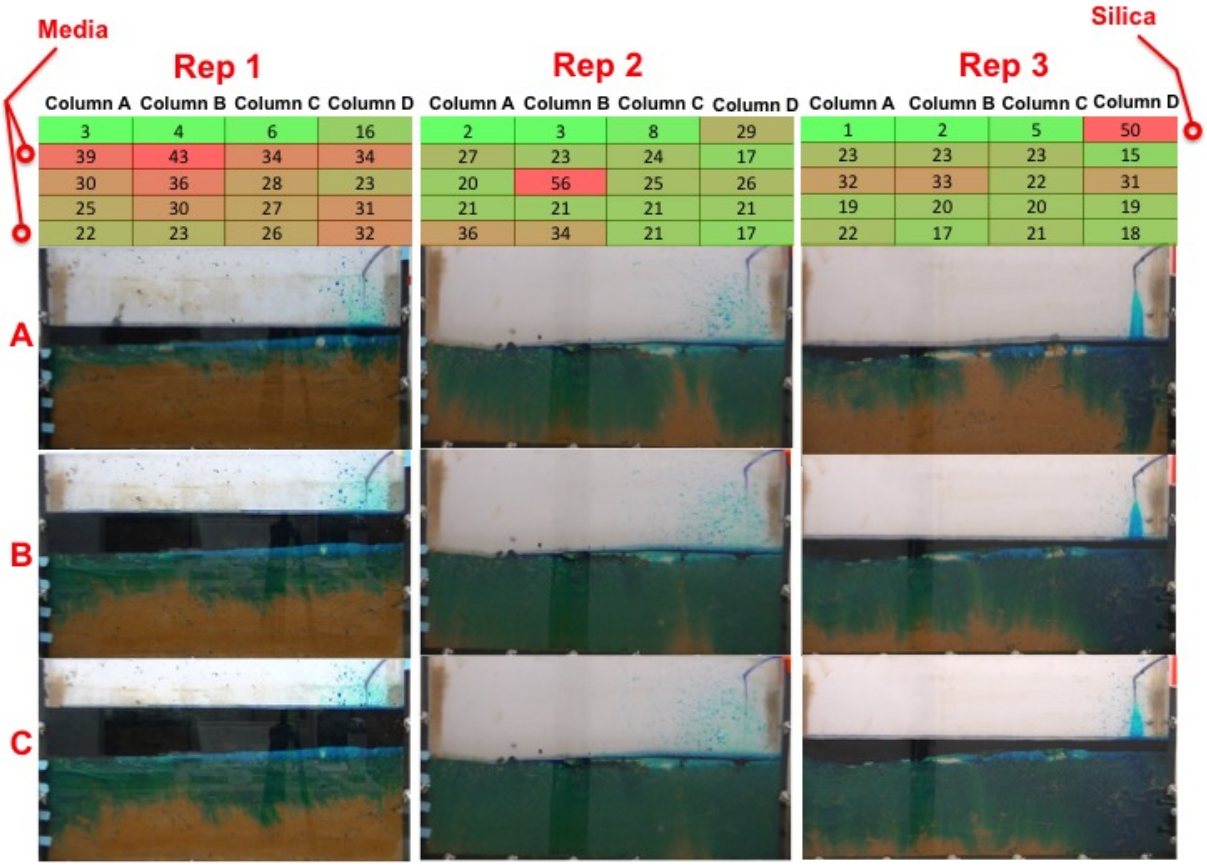

Figure 4.17: Comparison of blue dye flush with phosphorus retention (mg) across the media in Trial 2 Replicates 1, 2, and 3. Figures A, B, and C illustrate flow patterns after approximately 0.06, 1.5, and 1.75 L, respectively, of blue dye had been flushed through the media.

Figure 4.17 compared average phosphorus values of media samples 1 - 16 and silica samples 17 - 20 (mg/kg) to flow patterns within the media after 0.06 L (Figure 4.17 A), 1.5 L (Figure 4.17 B), and 1.75 L (Figure 4.17 C) of dye had been flushed through in Trial 2. Replicate 3 presented a fast flow rate through the media in Columns A, B, and D, compared to

surrounding media. Replicate 3 also presented the highest phosphorus value of 50 mg in the upper silica layer underneath the inflow tube. Replicates 1 and 3 demonstrated ponding on top of the silica layer, whereas replicate 2 did not demonstrate much ponding. Replicate 1 had several middle media sections with high phosphorus values along with relatively uniform flow patterns through the entire media surface. Replicates 2 and 3 showed a different story; overall phosphorus levels in the sections were low, with one section in each replicate containing unusually high phosphorus values compared to surrounding areas (56 mg in Rep 2 and 50 mg in Rep 3, with the next highest value being 36 and 33 mg, respectively). Additionally, flow of the dye through the media was not uniform; Rep 2 had non-uniform flow in Column C, and Rep 3 had non-uniform flow in Columns B and C, compared to surrounding dye flow. Along with the unusually high phosphorus concentrations found in those areas of uniform dye flow, it can be inferred that preferential flow occurred in Rep 2 and 3. The lack of ponding in Rep 2 compared to Rep 1 and 3 illustrates macropores or irregularities in the silica layer, allowing water to flow through faster than the surrounding media and preventing it from creating a "semi-clogged" condition, as originally intended. WCP results indicated a slower saturated hydraulic conductivity in Trial 2 compared to Trial 1, due to the addition of 300 g solids, based on ponding that occurred on the surface of Trial 2 compared to Trial 1.

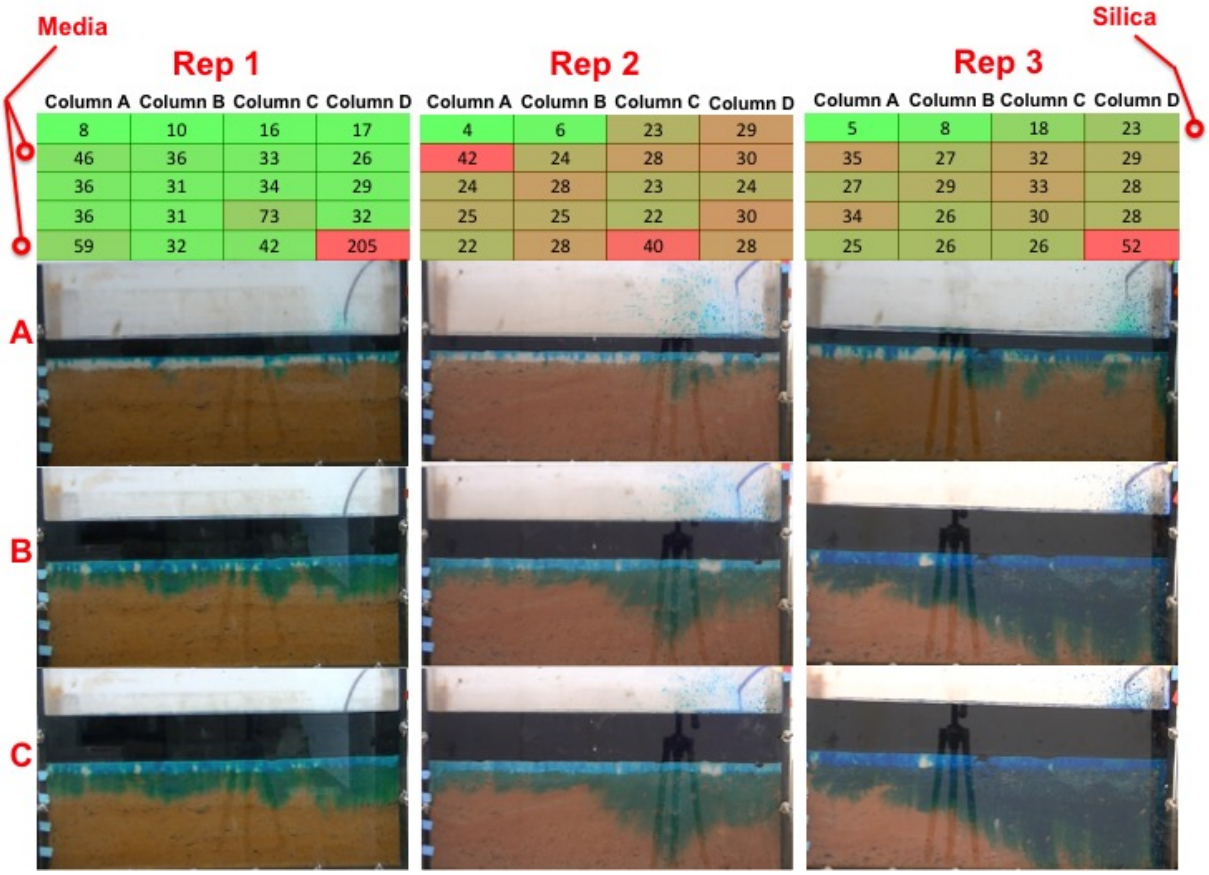

Figure 4.18: Comparison of blue dye flush with phosphorus retention (mg) across the media in Trial 3 Replicates 1, 2, and 3. Figures A, B, and C illustrate flow patterns after approximately 0.06, 1.5, and 1.75 L, respectively, of blue dye had been flushed through the media.

Figure 4.18 compared average phosphorus values (mg) of media samples 1 - 16 and silica samples 17 - 20 to flow patterns within the media after 0.06 L (Figure 4.18 A), 1.5 L (Figure 4.18 B), and 1.75 L (Figure 4.18 C) of dye had been flushed through in Trial 3. A barrier formed on the surface due to the placement of 600 g of silica, obstructing water flow. All 3 replicates demonstrated ponding on top of the silica layer; replicate 1 showed a relatively constant wetting front moving downward through the profile, whereas replicates 2 and 3 showed initial dye movement downward in Columns C and D, with little vertical and horizontal movement in Columns A and B. Replicate 3 demonstrated the highest amount of initial preferential flow through the silica layer after 0.06 L of dye had been flushed through.

For all 3 replicates, high phosphorus values were found in lowest media layer. Based on the constant dye flow throughout all columns, the high level in replicate 1 could be due to media mix variability, with a high amount of mulch located in the one section compared to the rest of the media. The high values in replicate 3 could be due to a preferential flow pathway, either through the center of the media or along the wall of the cell; flow patterns from Figure 4.18 A to Figure 4.18 B show an initial downward movement of dye in Columns C and D compared to the rest of the media. Phosphorus could have been transported faster into that area due to a preferential flow pathway that formed.

4.2.5 Background Phosphorus

Before placement in the cell for each trial replicate, the BRC media was sampled and analyzed for background phosphorus values (mg) (Table 4.4).

Table 4.4: Average total background phosphorus levels (mg) for the flow cell media volume sampled before each trial replicate began, analyzed three times and averaged. Error term reflects one standard error ($n = 3$).

Trial	**Replicate**	**Total Average P (mg) for flow cell**
1	1	264±85
1	2	311±55
1	3	232±45
2	1	277±28
2	2	131±44
2	3	167±40
3	1	189±46
3	2	55±32
3	3	254±24

Compared to the values in Table 4.4, the calculated value of the sum of each component was much higher (Table 4.5). This could be due to the non-homogenous nature of the media mix; the pine bark mulch had varying particle size, ranging from sand sized particles to longer pieces several centimeters in length. The small sample size (0.5 g) used for the microwave

digestion could have prevented the incorporation of mulch particles into the analysis. The lack of mulch incorporation underrepresented the BRC media component percentages; the percentage of background samples representing 85% sand, 10% fines and 5% mulch was very low if mulch was the limiting factor among samples.

Table 4.5: Background phosphorus levels (mg) for each individual media component per flow cell media volume, analyzed three times and averaged. Error term reflects one standard error ($n = 3$).

	— Media Component —			
	——— Phosphorus ———			
	Sand	**Fines**	**Mulch**	**Total Average (mg)**
1 (mg)	86	2689	1281	
2 (mg)	52	2092	1322	
3 (mg)	69	2304	1161	
Average (mg)	69±10	2362±175	1253±48	
Media Mix (%)	85	10	5	
	59	236	63	357

Wilcoxon Rank-Sum Test

The null hypothesis stated no differences between average background phosphorus (mg) and average phosphorus with background included (mg), and the alternative hypothesis stated that average phosphorus retained in the media after synthetic stormwater flush was higher than average background phosphorus. The α-value was set at 5%. Results are reported in Table 4.6.

Trial 1 Replicate 1 through Trial 3 Replicate 3 had p-values below 5%, therefore the null hypothesis is rejected and the alternative hypothesis accepted. Average phosphorus retained after synthetic stormwater flush was higher than average background phosphorus in the media. This analysis further exemplifies that the BRC media used in this research was retaining phosphorus from the synthetic strormwater.

Table 4.6: Wilcoxon rank-sum test p-values.

	Trial 1			Trial 2			Trial 3		
	R 1	**R 2**	**R 3**	**R 1**	**R 2**	**R 3**	**R 1**	**R 2**	**R 3**
p-value	<0.01	<0.01	<0.01	<0.01	<0.01	<0.01	<0.01	<0.01	<0.01

Abbreviations, R: Replicate.

4.2.6 Mass Balance

Mass balance was calculated after the phosphorus flow trials to determine phosphorus retention in the flow cell. Several assumptions were considered, including (a) equivalent media sampling volumes for samples 1 - 16 and 17 - 20, (b) silica layer volumes throughout all replicates of Trials 2 and 3 considered equivalent, and (c) mixing occurrences between media and silica layer during sampling considered negligible for inclusion of background phosphorus. Table 4.7 shows the results of the mass balance. For all trial replicates, 1,228 mg phosphorus was used in the synthetic stormwater.

Table 4.7: Mass balance of total initial versus outflow of Trials 1, 2, and 3.

		– P In (mg) –		—— P out (mg) ——				– Reduction (%)[6] –
Trial	**Rep**	**Media[1]**	**Total[2]**	**Media[3]**	**Sil[4]**	**Eff[5]**	**Total**	
1	1	264	1,492	170	-	1,248	1,418	5
1	2	310	1,538	306	-	1,021	1,327	14
1	3	230	1,458	592	-	1,098	1,690	-16
2	1	276	1,504	207	28	1,007	1,242	17
2	2	132	1,360	278	42	1,194	1,514	-11
2	3	167	1,395	192	59	1,096	1,348	3
3	1	190	1,418	591	51	1,020	1,662	-17
3	2	57	1,285	385	63	1,077	1,526	-19
3	3	253	1,481	233	55	1,013	1,301	12

[1] Average background phosphorus in BRC media.
[2] Total initial phosphours includes sum of 1,228 mg phosphorus in synthetic stormwater and background phosphorus.
[3] Average retained phosphorus in BRC media.
[4] Average retained phosphorus in silica.
[5] Phosphorus present in synthetic stormwater effluent.
[6] Reduction refers to percent phosphorus reduction.

The reduction column reports both positive and negative values. Negative reduction percentages correspond to to an export of phosphorus into the system by the media; it is when outflow values are greater then inflow values. A positive reduction percentage corresponds to a reduction in phosphorus values in the effluent compared to the influent.

Analysis

The mass balance results addressed Objective c and determined any correlations between background phosphorus values in BRC media and fine particle accumulation and clogging on phosphorus retention. Trial 1 Rep 1 and 2, Trial 2 Rep 1 and 3, and Trial 3 Rep 3 all reported a reduction in effluent phosphorus levels compared to influent; in the literature, field-scale BRCs have reported a range of reductions in effluent phosphorus levels (Li and Davis, 2016; Brown and Hunt, 2011b; Davis, 2007; Hunt et al., 2008; Komlos and Traver, 2012; Liu and Davis, 2014; Passeport et al., 2009). Trial 1 Rep 3, Trial 2 Rep 2, and Trial 3

Rep 1 and 2 reported increased phosphorus levels in the effluent compared to the influent; in the literature, field-scale BRCs have additionally reported a range of increases in phosphorus levels in the effluent compared to the influent (Li and Davis, 2016; Brown and Hunt, 2011a; Dietz and Clausen, 2005, 2006; Hunt et al., 2006; Li and Davis, 2009; Palmer et al., 2013; Sharkey, 2006).

All effluent values were relatively constant, which balanced out the total outflow value when compared to the retained phosphorus media values, which were highly variable, with values ranging from 170 - 592 mg. The silica layer contained the lowest amounts of phosphorus among all trial replicates. The two highest retained phosphorus media values, 591 and 592 mg, correlated to two of the total four negative reduction percentages, corresponding to an export of phosphorus into the system (outflow values greater than inflow). These two values corresponded to the background values of 190 and 230 mg, both located directly in the middle of the range of background values, from 57 to 310 mg.

4.3 Summary

By analyzing the results from the clogging experiments and phosphorus flow experiments, final tasks (e) and (f) in Section 1.5 were completed.

Chapter 5

Conclusions

5.1 Objective a: Solids Accumulation and Phosphorus Mobility

BRC media mix is variable due to the different component ratios and particle size differences. The phosphorus flow trials demonstrated preferential flow pathways in several trial replicates. Although the same media and packing method was used across all trial replicates, variability was present among each replicate. For each replicate in Trial 1, the highest phosphorus value (mg) for media samples 1 - 16 was found in the upper media layer, where preferential flow did not occur. Preferential flow potentially occurred in Trials 2 and 3, with high concentrations found sporadically in the middle and lower media layers. Preferential flow demonstrated variability among the media, which will occur in field scale BRCs as well, if a non-homogenous media mix is used. Current maintenance practices suggest removal of the top layer of accumulated sediments to promote surface storage volume and decrease overflow volume; Brown and Hunt (2012) reported removal of the top 7.5 cm (3 in) of media increased surface storage volume by 90%, and decreased overflow volume from 35-37% to 11-12% (Brown and Hunt, 2012). However, localized maintenance and replacement (i.e., at the stormwater inflow outlet) could provide similar benefits to storage volume and cost savings.

5.2 Objective b: Water Flow and Pollutant Load Simulations

Objective b simulated water flow and pollutant load multidimensionally. Previous research regarding bioretention media commonly used column studies as a means to simulate water and pollutant interaction (Hsieh and Davis, 2005a; Hsieh et al., 2007). By using the

flow cell, pollutant and water flow could be analyzed both vertically within the media, as well as spatially across the media surface. Average hydraulic conductivity data of the last two infiltration data points in Trial 2 showed no statistically signifiant difference in quadrants across the surface for both pre- and post-solids placement. There was no evidence to prove that flow was affected by the thickness of the accumulated solids layer.

When assessing field-scale BRCs in the literature, there is no known amount of accumulated solids that will render the cell incapable of filtering pollutants due to the wide range of BRC design, media mix, and external environmental conditions. However, the manner in which accumulated solids enters a BRC facility can result in drastically different clogged layers, including thin, patchy areas of solids and thick, evenly coated layers of solids; visually, a trend could be recognized as it did with the wedge shape in Trial 2, yet could be deemed equally as insignificant as it did in Trial 2. Overall, media with a larger amount of a clogged layer would not necessarily operate considerably worse than one with a thin layer; maintenance would be necessary on both.

Differences in hydraulic conductivity between the thick silica layer in Column D and the thin silica layer in Column A were considered insignificant; based on that observation, predictions can be made about the performance of a field-scale BRC under a similar solids load scaled from the flow cell data. BRCs with the same solids accumulation on the surface are predicted to decline in hydraulic conductivity regardless of the spatial variation of the solids; a BRC with a even, thin layer across the entire surface will demonstrate the same behavior as a BRC with the same amount of silica but in thicker patches covering a smaller percentage of the surface. Based on these findings, the decline of hydraulic conductivity in field scale BRCs can be predicted.

Table 5.1 presents the data involved in predicting hydraulic conductivity decline in a field scale BRC with the same amount of solids accumulation (scaled based on differences in media surface area) as in Trial 2 in order to schedule restorative maintenance at the optimum time. Predicted BRCs are located in Auburn, AL, USA, with annual rainfall of

152 cm (60 in, based on water year 2015), with the assumption that the total rainfall will be surface runoff within an urbanized watershed (USGS, 2016; NWS, 2017). A BRC with a surface area of 19 m^2 (200 ft^2) will be sized as 5% and 10% of the total impervious surface drainage area, to compare two different stormwater inflow conditions. The BRC sized as 5% of the total impervious surface area will receive 95% of total stormwater runoff, calculated as 608 m^3/year, and the BRC sized as 10% of the total impervious surface drainage area will receive 90% of total stormwater runoff, calculated as 304 m^3/year. Assuming that 300 g of accumulated solids from the flow cell surface area will have the same negative effect on hydraulic conductivity of the BRC, 190 kg of solids was considered the load necessary to clog the cell. Four different total suspended solids (TSS) concentrations were used based on land use to determine solids loading rate onto the BRC; the TSS data originated from the National Urban Runoff Program (NURP) which collected stormwater data between 1978 and 1983, considered the most comprehensive study of urban runoff (USEPA, 1996). Table 5.1 presents clogging predictions and subsequent maintenance schedules.

Table 5.1: Clogging predictions on a 20 m^2 BRC, sized at 5% and 10% of total impervious surface drainage area, using data collected from Trial 2, the semi-clogged condition (300 g).

Land Use - Sizing %	**TSS (mg/L)**	**Rain (cm/yr)**	**SW[1] (m^3/yr)**	**Solids (kg)**	**Clogging (years)**
Residential - 5%	101	152	608	190	3
Residential - 10%	101	152	304	190	6
Mixed - 5%	67	152	608	190	5
Mixed - 10%	67	152	304	190	9
Commercial - 5%	69	152	608	190	5
Commercial - 10%	69	152	304	190	9
Open - 5%	70	152	608	190	5
Open - 10%	70	152	304	190	9

[1] Volume stormwater received per year.

Maintenance is needed more often, every 3 - 5 years depending on the land use, in BRCs sized at 5% of the total impervious surface area (receiving 95% of total stormwater

runoff). For BRCs sized at 10% of the total impervious surface area (receiving 90% of total stormwater runoff), maintenance would be needed every 6 - 9 years based on the clogging patterns of 300 g on the flow cell media.

5.3 Objective c: Background Phosphorus

There were no correlations found between background phosphorus and amount of phosphorus retained in the media due to high amounts of variability. The two highest retained phosphorus media values, 591 and 592 mg, correlated to two of the total four negative reduction percentages, corresponding to an export of phosphorus into the system (outflow values greater than inflow). Background phosphorus values are highly correlated to media homogeneity. Field scale BRCs containing larger pieces of mulch and organic matter are potentially under representing background phosphorusvalues in sections of the media with lower amounts. Phosphorus retention in the media will differ in different areas of the cell.

5.4 Overall Conclusions

The success of field scale BRC application is highly dependent on media mix variability and packing, in addition to proper maintenance. Current research does not focus on maximizing the lifespan of a BRC; currently, the focus is on short term water quality monitoring and hydraulic performance. Very few studies look at long term BRC pollutant removal and if negative changes have occurred due to clogging of suspended solids. The flow cell research assists in predicting when maintenance may be needed (removal and replacement of media) due to surface solids accumulation. Using this prediction tool allows for better management, maintenance and cost savings of current and future BRC technology.

5.5 Research Limitations

Results from the clogging experiments and phosphorus flow experiments provided insight into the spatial variability of suspended solids on phosphorus mobility and BRC media pollutant retention. Several phases of the trials encountered error, potentially contributing to variability within the data set. Further experimentation could decrease variability.

The data collected from the clogging experiments and phosphorus flow experiments (infiltration rate, hydraulic conductivity, phosphorus levels) were analyzed collectively within each trial condition; data collection was conducted within the confines of the procedural methodology. The development of unique methodology provided opportunities of multiple data type comparisons, yet provided difficulty when comparing to outside literature.

5.5.1 Media Packing Method

A modified version of the dry packing method was used for the clogging experiments (Section 3.3.2), and a modified version of the wet packing method ASTM D 1557 (Section 3.4.2) was used for the phosphorus flow experiments (Lewis and Sjostrom, 2010; Begin et al., 2003; Communar et al., 2004; Ghodrati et al., 1999; Hrapovic et al., 2005; of Ecology Water Quality Program, 2014; ASTM, 2012; Lewis and Sjostrom, 2010; Seol and Lee, 2001). The methods were changed due to higher frequencies of macropores present in the dry packed media. Modification of the packing method altered media packing composition and created variability in hydraulic conductivity between trial replicates.

5.5.2 Synthetic Stormwater

Due to equipment limitations, the phosphorus in the synthetic stormwater was unable to remain in suspension for the duration of each phosphorus flow trial. The phosphorus and ferrihydrite remained in suspension for a portion of each trial, but not the entirety. This could create variability within each trial as a large majority of the phosphorus could have remained on the surface by chance due to accumulation at the bottom of the container and

independant of the media's phosphorus retention capacity. Additionally, phosphorus could have remained in the container and not been pumped through, accumulating in the container and altering all trials conducted afterwards.

Time was a determining factor for the phosphorus flow trials. The pumping rate of synthetic stormwater varied between each trial; due to the differences in hydraulic conductivity of the media between Trials 1 and 3 based on the amount of silica placed, the amount of time necessary to pump the given volume of synthetic stormwater varied. The hydraulic conductivity of the media in Trial 3 was much lower than that of Trial 1, therefore, more time was necessary to pump the volume of synthetic stormwater through the cell because a lower pumping rate was used otherwise overflow would occur. Trial 3 used an average pumping rate of 0.5 L/hour, compared to Trial 1, which used an average of 12 L/hour. If further experimentation occurred, time would no longer be a determining factor and a low pumping rate would be used for all three trials.

5.5.3 Silica Sampling

To ensure the same sample size was taken from each silica quadrant, samples should be weighed during each trial replicate. This will allow the mass balance calculation to be as accurate as possible. Additionally, dimensions of the silica layer volume must be measured during each replicate to maintain an equivalent layer volume among Trial 2 and 3 replicates.

5.5.4 Mass Balance

For the mass balance to produce more precise results, a higher frequency of composite samples needed to be taken. When the media was prepped for sampling of composite samples 1 - 16 for each trial replicate, the sample sizes taken needed to be weighed and recorded in order to ensure the same sample size was taken among trials. This will provide accuracy in the assumption that equivalent media sample volumes were taken among all trial replicates.

Silica samples 1 - 17 also needed the sample sizes to be weighed and recorded to ensure the same sampling volume was taken for all trial replicates and quadrants.

5.5.5 Infiltration Method

Due to time and space limitations of the flow cell methodology, the data was unable to fit the Philip's infiltration model; additionally, the dataset captured the infiltration process dominated by sorption and not conductivity as the first five infiltration data points were non-linear and not used in further analysis. The last two data points captured the very beginning of the linear portion of infiltration when quasi-steady state was reached and conductivity was the dominating process. In order to avoid this challenge in further experimentation, a larger infiltrometer must be built that can hold a larger volume of water. This will allow the quasi-steady state to be reached earlier in the infiltration trial, and can then be modeled using an infiltration model.

5.6 Future Research Recommendations

5.6.1 Methods of Phosphorus Delivery

Stormwater runoff can contain nutrients, heavy metals, and suspended solids depending on location; Hsieh and Davis (2005a) and Hsieh et al. (2007) mixed synthetic stormwater for bioretention column studies containing phosphorus, nitrate, ammonium, lead, suspended solids, and motor oil. In order to streamline the delivery process yet maintain real world conditions (66% of phosphorus found in stormwater is bound to other particles), ferrihydrite was mixed into the synthetic stormwater with phosphorus (Davis et al., 2009; Davis, 2007; Davis et al., 2001, 2006; Hunt et al., 2008).

The mixture of phosphorus and ferrihydrite focused on the phosphorus delivery; future experimentation could include sorption isotherms that analytically determined the percentage of phosphorus sorbed to other particles. Ferrihydrite could be further studied to determine if the BRC media had the capacity to sorb more phosphorus due to the presence of

the iron oxide. Alternative means of phosphorus delivery, including bound to sediments and heavy metals, could be further studied to determine if phosphorus was retained at higher rates or lower rates.

5.6.2 Media Variations

For this research, one type of media mix was used (85% sand, 10% fines, and 5% mulch) for the flow cell trials. Variations in the percentages of each media component could offer insight into a media type that retains the most phosphorus and reduces effluent levels, using the same clogging experiment and phosphorus flow experiment methodology.

Cost Benefit Analysis

A cost benefit analysis of different types and brands of mulch would determine the media mix that retains the most phosphorus at the lowest price. Mulch of different decomposition stages (aged mulch versus non aged) as well as different brands could be tested using the methodology used in this research. Mass balance calculations analyzing the inflow phosphorus versus outflow phosphorus would offer insight into if the media mix would be a viable BRC mix for field usage.

5.6.3 Plant and Root Growth Visualization

BRCs not only retain phosphorus from stormwater, they also provide habitat for native vegetation. Media mixes with varying levels of mulch, thus varying phosphorus levels in the media, could be packed into the flow cell and different types of vegetation used in BRCs could be planted. The flow cell panels are clear and detachable, thus root growth could be visualized and root density could be determined. Non-invasive sampling methods are possible with the flow cell methodology due to the detachable side; roots can be counted without adversely affecting the plant.

Appendix A

Clogging Trials Whole Cell Performance Data

Table A.1: Whole cell performance media height (cm), ponded water height (cm), and time data (s) for trials 1 - 48 with no replicates.

Experiment ID	Trial	Media Height (cm)	Ponded Water Height (cm)	Time (s)	Replicate
1	1	18.5	11	318	1
1	3	18.5	11	328	1
1	5	18.5	11	314	1
2	8	18.5	11	259	1
2	10	18.5	11	277	1
2	12	18.5	11	280	1
2	14	18.5	11	286	1
2	16	18.5	11	287	1
2	18	18.5	11	288	1
2	20	18.5	11	295	1
2	22	18.5	11	297	1
2	24	18.5	11	333	1
2	26	18.5	11	329	1
2	28	18.5	11	334	1
2	30	18.5	11	290	1
2	32	18.5	11	292	1
2	34	18.5	11	294	1
2	36	18.5	11	294	1
2	38	18.5	11	283	1
2	40	18.5	11	314	1
2	42	18.5	11	291	1
2	44	18.5	11	282	1
2	46	18.5	11	279	1
2	48	18.5	11	280	1

Table A.2: Whole cell performance media height (cm), ponded water height (cm), and time data (s) for trials 50 - 80. Trials 50 - 72 had no replicates, and trials 74 - 80 were analyzed in triplicate.

Experiment ID	**Trial**	**Media Height (cm)**	**Ponded Water Height (cm)**	**Time (s)**	**Replicate**
2	50	18.5	11	290	1
2	52	18.5	11	287	1
2	54	18.5	11	293	1
2	56	18.5	11	303	1
2	58	18.5	11	287	1
2	60	18.5	11	291	1
2	62	18.5	11	290	1
2	64	18.5	11	278	1
2	66	18.5	11	277	1
2	68	18.5	11	290	1
2	70	18.5	11	284	1
2	72	18.5	11	280	1
3	74	18.5	11	311	1
3	74	18.5	11	306	2
3	74	18.5	11	307	3
3	76	18.5	11	363	1
3	76	18.5	11	326	2
3	76	18.5	11	344	3
3	78	18.5	11	340	1
3	78	18.5	11	326	2
3	78	18.5	11	318	3
4	80	18.5	11	378	1

Table A.3: Whole cell performance media height (cm), ponded water height (cm), and time data (s) for trials 80 - 90, analyzed in triplicate.

Experiment ID	**Trial**	**Media Height (cm)**	**Ponded Water Height (cm)**	**Time (s)**	**Replicate**
4	80	18.5	11	355	2
4	80	18.5	11	364	3
5	82	18.5	11	571	1
5	82	18.5	11	602	2
5	82	18.5	11	600	3
5	84	18.5	11	971	1
5	84	18.5	11	1431	2
5	84	18.5	11	1571	3
5	86	18.5	11	2472	1
5	86	18.5	11	1295	2
5	86	18.5	11	1127	3
5	88	18.5	11	2563	1
5	88	18.5	11	2441	2
5	88	18.5	11	2470	3
5	90	18.5	11	5040	1
5	90	18.5	11	5640	2

Appendix B

Phosphorus Concentrations

Table B.1: Raw phosphorus values (mg). Background phosphorus values correspond to entire flow cell media volume, and sample values correspond to individual Section 1 - 16 media volume.

Trial	**Rep**	**Sample Position**	**Analytical Rep**	**Phosphorus (mg)**
1	1	1	1	20
1	1	1	2	42
1	1	1	3	34
1	1	2	1	36
1	1	2	2	39
1	1	2	3	36
1	1	3	1	29
1	1	3	2	51
1	1	3	3	47
1	1	4	1	45
1	1	4	2	61
1	1	4	3	59
1	1	5	1	13
1	1	5	2	33
1	1	5	3	26
1	1	6	1	15
1	1	6	2	28
1	1	6	3	30
1	1	7	1	13
1	1	7	2	24
1	1	7	3	36
1	1	8	1	13
1	1	8	2	24
1	1	8	3	23
1	1	9	1	9

Continued on next page

Continued from previous page

Trial	Rep	Sample Position	Analytical Rep	Phosphorus (mg)
1	1	9	2	33
1	1	9	3	30
1	1	10	1	17
1	1	10	2	29
1	1	10	3	26
1	1	11	1	10
1	1	11	2	27
1	1	11	3	27
1	1	12	1	10
1	1	12	2	26
1	1	12	3	22
1	1	13	1	13
1	1	13	2	25
1	1	13	3	26
1	1	14	1	12
1	1	14	2	23
1	1	14	3	25
1	1	15	1	10
1	1	15	2	34
1	1	15	3	37
1	1	16	1	7
1	1	16	2	26
1	1	16	3	21
1	1	Background	1	98
1	1	Background	2	317
1	1	Background	3	376
1	2	1	1	36
1	2	1	2	52
1	2	1	3	43
1	2	2	1	31
1	2	2	2	41
1	2	2	3	37
1	2	3	1	64
1	2	3	2	88
1	2	3	3	60

Continued on next page

Continued from previous page

Trial	Rep	Sample Position	Analytical Rep	Phosphorus (mg)
1	2	4	1	84
1	2	4	2	70
1	2	4	3	66
1	2	5	1	24
1	2	5	2	36
1	2	5	3	33
1	2	6	1	23
1	2	6	2	30
1	2	6	3	31
1	2	7	1	27
1	2	7	2	36
1	2	7	3	34
1	2	8	1	28
1	2	8	2	45
1	2	8	3	30
1	2	9	1	23
1	2	9	2	34
1	2	9	3	35
1	2	10	1	23
1	2	10	2	48
1	2	10	3	37
1	2	11	1	25
1	2	11	2	34
1	2	11	3	33
1	2	12	1	29
1	2	12	2	37
1	2	12	3	33
1	2	13	1	24
1	2	13	2	31
1	2	13	3	56
1	2	14	1	26
1	2	14	2	58
1	2	14	3	34
1	2	15	1	25
1	2	15	2	33

Continued on next page

Continued from previous page

Trial	Rep	Sample Position	Analytical Rep	Phosphorus (mg)
1	2	15	3	37
1	2	16	1	22
1	2	16	2	37
1	2	16	3	26
1	2	Background	1	218
1	2	Background	2	408
1	2	Background	3	306
1	3	1	1	40
1	3	1	2	45
1	3	1	3	174
1	3	2	1	40
1	3	2	2	113
1	3	2	3	46
1	3	3	1	92
1	3	3	2	55
1	3	3	3	78
1	3	4	1	128
1	3	4	2	107
1	3	4	3	88
1	3	5	1	37
1	3	5	2	49
1	3	5	3	44
1	3	6	1	32
1	3	6	2	37
1	3	6	3	42
1	3	7	1	36
1	3	7	2	45
1	3	7	3	114
1	3	8	1	24
1	3	8	2	38
1	3	8	3	99
1	3	9	1	30
1	3	9	2	70
1	3	9	3	41
1	3	10	1	22

Continued on next page

Continued from previous page

Trial	Rep	Sample Position	Analytical Rep	Phosphorus (mg)
1	3	10	2	44
1	3	10	3	72
1	3	11	1	19
1	3	11	2	38
1	3	11	3	33
1	3	12	1	23
1	3	12	2	37
1	3	12	3	40
1	3	13	1	24
1	3	13	2	42
1	3	13	3	34
1	3	14	1	23
1	3	14	2	26
1	3	14	3	27
1	3	15	1	29
1	3	15	2	64
1	3	15	3	36
1	3	16	1	20
1	3	16	2	41
1	3	16	3	28
1	3	Background	1	264
1	3	Background	2	289
1	3	Background	3	143
2	1	1	1	26
2	1	1	2	23
2	1	1	3	68
2	1	2	1	34
2	1	2	2	46
2	1	2	3	50
2	1	3	1	27
2	1	3	2	33
2	1	3	3	40
2	1	4	1	31
2	1	4	2	33
2	1	4	3	38

Continued on next page

Continued from previous page

Trial	Rep	Sample Position	Analytical Rep	Phosphorus (mg)
2	1	5	1	31
2	1	5	2	30
2	1	5	3	29
2	1	6	1	25
2	1	6	2	47
2	1	6	3	36
2	1	7	1	25
2	1	7	2	30
2	1	7	3	27
2	1	8	1	27
2	1	8	2	25
2	1	8	3	18
2	1	9	1	27
2	1	9	2	25
2	1	9	3	23
2	1	10	1	30
2	1	10	2	29
2	1	10	3	30
2	1	11	1	21
2	1	11	2	32
2	1	11	3	29
2	1	12	1	26
2	1	12	2	30
2	1	12	3	39
2	1	13	1	19
2	1	13	2	24
2	1	13	3	23
2	1	14	1	17
2	1	14	2	28
2	1	14	3	23
2	1	15	1	23
2	1	15	2	21
2	1	15	3	34
2	1	16	1	17
2	1	16	2	23

Continued on next page

Continued from previous page

Trial	Rep	Sample Position	Analytical Rep	Phosphorus (mg)
2	1	16	3	56
2	1	17	1	3
2	1	17	2	3
2	1	17	3	2
2	1	18	1	4
2	1	18	2	3
2	1	18	3	4
2	1	19	1	7
2	1	19	2	6
2	1	19	3	6
2	1	20	1	16
2	1	20	2	15
2	1	20	3	15
2	1	Background	1	322
2	1	Background	2	285
2	1	Background	3	226
2	2	1	1	27
2	2	1	2	27
2	2	1	3	28
2	2	2	1	22
2	2	2	2	23
2	2	2	3	26
2	2	3	1	18
2	2	3	2	19
2	2	3	3	34
2	2	4	1	15
2	2	4	2	18
2	2	4	3	18
2	2	5	1	18
2	2	5	2	20
2	2	5	3	21
2	2	6	1	18
2	2	6	2	19
2	2	6	3	131
2	2	7	1	21

Continued on next page

Continued from previous page

Trial	Rep	Sample Position	Analytical Rep	Phosphorus (mg)
2	2	7	2	35
2	2	7	3	20
2	2	8	1	25
2	2	8	2	23
2	2	8	3	29
2	2	9	1	21
2	2	9	2	21
2	2	9	3	21
2	2	10	1	19
2	2	10	2	19
2	2	10	3	25
2	2	11	1	18
2	2	11	2	22
2	2	11	3	23
2	2	12	1	22
2	2	12	2	21
2	2	12	3	21
2	2	13	1	19
2	2	13	2	55
2	2	13	3	33
2	2	14	1	19
2	2	14	2	30
2	2	14	3	54
2	2	15	1	14
2	2	15	2	33
2	2	15	3	17
2	2	16	1	14
2	2	16	2	20
2	2	16	3	19
2	2	17	1	2
2	2	17	2	2
2	2	17	3	2
2	2	18	1	4
2	2	18	2	3
2	2	18	3	3

Continued on next page

Continued from previous page

Trial	Rep	Sample Position	Analytical Rep	Phosphorus (mg)
2	2	19	1	7
2	2	19	2	8
2	2	19	3	9
2	2	20	1	30
2	2	20	2	30
2	2	20	3	28
2	2	Background	1	52
2	2	Background	2	138
2	2	Background	3	205
2	3	1	1	23
2	3	1	2	20
2	3	1	3	26
2	3	2	1	22
2	3	2	2	26
2	3	2	3	22
2	3	3	1	18
2	3	3	2	28
2	3	3	3	21
2	3	4	1	15
2	3	4	2	16
2	3	4	3	14
2	3	5	1	21
2	3	5	2	46
2	3	5	3	28
2	3	6	1	21
2	3	6	2	57
2	3	6	3	20
2	3	7	1	16
2	3	7	2	22
2	3	7	3	29
2	3	8	1	17
2	3	8	2	36
2	3	8	3	39
2	3	9	1	18
2	3	9	2	18

Continued on next page

Continued from previous page

Trial	Rep	Sample Position	Analytical Rep	Phosphorus (mg)
2	3	9	3	22
2	3	10	1	20
2	3	10	2	20
2	3	10	3	19
2	3	11	1	15
2	3	11	2	17
2	3	11	3	29
2	3	12	1	13
2	3	12	2	18
2	3	12	3	26
2	3	13	1	18
2	3	13	2	20
2	3	13	3	27
2	3	14	1	13
2	3	14	2	25
2	3	14	3	14
2	3	15	1	15
2	3	15	2	20
2	3	15	3	27
2	3	16	1	17
2	3	16	2	20
2	3	16	3	18
2	3	17	1	1
2	3	17	2	1
2	3	17	3	2
2	3	18	1	2
2	3	18	2	2
2	3	18	3	2
2	3	19	1	5
2	3	19	2	5
2	3	19	3	6
2	3	20	1	51
2	3	20	2	53
2	3	20	3	46
2	3	Background	1	138

Continued on next page

Continued from previous page

Trial	Rep	Sample Position	Analytical Rep	Phosphorus (mg)
2	3	Background	2	247
2	3	Background	3	118
3	1	1	1	57
3	1	1	2	44
3	1	1	3	36
3	1	2	1	24
3	1	2	2	50
3	1	2	3	34
3	1	3	1	21
3	1	3	2	41
3	1	3	3	36
3	1	4	1	20
3	1	4	2	30
3	1	4	3	29
3	1	5	1	26
3	1	5	2	47
3	1	5	3	36
3	1	6	1	20
3	1	6	2	40
3	1	6	3	33
3	1	7	1	37
3	1	7	2	32
3	1	7	3	33
3	1	8	1	15
3	1	8	2	37
3	1	8	3	34
3	1	9	1	36
3	1	9	2	38
3	1	9	3	34
3	1	10	1	19
3	1	10	2	38
3	1	10	3	35
3	1	11	1	35
3	1	11	2	138
3	1	11	3	48

Continued on next page

Continued from previous page

Trial	Rep	Sample Position	Analytical Rep	Phosphorus (mg)
3	1	12	1	29
3	1	12	2	39
3	1	12	3	26
3	1	13	1	24
3	1	13	2	42
3	1	13	3	110
3	1	14	1	15
3	1	14	2	38
3	1	14	3	42
3	1	15	1	30
3	1	15	2	45
3	1	15	3	51
3	1	16	1	90
3	1	16	2	331
3	1	16	3	193
3	1	17	1	5
3	1	17	2	10
3	1	17	3	9
3	1	18	1	7
3	1	18	2	11
3	1	18	3	11
3	1	19	1	12
3	1	19	2	20
3	1	19	3	17
3	1	20	1	16
3	1	20	2	18
3	1	20	3	17
3	1	Background	1	98
3	1	Background	2	248
3	1	Background	3	222
3	2	1	1	31
3	2	1	2	39
3	2	1	3	57
3	2	2	1	20
3	2	2	2	29

Continued on next page

Continued from previous page

Trial	Rep	Sample Position	Analytical Rep	Phosphorus (mg)
3	2	2	3	21
3	2	3	1	25
3	2	3	2	32
3	2	3	3	26
3	2	4	1	28
3	2	4	2	31
3	2	4	3	30
3	2	5	1	16
3	2	5	2	26
3	2	5	3	28
3	2	6	1	29
3	2	6	2	30
3	2	6	3	24
3	2	7	1	17
3	2	7	2	27
3	2	7	3	26
3	2	8	1	18
3	2	8	2	26
3	2	8	3	30
3	2	9	1	23
3	2	9	2	31
3	2	9	3	22
3	2	10	1	18
3	2	10	2	29
3	2	10	3	28
3	2	11	1	15
3	2	11	2	29
3	2	11	3	23
3	2	12	1	26
3	2	12	2	36
3	2	12	3	26
3	2	13	1	15
3	2	13	2	27
3	2	13	3	26
3	2	14	1	22

Continued on next page

Continued from previous page

Trial	Rep	Sample Position	Analytical Rep	Phosphorus (mg)
3	2	14	2	32
3	2	14	3	31
3	2	15	1	19
3	2	15	2	37
3	2	15	3	63
3	2	16	1	13
3	2	16	2	51
3	2	16	3	20
3	2	17	1	4
3	2	17	2	4
3	2	17	3	4
3	2	18	1	7
3	2	18	2	6
3	2	18	3	6
3	2	19	1	23
3	2	19	2	20
3	2	19	3	26
3	2	20	1	28
3	2	20	2	29
3	2	20	3	31
3	2	Background	1	0
3	2	Background	2	54
3	2	Background	3	112
3	3	1	1	29
3	3	1	2	45
3	3	1	3	30
3	3	2	1	29
3	3	2	2	24
3	3	2	3	28
3	3	3	1	35
3	3	3	2	32
3	3	3	3	27
3	3	4	1	28
3	3	4	2	30
3	3	4	3	29

Continued on next page

Continued from previous page

Trial	Rep	Sample Position	Analytical Rep	Phosphorus (mg)
3	3	5	1	27
3	3	5	2	30
3	3	5	3	23
3	3	6	1	29
3	3	6	2	20
3	3	6	3	38
3	3	7	1	27
3	3	7	2	29
3	3	7	3	42
3	3	8	1	25
3	3	8	2	27
3	3	8	3	32
3	3	9	1	27
3	3	9	2	27
3	3	9	3	47
3	3	10	1	28
3	3	10	2	24
3	3	10	3	26
3	3	11	1	34
3	3	11	2	28
3	3	11	3	28
3	3	12	1	27
3	3	12	2	26
3	3	12	3	32
3	3	13	1	25
3	3	13	2	25
3	3	13	3	24
3	3	14	1	25
3	3	14	2	29
3	3	14	3	24
3	3	15	1	25
3	3	15	2	25
3	3	15	3	29
3	3	16	1	24
3	3	16	2	26

Continued on next page

Continued from previous page

Trial	Rep	Sample Position	Analytical Rep	Phosphorus (mg)
3	3	16	3	107
3	3	17	1	4
3	3	17	2	7
3	3	17	3	5
3	3	18	1	9
3	3	18	2	7
3	3	18	3	8
3	3	19	1	17
3	3	19	2	20
3	3	19	3	17
3	3	20	1	22
3	3	20	2	22
3	3	20	3	26
3	3	Background	1	287
3	3	Background	2	266
3	3	Background	3	208

Bibliography

L. M. Ahiablame, B. A. Engel, and I. Chaubey. Effectiveness of low impact development practices in two urbanized watersheds: Retrofitting with rain barrel/cistern and porous pavement. *Journal of Environmental Management*, 119:151–161, 2013.

A. O. Akan. *Urban stormwater hydrology: A guide to engineering calculations*. Technomic Publishing Company, Lancaster, PA, 1993.

M. Alberti, D. Booth, K. Hill, B. Coburn, C. Avolio, S. Coe, and D. Spirandelli. The impact of urban patterns on aquatic ecosystems: An empirical analysis in puget lowland sub-basins. *Landscape and Urban Planning*, 80(4):345–361, 2007.

K. T. Aldridge and G. G. Ganf. Modification of sediment redox potential by three contrasting macrophytes: Implications for phosphorus adsorption/desorption. *Marine and Freshwater Research*, 54(1):87–94, 2003.

M. Ankeny, M. Ahmed, T. Kaspar, and R. Horton. Simple field method for determining unsaturated hydraulic conductivity. *Soil Science Society of America Journal*, 55(2):467–470, 1991.

C. L. Arnold and C. J. Gibbons. Impervious surface coverage - the emergence of a key environmental indicator. *Journal of the American Planning Association*, 62(2):243–258, 1996.

A. Askarizadeh, M. A. Rippy, T. D. Fletcher, D. L. Feldman, J. Peng, P. Bowler, A. S. Mehring, B. K. Winfrey, J. A. Vrugt, A. AghaKouchak, S. C. Jiang, B. F. Sanders, L. A.

Levin, S. Taylor, and S. B. Grant. From rain tanks to catchments: Use of low-impact development to address hydrologic symptoms of the urban stream syndrome. *Environmental Science & Technology*, 49(19):11264–11280, 2015.

B. C. Asleson, R. S. Nestingen, J. S. Gulliver, R. M. Hozalski, and J. L. Nieber. Performance assessment of rain gardens(1). *Journal of the American Water Resources Association*, 45 (4):1019–1031, 2009.

ASTM. Standard test method for particle-size analysis of soils. In *Annual Book of ASTM Standards*. American Society of Testing and Materials, Philadelphia, PA, 1985.

ASTM. Standard test methods for laboratory compaction characteristics of soil using modified effort (56,000 ft-lbft$\hat{3}$). Technical Report D1557, 2012.

S. Baken, C. Moens, B. van der Grift, and E. Smolders. Phosphate binding by natural iron-rich colloids in streams. *Water Research*, 98:326–333, 2016.

N. Barrow. A mechanistic model for describing the sorption and desorption of phosphate by soil. *Journal of Soil Science*, 34(4):733–750, 1983.

E. Z. Bean, W. F. Hunt, and D. A. Bidelspach. Field survey of permeable pavement surface infiltration rates. *Journal of Irrigation and Drainage Engineering*, 133(3):249–255, 2007.

L. Begin, J. Fortin, and J. Caron. Evaluation of the fluoride retardation factor in unsaturated and undisturbed soil columns. *Soil Science Society of America Journal*, 67(6):1635–1646, 2003.

D. B. Booth, D. Hartley, and R. Jackson. Forest cover, impervious-surface area, and the mitigation of stormwater impacts. *Journal of the American Water Resources Association*, 38(3):835–845, 2002.

E. C. Bortoluzzi, C. A. S. Perez, J. D. Ardisson, T. Tiecher, and L. Caner. Occurrence of iron and aluminum sesquioxides and their implications for the p sorption in subtropical soils. *Applied Clay Science*, 104:196–204, 2015.

R. A. Brown and W. F. Hunt. Bioretention performance in the upper coastal plain of north carolina. In *Low Impact Development for Urban Ecosystem and Habitat Protection*, pages 1–10. American Society of Civil Engineers, 2008.

R. A. Brown and W. F. Hunt. Impacts of media depth on effluent water quality and hydrologic performance of undersized bioretention cells. *Journal of Irrigation and Drainage Engineering*, 137(3):132–143, 2011a.

R. A. Brown and W. F. Hunt. Underdrain configuration to enhance bioretention exfiltration to reduce pollutant loads. *Journal of Environmental Engineering*, 137(11):1082–1091, 2011b.

R. A. Brown and W. F. Hunt. Improving bioretention/biofiltration performance with restorative maintenance. *Water Science and Technology*, 65(2):361–367, 2012.

R. Burgy and J. Luthin. A test of the single- and double-ring types of infiltrometers. *Transactions of the American Geophysical Union*, 37(2), 1956.

R. O. Carey, G. J. Hochmuth, C. J. Martinez, T. H. Boyer, M. D. Dukes, G. S. Toor, and J. L. Cisar. Evaluating nutrient impacts in urban watersheds: Challenges and research opportunities. *Environmental Pollution*, 173:138–149, 2013.

D. D. Carpenter and L. Hallam. Influence of planting soil mix characteristics on bioretention cell design and performance. *Journal of Hydrologic Engineering*, 15(6):404–416, 2010.

R. Carsel and R. Parrish. Developing joint probability-distributions of soil-water retention characteristics. *Water Resources Research*, 24(5):755–769, 1988.

F. X. M. Casey, R. P. Ewing, and R. Horton. Automated system for miscible displacement through soil of multiple volatile organic compounds. *Soil Science*, 165(11):841–847, 2000.

C. M. Cianfrani, W. C. Hession, and D. M. Rizzo. Watershed imperviousness impacts on stream channel condition in southeastern pennsylvania. *Journal of the American Water Resources Association*, 42(4):941–956, 2006.

G. Communar, R. Keren, and F. H. Li. Deriving boron adsorption isotherms from soil column displacement experiments. *Soil Science Society of America Journal*, 68(2):481–488, 2004.

M. Crawley. *Statistics: An introduction using R.* Wiley, United Kingdom, 2 edition, 2015.

A. P. Davis. Field performance of bioretention: Water quality. *Environmental Engineering Science*, 24(8):1048–1064, 2007.

A. P. Davis. Field performance of bioretention: Hydrology impacts. *Journal of Hydrologic Engineering*, 13(2):90–95, 2008.

A. P. Davis, M. Shokouhian, H. Sharma, and C. Minami. Laboratory study of biological retention for urban stormwater management. *Water Environment Research*, 73(1):5–14, 2001.

A. P. Davis, M. Shokouhian, H. Sharma, C. Minami, and D. Winogradoff. Water quality improvement through bioretention: Lead, copper, and zinc removal. *Water Environment Research*, 75(1):73–82, 2003.

A. P. Davis, M. Shokouhian, H. Sharma, and C. Minami. Water quality improvement through bioretention media: Nitrogen and phosphorus removal. *Water Environment Research*, 78 (3):284–293, 2006.

A. P. Davis, W. F. Hunt, R. G. Traver, and M. Clar. Bioretention technology: Overview of current practice and future needs. *Journal of Environmental Engineering*, 135(3):109–117, 2009.

P. Day. Particle fractionation and particle-size analysis. In *Methods of Soil Analysis, Part I - Physical and Mineralogical Methods*, pages 545–567. 1965.

I. Decagon Devices. Mini disk infiltrometer manual, 2016.

M. Dechesne, S. Barraud, and J.-P. Bardin. Experimental assessment of stormwater infiltration basin evolution. *Journal of Environmental Engineering*, 131(7):1090–1098, 2005.

M. E. Dietz and J. C. Clausen. A field evaluation of rain garden flow and pollutant treatment. *Water Air and Soil Pollution*, 167(1-4):123–138, 2005.

M. E. Dietz and J. C. Clausen. Saturation to improve pollutant retention in a rain garden. *Environmental Science & Technology*, 40(4):1335–1340, 2006.

T. Economist. Open-air computers: Cities are turning into vast data factories, 2016.

D. Elrick, W. Reynolds, and K. Tan. Hydraulic conductivity measurements in the unsaturated zone using improved well analyses. *Ground Water Monitoring and Remediation*, 9 (3):184–193, 1989.

A. J. Erickson, J. S. Gulliver, and P. T. Weiss. Enhanced sand filtration for storm water phosphorus removal. *Journal of Environmental Engineering*, 133(5):485–497, 2007.

C. Everts and R. Kanwar. Interpreting tension-infiltrometer data for quantifying soil macropores - some practical considerations. *Transactions of the ASAE*, 36(2):423–428, 1993.

E. A. Fassman and S. Blackbourn. Urban runoff mitigation by a permeable pavement system over impermeable soils. *Journal of Hydrologic Engineering*, 15(6):475–485, 2010.

M. Flury and N. N. Wai. Dyes as tracers for vadose zone hydrology. *Reviews of Geophysics*, 41(1):1002, 2003.

M. Ghodrati, M. Chendorain, and Y. J. Chang. Characterization of macropore flow mechanisms in soil by means of a split macropore column. *Soil Science Society of America Journal*, 63(5):1093–1101, 1999.

P. Gobel, C. Dierkes, and W. G. Coldewey. Storm water runoff concentration matrix for urban areas. *Journal of Contaminant Hydrology*, 91(1-2):26–42, 2007.

W. Green and G. Ampt. Studies in soil physics: I. The flow of air and water through soils. *Journal of Agricultural Science*, 4:1–24, 1911.

J. M. Hathaway and W. F. Hunt. Evaluation of first flush for indicator bacteria and total suspended solids in urban stormwater runoff. *Water Air and Soil Pollution*, 217(1-4): 135–147, 2011.

B. E. Hatt, T. D. Fletcher, and A. Deletic. Treatment performance of gravel filter media: Implications for design and application of stormwater infiltration systems. *Water Research*, 41(12):2513–2524, 2007.

C. Henderson. *The chemical and biological mechanisms of nutrient removal from stormwater in bioretention systems*. Griffith University, Nathan, Australia, 2008.

D. Hillel. *Soil and water: Physical principles and processes*. Academic Press, New York, 1971.

D. Hillel. *Environmental soil physics*. Academic Press, San Diego, CA, 1998.

D. Hillel. *Introduction to environmental soil physics*. Elsevier Academic Press, 2004.

R. Horton. Analysis of runoff-plot experiments with varying infiltration capacity. *Transactions, American Geophysical Union*, pages 693–964, 1939.

R. Horton. An approach toward a physical interpretation of infiltration capacity. *Soil Science Society Proceedings*, pages 400–417, 1940.

R. E. Horton. The role of infiltration in the hydrologic cycle. *Transactions, American Geophysical Union*, 14:446–460, 1933.

L. Hrapovic, B. E. Sleep, D. J. Major, and E. D. Hood. Laboratory study of treatment of trichloroethene by chemical oxidation followed by bioremediation. *Environmental Science & Technology*, 39(8):2888–2897, 2005.

C. H. Hsieh and A. P. Davis. Multiple-event study of bioretention for treatment of urban storm water runoff. *Water Science and Technology*, 51(3-4):177–181, 2005a.

C. H. Hsieh and A. P. Davis. Evaluation and optimization of bioretention media for treatment of urban storm water runoff. *Journal of Environmental Engineering*, 131(11):1521–1531, 2005b.

C.-h. Hsieh, A. P. Davis, and B. A. Needelman. Bioretention column studies of phosphorus removal from urban stormwater runoff. *Water Environment Research*, 79(2):177–184, 2007.

W. Hunt. *Pollutant removal evaluation and hydraulic characterization for bioretention stormwater treatment devices*. Ph.d, Pennsylvania State University, State College, PA, 2003.

W. F. Hunt, A. R. Jarrett, J. T. Smith, and L. J. Sharkey. Evaluating bioretention hydrology and nutrient removal at three field sites in North Carolina. *Journal of Irrigation and Drainage Engineering*, 132(6):600–608, 2006.

W. F. Hunt, J. T. Smith, S. J. Jadlocki, J. M. Hathaway, and P. R. Eubanks. Pollutant removal and peak flow mitigation by a bioretention cell in urban Charlotte, NC. *Journal of Environmental Engineering*, 134(5):403–408, 2008.

A. Jain and R. H. Loeppert. Effect of competing anions on the adsorption of arsenate and arsenite by ferrihydrite. *Journal of Environmental Quality*, 29(5):1422–1430, 2000.

Y. Jin, M. V. Yates, S. S. Thompson, and W. A. Jury. Sorption of viruses during flow through saturated sand columns. *Environmental Science & Technology*, 31(2):548–555, 1997.

P. S. Jones and A. P. Davis. Spatial accumulation and strength of affiliation of heavy metals in bioretention media. *Journal of Environmental Engineering*, 139(4):479–487, 2013.

W. A. Jury and R. Horton. *Soil Physics*. John Wiley & Sons, Inc., sixth edition, 2004.

H. H. Kim, E. A. Seagren, and A. P. Davis. Engineered bioretention for removal of nitrate from stormwater runoff. *Water Environment Research*, 75(4):355–367, 2003.

A. Klute. Physical and mineralogical methods. In *Methods of Soil Analysis*, pages 404–406. 2nd edition, 1986.

A. Klute and C. Dirksen. *Hydraulic conductivity and diffusivity: Laboratory methods.* American Society of Agronomy, Madison, WI, 1986.

J. Komlos and R. G. Traver. Long-term orthophosphate removal in a field-scale storm-water bioinfiltration rain garden. *Journal of Environmental Engineering*, 138(10):991–998, 2012.

G. F. Koopmans, W. J. Chardon, P. a. I. Ehlert, J. Dolfing, R. a. A. Suurs, O. Oenema, and W. H. van Riemsdijk. Phosphorus availability for plant uptake in a phosphorus-enriched noncalcareous sandy soil. *Journal of Environmental Quality*, 33(3):965–975, 2004.

K. Kung. Preferential flow in a sandy vadose zone .1. field observation. *Geoderma*, 46(1-3): 51–58, 1990a.

K. Kung. Preferential flow in a sandy vadose zone .2. mechanism and implications. *Geoderma*, 46(1-3):59–71, 1990b.

G. Langergraber, R. Haberl, J. Laber, and A. Pressl. Evaluation of substrate clogging processes in vertical flow constructed wetlands. *Water Science and Technology*, 48(5): 25–34, 2003.

S. Le Coustumer, T. D. Fletcher, A. Deletic, S. Barraud, and J. F. Lewis. Hydraulic performance of biofilter systems for stormwater management: Influences of design and operation. *Journal of Hydrology*, 376(1-2):16–23, 2009.

S. Le Coustumer, T. D. Fletcher, A. Deletic, S. Barraud, and P. Poelsma. The influence of design parameters on clogging of stormwater biofilters: A large-scale column study. *Water Research*, 46(20):6743–6752, 2012.

N.-J. B. LeFevre, D. W. Watkins, J. S. Gierke, and J. Brophy-Price. Hydrologic performance monitoring of an underdrained low-impact development storm-water management system. *Journal of Irrigation and Drainage Engineering*, 136(5):333–339, 2010.

J. Lewis and J. Sjostrom. Optimizing the experimental design of soil columns in saturated and unsaturated transport experiments. *Journal of Contaminant Hydrology*, 115(1-4): 1–13, 2010.

H. Li and A. P. Davis. Urban particle capture in bioretention media. I: Laboratory and field studies. *Journal of Environmental Engineering*, 134(6):409–418, 2008a.

H. Li and A. P. Davis. Urban particle capture in bioretention media. II: Theory and model development. *Journal of Environmental Engineering*, 134(6):419–432, 2008b.

H. Li and A. P. Davis. Heavy metal capture and accumulation in bioretention media. *Environmental Science & Technology*, 42(14):5247–5253, 2008c.

H. Li and A. P. Davis. Water quality improvement through reductions of pollutant loads using bioretention. *Journal of Environmental Engineering*, 135(8):567–576, 2009.

H. Li, L. J. Sharkey, W. F. Hunt, and A. P. Davis. Mitigation of impervious surface hydrology using bioretention in North Carolina and Maryland. *Journal of Hydrologic Engineering*, 14(4):407–415, 2009.

J. Li and A. P. Davis. A unified look at phosphorus treatment using bioretention. *Water Research*, 90:141–155, 2016.

G. Lindsey, L. Roberts, and W. Page. Inspection and maintenance of infiltration facilities. *Journal of Soil and Water Conservation*, 47(6):481–486, 1992.

J. Liu and A. P. Davis. Phosphorus speciation and treatment using enhanced phosphorus removal bioretention. *Environmental Science & Technology*, 48(1):607–614, 2014.

J. Liu, D. J. Sample, C. Bell, and Y. Guan. Review and research needs of bioretention used for the treatment of urban stormwater. *Water*, 6(4):1069–1099, 2014a.

J. Liu, D. J. Sample, J. S. Owen, J. Li, and G. Evanylo. Assessment of selected bioretention blends for nutrient retention using mesocosm experiments. *Journal of Environmental Quality*, 43(5):1754–1763, 2014b.

P.-W. G. Liu, L.-M. Whang, M.-C. Yang, and S.-S. Cheng. Biodegradation of diesel-contaminated soil: A soil column study. *Journal of the Chinese Institute of Chemical Engineers*, 39(5):419–428, 2008.

R. Lookman, D. Freese, R. Merckx, K. Vlassak, and W. Vanriemsdijk. Long-term kinetics of phosphate release from soil. *Environmental Science & Technology*, 29(6):1569–1575, 1995.

W. C. Lucas and M. Greenway. Nutrient retention in vegetated and nonvegetated bioretention mesocosms. *Journal of Irrigation and Drainage Engineering*, 134(5):613–623, 2008.

W. C. Lucas and M. Greenway. Phosphorus retention by bioretention mesocosms using media formulated for phosphorus sorption: Response to accelerated loads. *Journal of Irrigation and Drainage Engineering*, 137(3):144–153, 2011.

M. A. Mallin, V. L. Johnson, and S. H. Ensign. Comparative impacts of stormwater runoff on water quality of an urban, a suburban, and a rural stream. *Environmental Monitoring and Assessment*, 159(1-4):475–491, 2009.

M. G. Miguez, O. M. Rezende, and A. P. Verol. City growth and urban drainage alternatives: Sustainability challenge. *Journal of Urban Planning and Development*, 141(3):04014026, 2015.

B. P. Mohanty, T. H. Skaggs, and M. T. van Genuchten. Impact of saturated hydraulic conductivity on the prediction of tile flow. *Soil Science Society of America Journal*, 62(6): 1522–1529, 1998.

D. M. Nash and D. J. Halliwell. Tracing phosphorous transferred from grazing land to water. *Water Research*, 34(7):1975–1985, 2000.

V. Novotny. *Water quality: Diffuse pollution and watershed management*. J. Wiley, Hoboken, NJ, 2003.

NWS. AHPS precipitation analysis. `http://water.weather.gov/precip/`, 2017.

W. S. D. of Ecology Water Quality Program. 2014 Stormwater management manual for Western Washington. Technical report, 2014.

S. W. O'Neill and A. P. Davis. Analysis of bioretention media specifications and relationships to overall performance. In *Low Impact Development 2010*, pages 1223–1233. American Society of Civil Engineers, 2010.

J. L. Page, R. J. Winston, D. B. Mayes, C. Perrin, and W. F. Hunt. Retrofitting with innovative stormwater control measures: Hydrologic mitigation of impervious cover in the municipal right-of-way. *Journal of Hydrology*, 527:923–932, 2015.

E. T. Palmer, C. J. Poor, C. Hinman, and J. D. Stark. Nitrate and phosphate removal through enhanced bioretention media: Mesocosm study. *Water Environment Research*, 85 (9):823–832, 2013.

E. Passeport, W. F. Hunt, D. E. Line, R. A. Smith, and R. A. Brown. Field study of the ability of two grassed bioretention cells to reduce storm-water runoff pollution. *Journal of Irrigation and Drainage Engineering*, 135(4):505–510, 2009.

K. Perroux and I. White. Designs for disc permeameters. *Soil Science Society of America Journal*, 52(5):1205–1215, 1988.

J. Philip. The theory of infiltration: 1. the infiltration equation and its solution. *Soil Science*, 83:345–357, 1957a.

J. Philip. The theory of infiltration: 2. the profile at infinity. *Soil Science*, 83:435–448, 1957b.

J. Philip. The theory of infiltration: 3. moisture profiles and relation to experiment. *Soil Science*, 84:163–178, 1957c.

J. Philip. The theory of infiltration: 4. sorptivity and algebraic infiltration equations. *Soil Science*, 84:257–264, 1957d.

J. Philip. The theory of infiltration: 5. influence of initial moisture content. *Soil Science*, 84:329–339, 1957e.

J. Philip. Evaporation, and moisture and heat fields in the soil. *Journal of Meteorology*, 14 (4):354–366, 1957f.

J. Philip. Infiltration in one, two, and three dimensions. In *National Conference of American Society of Agricultural Engineers*, pages 1–13, St. Josephs, MI, 1983.

R. Pitt, A. Maestre, and R. Morquecho. The National Stormwater Quality Database (NSQD, Version 1.1). Technical report, 2004.

Prince George's County Department of Environmental Resources. Design manual for use of bioretention in stormwater management. Technical report, Prince George's County (MD)

Government, Department of Environmental Protection, Watershed Protection Branch, Landover, MD, 1993.

Prince George's County Department of Environmental Resources. Low impact development hydrologic analysis. Technical report, Department of Environmental Resources, Largo, MD, 1999a.

Prince George's County Department of Environmental Resources. Low impact development design strategies, an integrated design approach. Technical report, Department of Environmental Resources, Programs and Planning Division, Largo, MD, 1999b.

P. Raats. Analytical solutions of a simplified flow equation. *Transactions of the ASAE*, 19 (4):683–689, 1976.

K. P. Raven, A. Jain, and R. H. Loeppert. Arsenite and arsenate adsorption on ferrihydrite: Kinetics, equilibrium, and adsorption envelopes. *Environmental Science & Technology*, 32 (3):344–349, 1998.

W. Reynolds and D. Elrick. Ponded infiltration from a single ring: I. analysis of steady flow. *Soil Science Society of America Journal*, 54:1233–1241, 1990.

W. Reynolds and D. Elrick. Determination of hydraulic conductivity using a tension infiltrometer. *Soil Science Society of America Journal*, 55(3):633–639, 1991.

W. Reynolds, D. E. Elrick, E. Youngs, A. Amoozegar, H. Bootlink, and J. Bouma. Saturated and field-saturated water flow parameters. In *Methods of Soil Analysis Part 4: Physical Methods*, number 5 in Soil Science Society of America Book Series. Soil Science Society of America, Inc., Madison, WI, 2002.

W. D. Reynolds, B. T. Bowman, R. R. Brunke, C. F. Drury, and C. S. Tan. Comparison of tension infiltrometer, pressure infiltrometer, and soil core estimates of saturated hydraulic conductivity. *Soil Science Society of America Journal*, 64(2):478–484, 2000.

L. Rhea, T. Jarnagin, D. Hogan, J. V. Loperfido, and W. Shuster. Effects of urbanization and stormwater control measures on streamflows in the vicinity of Clarksburg, Maryland, USA. *Hydrological Processes*, 29(20):4413–4426, 2015.

L. Richards. Capillary conduction of liquids through porous mediums. *Physics*, 1:318–333, 1931.

D. T. Saalfeld, E. M. Reutebuch, R. J. Dickey, W. C. Seesock, C. Webber, and D. R. Bayne. Effects of landscape characteristics on water quality and fish assemblages in the Tallapoosa River Basin, Alabama. *Southeastern Naturalist*, 11(2):239–252, 2012.

D. Schindler. Evolution of phosphorus limitation in lakes. *Science*, 195(4275):260–262, 1977.

W. Schuh. Seasonal-variation of clogging of an artificial recharge basin in a northern climate. *Journal of Hydrology*, 121(1-4):193–215, 1990.

U. Schwertmann and R. Cornell. *Iron oxides in the laboratory*. Wiley-VCH, 2nd edition, 2000.

D. Scotter, B. Clothier, and E. Harper. Measuring saturated hydraulic conductivity and sorptivity using twin rings. *Australian Journal of Soil Research*, 20(4):295–304, 1982.

Y. Seol and L. S. Lee. Coupled effects of treated effluent irrigation and wetting-drying cycles on transport of triazines through unsaturated soil columns. *Journal of Environmental Quality*, 30(5):1644–1652, 2001.

L. Sharkey. The performance of bioretention areas in North Carolina: A study of water quality, water quantity, and soil media. Technical report, North Carolina State University, Raleigh, NC, 2006.

J. T. Sims, R. R. Simard, and B. C. Joern. Phosphorus loss in agricultural drainage: Historical perspective and current research. *Journal of Environmental Quality*, 27(2):277–293, 1998.

E. K. Stander and M. Borst. Hydraulic test of a bioretention media carbon amendment. *Journal of Hydrologic Engineering*, 15(6):531–536, 2010.

T. Thompson. Low impact development, 2009.

UN Department of Economic and Social Affairs. World's population increasingly urban with more than half living in urban areas, 2016.

University of Arkansas. Low impact development: A design manual for urban areas. Technical report, University of Arkansas, Fayetteville, AR, 2010.

US Dep of Housing and Urban Development. The practice of low impact development. Technical report, Office of Policy Development and Research, Washington, D.C., 2003.

USEPA. *Quality criteria for water (Gold book)*. EPA 440/5-86-001. Office of Water, Regulations and Standards, Washington, DC, 1986.

USEPA. Urban storm water preliminary data summary. Technical report, 1996.

USEPA. Method 3051A Microwave assisted acid digestion of sediments, sludges, soils, and oils. Manual, 2007.

USGS. Rain and precipitation, USGS water science school. `https://water.usgs.gov/edu/earthrain.html`, 2016.

W. Wang, T. Liang, L. Wang, Y. Liu, Y. Wang, and C. Zhang. The effects of fertilizer applications on runoff loss of phosphorus. *Environmental Earth Sciences*, 68(5):1313–1319, 2013.

I. White and M. Sully. Macroscopic and microscopic capillary length and time scales from field infiltration. *Water Resources Research*, 23(8):1514–1522, 1987.

C. E. Wilson, W. F. Hunt, R. J. Winston, and P. Smith. Comparison of runoff quality and quantity from a commercial low- impact and conventional development in Raleigh, North Carolina. *Journal of Environmental Engineering*, 141(2), 2015.

A. Wossink and W. F. Hunt. Cost effectiveness analysis of structural stormwater best management practices in North Carolina. Technical report, North Carolina Water Resources Research Institute, Raleigh, NC, 2003.

E. Youngs, P. Leedsharrison, and D. Elrick. The hydraulic conductivity of low permeability wet soils used as landfill lining and capping material - analysis of pressure infiltrometer measurements. *Soil Technology*, 8(2):153–160, 1995.

M. Zhang, A. K. Alva, Y. C. Li, and D. V. Calvert. Aluminum and iron fractions affecting phosphorus solubility and reactions in selected sandy soils. *Soil Science*, 166(12):940–948, 2001.

R. D. Zhang. Determination of soil sorptivity and hydraulic conductivity from the disk infiltrometer. *Soil Science Society of America Journal*, 61(4):1024–1030, 1997.

Y. Zinger, T. Fletcher, A. Deletic, G. Blecken, and M. Viklander. Optimisation of the nitrogen retention capacity of stormwater biofiltration systems. pages 893–900, 2007.